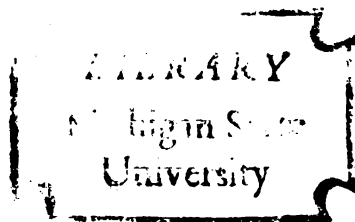




THESIS



This is to certify that the  
thesis entitled

Considerations in the Design of Solar Engines

presented by

L. D. Ryan

has been accepted towards fulfillment  
of the requirements for

Ph.D degree in Ag. Eng.

  
Major professor

Date August 7, 1980



OVERDUE FINES:

25¢ per day per item

RETURNING LIBRARY MATERIALS:

Place in book return to remove  
charge from circulation records

© Copyright by

L.D. RYAN

1980



CONSIDERATIONS IN THE DESIGN OF SOLAR ENGINES

By

L.D. Ryan

A DISSERTATION

Submitted to  
Michigan State University  
in partial fulfillment of the requirements  
for the degree of

DOCTOR OF PHILOSOPHY

Department of Agricultural Engineering

1980

## ABSTRACT

### CONSIDERATIONS IN THE DESIGN OF SOLAR ENGINES

By

L.D. Ryan

The basic problem is to develop simple engines to convert solar radiation into useful work. Since the conversion of radiation to work is presently undeveloped, it became necessary to assemble information on related subjects. Chapters are included on solar insolation and solar collectors, both flat plate and concentrators.

Over a century ago operational solar engines were being built. As low cost fossil fuel became available, the solar engines became novelties that could not economically compete. This fledgling technology went to an early grave with its inventors. Enough information of past engines was assembled to estimate probable efficiency. Ericsson built an engine that produced one brake horsepower per one hundred square feet of collector. This engine was approximately twelve per cent efficient which will be a goal to achieve for modern researchers.

Cost effective design is one that can economically compete with diesel engines. Chapter 5 studies this problem. With inflated fuel prices it appears that solar engines have a place in the free market system.

The initial research centered on the Stirling engine.

It became obvious that the displacement piston was an expensive means to add and reject heat. The displacement piston was eliminated by rotating the entire engine through the heat source for  $180^\circ$  of rotation and cooling over the remaining  $180^\circ$ . This modification resulted in the development of a new engine.

The engine consists of a hollow-bored cylinder with head caps on each end. Inside the cylinder are two pistons at each end of the tube. These pistons are connected to a common pitman crank that is stationary. The entire engine, consisting of cylinder, pistons, and connecting rods, rotates while the crank shaft remains stationary. Energy conducting rings are added to the cylinder head with internal connection between the ring and the gas above the cylinder. These rings were originally hollow tubes formed into circles of  $180^\circ$ . To make this engine operational, the solid rings were redesigned. The side facing the mirror is transparent. The solar radiation passes through the transparent cover and is trapped. Each piston has one energy ring. Solar energy from a concentrating collector focuses inside the rotating ring, adding energy to the gas above the piston. The ring rotates out from under the focal point and is cooled, which completes the cycle.

Limited studies were conducted on the gas inside the heat ring. Pressure versus time was measured for air and Freon-12 when subjected to radiation. Freon-12 responded significantly better. This indicated a need for further

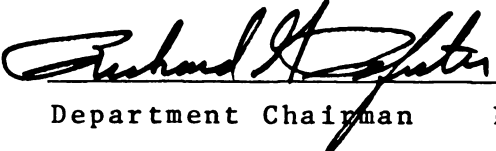
tests to find the best gas to absorb solar radiation.

A very simple fundamental fact came from the evolutionary design process of the rotating engine. The ideal gas law is valid when gas is enclosed in flat plate collectors. With the proper design, the pressure will increase with the temperature. It was found that 13.8 kPa pressure increase is possible with a concentration ratio of one. From this knowledge, other engine designs became feasible. The author easily constructed models to operate from flat plate collectors. The increased pressure produced work. The motion of the piston could be used to provide a cooling cycle either with valving or through shading.

Since friction is a deterrent to solar engine development, methods to minimize friction are discussed. A specific design using rolling diaphragms with a piston held concentric with a bushing has solved this problem. By using the piston-cylinder arrangement and a flat plate collector, a low cost engine is possible.

Approved by

 7 Aug. 1980  
Major Professor Date

 7 Aug 80  
Department Chairman Date

## DEDICATION

This dissertation is dedicated to the One who created the Sun, and to Susan, my wife, who gave me five sons.

## ACKNOWLEDGEMENTS

I want to thank all that have been a part of making this dissertation possible. To Jennifer Graney and Marilyn Duke, who have given up their free time to type the final document, thank you. To my committee and major advisor, Dr. Larry Segerlind, thank you. To my beloved wife, Susan, who has been with me through three degrees, thank you. I particularly want to praise the Lord for His daily help and encouragement in this work, which by His Grace will be used for His Kingdom.

August 6, 1980

## TABLE OF CONTENTS

	Page
LIST OF TABLES . . . . .	vi
LIST OF FIGURES . . . . .	viii
 Chapter	
1. BRIEF HISTORY OF SOLAR ENGINES. . . . .	1
1.1 Introduction . . . . .	1
1.2 Early French Solar Engines . . . . .	3
1.3 Ericsson's Sun Motor . . . . .	6
1.4 Other Solar Engines. . . . .	10
1.5 Stirling Engine . . . . .	16
1.6 Patent Search of Solar Devices . . . . .	20
1.7 Summary. . . . .	27
1.8 Objectives. . . . .	31
2. SOLAR INSOLATION . . . . .	32
2.1 Solar Constant and Surface Insolation. . . . .	32
2.2 Transmittance of Solar Radiation Through the Air Mass . . . . .	34
2.3 Solar Geometry . . . . .	38
2.4 Solar Time. . . . .	43
3. SOLAR COLLECTORS . . . . .	45
3.1 Introduction . . . . .	45
3.2 Flat Plate Collector Analysis . . . . .	48
3.3 Simplified Analysis for Flat Plate Collectors . . . . .	59
3.4 Solar Concentrators. . . . .	63
4. ACTUAL COLLECTOR TESTS COMPARED WITH ANALYSIS. . . . .	72
4.1 Parabolic Collector Tests and Comparison	72
4.2 Flat Plate Collector Tests and Comparison	83

Chapter	Page
5. SOLAR ENGINE ECONOMICS . . . . .	89
5.1 Introduction . . . . .	89
5.2 Simple Payback Costing. . . . .	89
5.3 Flat Plate Versus Concentrating Collector as Engine Power Source . . . . .	93
6. SOLAR ENGINE CYCLES . . . . .	96
6.1 Second Law Considerations. . . . .	96
6.2 Rankine Cycle. . . . .	101
6.3 Ericsson Cycle . . . . .	103
6.4 Stirling Cycle . . . . .	107
7. SOLAR ENGINE DESIGN . . . . .	109
7.1 Economic Comparison of Solar Designs . . . . .	109
7.2 Engine Design to Minimize Cost . . . . .	111
7.3 Minimizing Friction in Solar Engines . . . . .	118
7.4 Material Selection for Solar Engine Applications. . . . .	126
7.5 Working Media in Solar Engines . . . . .	135
7.6 Design of Machine Elements . . . . .	139
8. ENGINEERING ANALYSIS OF A ROTATING SOLAR ENGINE . . . . .	153
8.1 Introduction and Engine Description . . . . .	153
8.2 Cycle Analysis of the New Engine . . . . .	157
8.3 Solar Insolation. . . . .	166
8.4 Energy Transferred to the Gas . . . . .	167
8.5 Engine Efficiency . . . . .	174
8.6 Mechanism and Stress Analysis . . . . .	175
8.7 Servicing and Engine Life. . . . .	175
9. OPERATION OF THE SOLAR ENGINE . . . . .	177
9.1 Discussion of the Rotating Engine . . . . .	177
9.2 Results of Tests. . . . .	182
9.3 Proposed Solar Engine Design. . . . .	186
9.4 Failures . . . . .	190
10. CONCLUSION . . . . .	193
11. RECOMMENDATIONS. . . . .	198
BIBLIOGRAPHY . . . . .	199



## LIST OF TABLES

Table	Page
1-1. Patent Search on Solar Engines. . . . .	21
1-2. Solar Engine Developers . . . . .	27
1-3. Past Performances . . . . .	29
2-1. Coefficiencts of $a_0$ , $a_1$ , and $k$ . . . . .	38
2-2. Constant for Equation 2.11 . . . . .	42
2-3. Equation of Time "E" . . . . .	44
2-4. Standard Meridian for Local Time Zone . . . . .	44
3-1. Convective Heat Transfer Coefficients . . . . .	52
3-2. Diffuse Reflectance $\rho_d$ . . . . .	57
3-3. Absorption Emissivity of Various Surfaces . . . . .	58
3-4. Specular Solar Reflectance . . . . .	68
4-1. Data for Solar Concentrator. . . . .	73
4-2. Factors for Equation 4.2. . . . .	79
4-3. Absorber Tests . . . . .	85
5-1. Price/Horsepower for Solar Engine System . . . . .	92
5-2. Economic Comparison of Flat Plate to Concen- trator for Systems Operating Solar Engines . . . . .	95
7-1. Typical Sizes of Diaphragms. . . . .	125
7-2. Effect of Temperature on Material Strength. . . . .	129
7-3. Thermal Conductivities of Various Metals . . . . .	139

Table	Page
7-4. Properties of 1100 Aluminum Alloy. . . . .	141
7-5. Bearing Design Pressure . . . . .	144
7-6. Ball Bushing. . . . .	150
7-7. Coefficient of Friction . . . . .	151

## LIST OF FIGURES

Figure	Page
1-1. Solar Engine System . . . . .	1
1-2. Mouchot's Engine . . . . .	4
1-3. Pifre's Sun-Power Plant of 1878 Driving A Printing Press. . . . .	4
1-4. Solar Furnace Used by Lavoisier, 1774 . . . .	5
1-5. The Novelty Locomotive by Ericsson to Compete with Stephenson's Rocket, 1929 . . . . .	7
1-6. Ericsson's Caloric Engine . . . . .	8
1-7. Ericsson's Solar Engine. . . . .	11
1-8. Pasadena Sun Heat Absorber of 1901 . . . .	12
1-9. Shuman-Boys System Meadi, 1913 . . . . .	15
1-10. Shuman-Boys System Meadi, 1913 . . . . .	15
1-11. Stirling Engine . . . . .	17
1-12. Stirling Cycle for a Gaseous Substance. . . .	18
1-13. Stirling Engine with Regenerators . . . . .	19
1-14. W.W. White Radiation Turbine . . . . .	22
1-15. Newland Solar Energy Device. Patent No. 4 033 126. . . . .	23
1-16. Solar Engine Based on Thermal Expansion . . .	24
1-17. Horton Solar Power Plant . . . . .	24

Figure	Page
1-18. Bentley's Heat Engine. Patent No. 4 033 134. . . . .	25
1-19. Bell's Solar Energy Converter with Waste Engine. Patent No. 4 002 031 . . . . .	26
2-1. Solar Insolation 40° North Latitude - February 21 . . . . .	33
2-2. ASHRAE Tables . . . . .	34
2-3. Air Mass. . . . .	36
2-4. Projected Area. . . . .	38
2-5. Angles Defined. . . . .	40
2-6. Hourly Radiation Chart . . . . .	43
3-1. Patent No. 4 033 118 by Powell . . . . .	47
3-2. Solarometer Measuring $A(H_D + H_d)$ . . . . .	50
3-3. Heat Transfer Through Cover . . . . .	53
3-4. Energy Balance on Cover. . . . .	55
3-5. Transmittance, $\tau$ , Neglecting Absorption . . . . .	58
3-6. Solar Test Module. . . . .	60
3-7. Vertical Solar Collector . . . . .	60
3-8. Heat Flow from Collector (Simplified) . . . . .	61
3-9. Heat Transfer into Receiver . . . . .	70
4-1. Testing System for Table 4-1 . . . . .	72
4-2. Hand-Held Solarometer . . . . .	74
4-3. Auxiliary Space Heating System . . . . .	83
4-4. Vertical Solar Collector at Western Michigan University. . . . .	84

Figure	Page
4-5. Solar Test Panel . . . . .	85
6-1. Carnot Engine . . . . .	98
6-2. Carnot Cycle . . . . .	100
6-3. Heat Engine Cycle Comparison . . . . .	101
6-4. Rankine Cycle . . . . .	102
6-5. Rankine Cycle Schematic. . . . .	102
6-6. Solar Engine Adapted to Use Hot Air (1880) .	104
6-7. Schematic of One Type of John Ericsson's Hot Air Engine (Mernel) . . . . .	105
6-8. Ericsson Cycle. . . . .	106
6-9. Stirling Cycle. . . . .	107
7-1. Savery's Steam Pump . . . . .	112
7-2. Solar Pump . . . . .	113
7-3a. Solar Engine Front View. . . . .	114
7-3b. Solar Engine Side View . . . . .	116
7-4. Flat Plate Solar Engine. . . . .	119
7-5. Rolling Diaphragms Concept. . . . .	122
7-6. Free Body of Side Walls of Diaphragm . . .	122
7-7. Diaphragm, Up-stroke Position. . . . .	124
7-8. Diaphragm, Down-stroke Position . . . . .	124
7-9. The Creep Curve . . . . .	130
7-10. Fatigue Strength as a Function of $\sigma_{ult}$ and Surface Finish . . . . .	133
7-11. Effect of Temperature on the Fatigue Limits of Steels . . . . .	133

Figure	Page
7-12. T-S Diagram of H <sub>2</sub> O . . . . .	136
7-13. Vapor Pressure of Various Temperatures for Solar Working Media. . . . .	138
7-14. Hot Air Engine. . . . .	139
7-15. Forces on the Guide Bushing . . . . .	145
7-16. Force Distribution in Bushing. . . . .	145
7-17. Typical Ball Bushing. . . . .	147
7-19. Ball Bushing Design Chart . . . . .	148
7-20. Ball Bushing Design Chart . . . . .	148
8-1. Solar Engine Frame . . . . .	154
8-2. Solar Engine Piston Assembly . . . . .	155
8-3. Solar Engine Assembly . . . . .	156
8-4. Cycle Diagram . . . . .	157
8-5. Solar Engine Schematic . . . . .	160
8-6. Energy Balance on Heat Ring . . . . .	170
9-1. Solar Engine Schematic with Revised Heat Ring . . . . .	177
9-2. Four Inch Bore Engine . . . . .	179
9-3. Four Inch Bore Engine . . . . .	180
9-4. Small Model of Solar Engine . . . . .	181
9-5. Test Chamber . . . . .	182
9-6. Test Results . . . . .	184
9-7. Flat Plate Collector Engine . . . . .	185

CHAPTER 1  
BRIEF HISTORY OF SOLAR ENGINES

1.1 Introduction

Solar engines have inherent limitations that have baffled developers for centuries. First, the sun is an intermittent energy source which is unpredictable in many regions because of climatic conditions. This variableness requires a method of energy storage or limits the engines use to specific applications. Second, the overall efficiency is low. The energy density of the sunlight is not high. Thus, large collecting areas are needed. Collector efficiency may range from 0.30 to 0.70. The engine will have an efficiency much less than the theoretical Carnot engine. The Carnot efficiency is

$$\eta_c = 1 - \frac{T_L}{T_H} \quad (1.1)$$

where  $T_L$  is the environmental temperature in degrees absolute, and  $T_H$  is the receiver temperature in degrees absolute (15). Behind the engine must come some device such as a pump, generator, or other apparatus. A schematic of such an arrangement is shown in Figure 1-1.

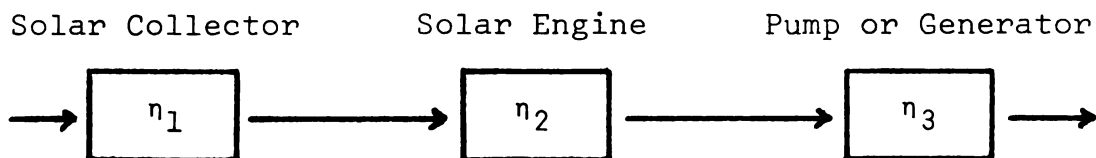


FIGURE 1-1. Solar Engine System

$\eta_1$ ,  $\eta_2$ , and  $\eta_3$  represent efficiency of each component. The efficiency of the total system is:

$$\eta = \eta_1 \eta_2 \eta_3 \dots \eta_n \quad (1.2)$$

The overall efficiency is the product of the efficiencies of the various components. Low combined efficiency will, in general, increase the cost per unit of energy output for a solar engine. Solar energy is free, but the equipment to convert the radiation to work is not free. Capital equipment will depreciate, and the value of the energy captured must be used to recover the depreciated capital. Chapter Five is devoted to the economics of solar engines, but to understand the significance of the historical development, the low overall efficiency must be considered a deterrent to development.

The research objectives of solar engine developers must be to develop low-cost, reliable and efficient engines. The overall low efficiency and complicated designs have contributed to the slow development of solar engines. John Ericsson, the famous developer of an engine by his name, summarized the problem in 1878. He wrote, "that although the heat is obtained for nothing, so expensive, costly, and complex is the concentration apparatus, that solar steam is many times more costly than steam produced by burning coal" (3).



## 1.2 Early French Solar Engines

Some of the earliest known solar engines came from the French. In 1615, Solomon de Caux pumped water by heating air from the sun. This is the first known solar machine developed for such a purpose. Little is known about the performance. August Mouchot, 1866-72, used a truncated cone with four square meters of surface to concentrate the sun's rays on a water boiler. The copper boiler developed a pressure of 517 kPa (75 lb/in<sup>2</sup>) and 140°C. (284°F.). The boiler initially powered a reciprocating steam engine that moved slowly at 80 rpm. Later, the reciprocating engine was replaced with a rotary engine which powered a pump. In 1878, Mouchot developed a water distiller. Two identical water distillers were tested at Constantine and Montpellier, France. The tests resulted in an efficiency of 49% which were witnessed by two appointed commissioners. Mouchot received support from Napoleon and several steam driven solar plants were constructed, but the French government eventually abandoned their support. It was concluded that the engine was too expensive and other alternatives seemed more appropriate (2).

Another Frenchman, M. Abel Pifre, in 1880, developed a steam-powered engine to run a printing press and a rotary pump, which is shown in Figure 1-3. Pifre used a parabolic collector with a 100 square foot radiator intercept (11.333 ft. diameter). The output was a .065 hp. The overall efficiency from this data would be a meager 0.54%. The

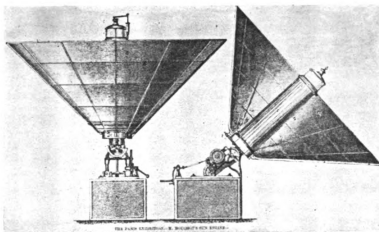


FIGURE 1-2. Mouchot's Engine.

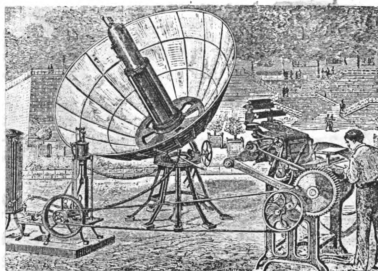


FIGURE 1-3. Pifre's Sun-Power Plant of 1878 Driving a Printing Press.

boiler chamber was at the focal point with an 11 gallon capacity (1).

C.L.A. Tellier, five years later (1885), used ammonia to power a small vertical engine. The system did not use a solar concentrator, but instead employed a simple flat plate collector. The flat plate collector was 215 square feet in size. The boiler charged with ammonium hydrate produced ammonia when heated. The boiler was constructed of segmented components that were 3.5 x 1.12 meters in dimension (1).

A solar furnace used by Lavoisier in 1774 is shown in Figure 1-4.

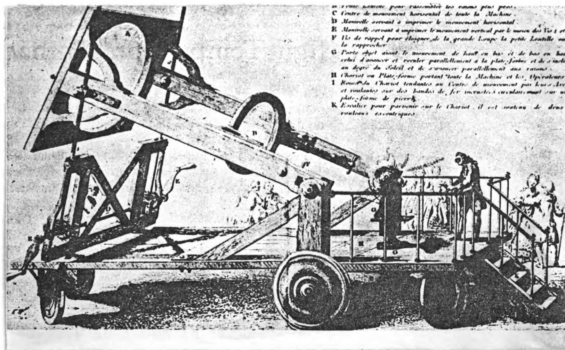


FIGURE 1-4. Solar Furnace Used by Lavoisier, 1774.

The French today are continuing their thrust into solar research. Perhaps the earlier uncoordinated efforts by their countrymen have set the stage for continued interest in the subject and eventual "break-throughs" in solar furnaces and engine technology will certainly result.

### 1.3 Ericsson's Sun Motor

An old adage -- "Nothing ventured, nothing gained" -- could certainly have been John Ericsson's motto. Many historians would view his life as a series of failures dotted with an occasional success. One historian of technology stated "With each failure, Ericsson gained more notoriety and was able to find more investors for his next project" (32). The truth of the matter is that John Ericsson was a courageous genius.

Ericsson left his native Sweden in 1826 and moved to England. He soon developed new pumps and made improvements on steam engines while a junior partner with John Braithwaite, a mechanical constructor. With only two months notice, Ericsson prepared an entry in a steam locomotive race. The winner of the race would become the father of steam railroads. He created the Novelty which easily outdistanced the competition. On the second day, minor problems (steam leaks) put Ericsson out of the race. The Novelty is shown in Figure 1-5 (3).

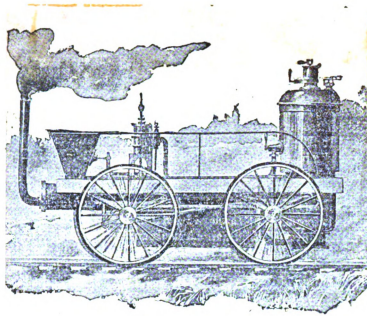


FIGURE 1-5. The Novelty Locomotive by Ericsson to Compete with Stephenson's Rocket, 1929.

By 1830 Ericsson had invented the screw propeller, fire engine and wrought iron cannon, but at that time, he could not find investors. He had also invented the hot air engine. Many of his inventions were before their times. It was in 1849 that Joules established the mechanical equivalent of heat. Joules discovered that one BTU was equivalent to 778 foot-pounds of work. Also, heat was explained with the caloric theory. In other words, thermodynamics was in its infancy. In those days, few could understand Ericsson's hot air engine or caloric engine. The caloric engine is shown in Figure 1-6 (3).

Professor Michael Faraday did not accept the condemnation of Ericsson by the leading scientific community of that day. The general opinion was that Ericsson's engine was

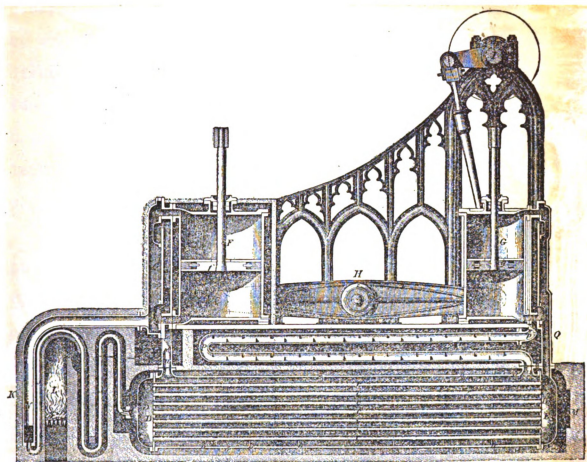


FIGURE 1-6. Ericsson's Caloric Engine.

based on unsound scientific principles. A large audience attended the Royal Institution in London to hear Faraday supposedly explain and support the engine. Ericsson was disappointed when Professor Faraday opened the lecture by stating he did not know how the engine worked and would direct his lecture to how the regenerative apparatus functioned. The theoreticians of 1833 could not accept Ericsson's theories and claims as sound, yet because of a lack of understanding in thermodynamics, they could not explain their skepticism.

Ericsson attracted attention when he published his paper on a solar motor. In his paper, he said "Adverting to the insignificance of the dynamic energy which the entire exhaustion of our coal fields would produce, compared with the incalculable amount of force at our command, if we avail ourselves of the concentrated heat of the solar rays. Already Englishmen have estimated the near approach of the time when the supply of coal will end, although their mines, so to speak, have just been opened. A couple of thousand years dropped in the ocean of time will completely exhaust the coal fields of Europe, unless, in the meantime, the heat of the sun be employed." It seems John Ericsson could foresee the energy crisis coming at the beginning of the fossil fuel age (3).

Ericsson ran experiments that showed he could evaporate 489 cubic inches of water per hour with a collecting surface of 100 square feet, which he stated would be over one

horsepower (3). By assuming 300 BTU/hour with a collector efficiency of 70%, the engine efficiency would be twelve per cent. The efficiency is calculated by converting one horsepower to BTU/hr by multiplying by 2545 BTU/hr-hp and dividing by the collector area, the insolation (solar radiation) and the collector efficiency.

$$\eta = \frac{1 \text{ hp} \times 2545 \text{ BTU/hr hp}}{100 \text{ ft}^2 \times 300 \text{ BTU/hr ft}^2 \times .70} = .12$$

The Ericsson sun power plant shown in Figure 1-7 must have been approximately 12% efficient. The engine which had a six inch diameter piston with an eight inch stroke was driven with steam. The engine operated a five inch diameter pump. The engine could also operate a mill running off the flywheel. The average speed was 120 rpm with 35 psia pressure on the piston. There was a steam condenser in a closed system. Therefore, the engine of Figure 1-7 was probably a basic rankine cycle.

#### 1.4 Other Solar Engines

In 1876, W. Adams ran a steam engine from the sun in Bombay, India with a 40 foot diameter hemispherical collector formed from many 10 inch by 17 inch plane mirrors. The water boiler ran a 2.5 hp steam pump (1). Calculating the overall efficiency assuming 310 BTU/ft<sup>2</sup>hr and 70% collector efficiency:

$$\eta = \frac{2.5 \times 100 \times 2545}{310 \times \frac{\pi}{4}(40)^2 \times .70}$$

$$\eta = 2.3\%$$



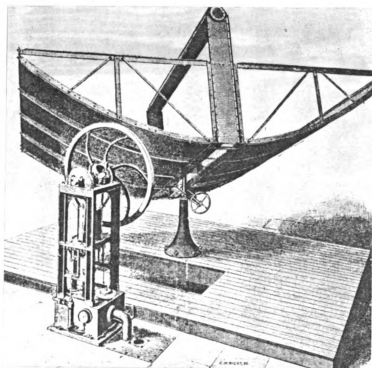


FIGURE 1-7. Ericsson's Solar Engine.

A.G. Eneas in 1901 in Pasadena, California, developed a truncated cone with 642 square feet area that had a stated collector efficiency of 74.6%. In 1903, in Mesa, Arizona, with a 700 square foot collector, he claimed 73.3% efficiency. Later in 1904, in Wilcox, Arizona, another truncated 700 square foot cone had a supposed efficiency of 79.6% (1). Engines were used with Eneas' system, but they were not loaded during tests.

The Pasadena solar engine by an unnamed group called the "Party of Boston Inventors" is shown in Figure 1-8 (2). The design and erection was done by this "Party of Boston Inventors". It was a truncated cone 33.5 feet in diameter at one end and 15 feet at the other end. The boiler was 13.5 feet long with a 100 gallon water capacity with 8 cubic feet

of vapor space. The engine pumped water. The rated output was about 4.25 hp. The overall efficiency would be approximately:

$$\eta = \frac{4.25 \times 100 \times 2545}{300 \times .70 \times \frac{\pi}{4} \left( (33.5)^2 - 15^2 \right)}$$

$$\eta = 7.3\%$$

The concentration ratio (area of aperture to receiver area) appeared to have been 13.4. The plant required 150 square feet of radiation per horsepower.

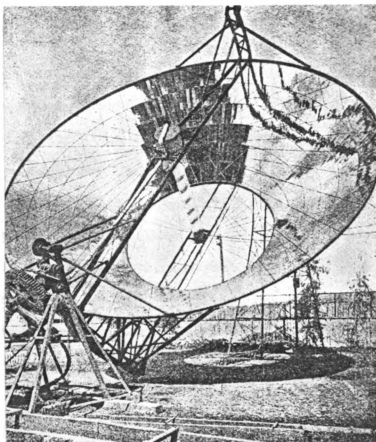


FIGURE 1-8. Pasadena Sun Heat Absorber of 1901.

In 1902 in Olney, Illinois, H.E. Willsie and John Boyle, Jr. used a shallow wooden tank covered with two glass windows (2). The sides and bottom were double walls stuffed with hay. This flat plate collector had three inches of water. The bottom of the wood tank was covered with tarpaper that was well pitched. The flat plate collector efficiency was approximately 50%. Later renditions of this collector supposedly reached 85% efficiency but was impossible due to an error on the amount of insolation hitting the collector. The flat plate design heated water which transferred its energy to sulphur dioxide which in turn ran an engine. From the results, the probable overall efficiency would be:

$$\eta = \frac{6 \times 100 \times 2545}{600 \times 300 \times .50}$$

$$\eta = 16.96\%$$

The glass area was 600 ft<sup>2</sup> and the engine produced 6 hp. In 1905, a similar type of system ran a 20 horsepower slide-valve engine.

In 1908, the Willsie and Boyle design with 1000 ft<sup>2</sup> of collector developed 15 horsepower (2). The efficiency of this system was:

$$\eta = \frac{15 \times 100 \times 2545}{1000 \times 300 \times .50}$$

$$\eta = 25\%$$

These figures should be questioned or the design resurrected and used.

In 1907 in Tacony, Pennsylvania, Frank Shuman had a 3.5 horsepower solar engine operating from 1200 square feet of glass (2). This was essentially a flat plate collector heating ether which vaporized and ran a small vertical engine. The ether left the engine and went into an air to ether condenser before being recirculated to the solar collector. This efficiency would be:

$$\eta = \frac{3.5 \times 100 \times 2545}{300 \times .50 \times 1200}$$

$$\eta = 4.94\%$$

In 1911, Shuman added tilted sides to act as a concentrator to the flat plate system described above (1).

In 1912, seven miles south of Cairo, the Shuman-Boys absorber was constructed (1). The distinguished physicist, C.V. Boys, along with consulting engineers Ackermann and Walrond, joined their efforts with Shuman's blessings to build the plant pictured in Figures 1-9 and 1-10.

The collector area was 13,269 square feet. The boiler was at the focal point of the parabolic collector. A single glass cover enclosed the boiler. The boiler was 205 feet long with a 4 1/2 to 1 concentration of solar radiation. The solar collector efficiency was 40.1%. It took 183 square feet of collector to produce one brake horsepower. This 13,269 square foot collector produced 55.5 bhp. The collector followed the east-west motion of the sun, and it was reported that the output did not drop much in the morning or evening. The efficiency by calculation would be

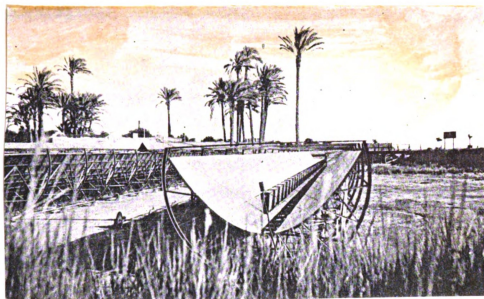


FIGURE 1-9. Shuman-Boys System Meadi, 1913.

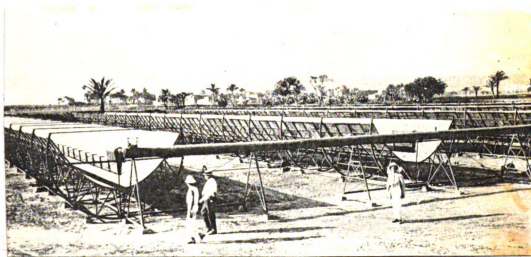


FIGURE 1-10. Shuman-Boys System Meadi, 1913.

approximately:

$$\eta = \frac{55.5 \times 100 \times 2545}{13,269 \times 310 \times .40}$$

$$\eta = 8.6\%$$

The collector efficiency has been published as 40%.

C.G. Abbott, in 1936, used a parabolic trough to produce 1/2 hp. In Florida, another system was constructed using a parabolic trough with 60% efficiency. The solar engine was 1/5 hp. Water was the working medium (2).

Frederico Molero, a Russian, in 1941-46 used a 33 foot diameter tracking parabolic collector. No load was used, but it was claimed that steam could be produced at all temperatures and pressures (2).

M.L. Ghai and M.L. Khanna, 1950-1955, used a parabolic collector with air to produce 1/8 to 1/6 hp. Temperatures of 700 degrees to 1200 degrees F. were obtained. M.L. Khanna used a parabolic flat mirror collector to operate an open cycle hot air engine. Chai and Khanna have experimented in New Delhi, India with small open cycle piston engines. These engines are essentially Ericsson engines (2).

### 1.5 Stirling Engine

Ericsson's engine was an open cycle engine. Air is pulled into the heating zone and when heated, expands and does work. This air is then dumped into the atmosphere. Ericsson used two 330 hp engines of this type to drive a 2000-ton paddle wheel ship (3).

The Stirling engine developed by Robert Stirling was first built in 1827. This engine is a closed system. The operation is shown in Figure 1-11 (15).

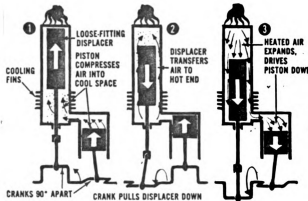


FIGURE 1-11. Stirling Engine.

The work piston in Figure 1-11 is the short piston. The displacement piston is the long, loosely fitting piston. The work piston in position one (left-hand figure) is pushing upward forcing the gas into the cooling area that is finned. The loose fitting displacement piston is at the top of its stroke so that it forced the gas away from the heating section. Heat is rejected and the pressure is reduced. The cycle continues in position two (center figure) of Figure 1-11.

The displacement piston moves downward forcing the gas back up into the hot region. As heat is added, the pressure increases and the work piston moves downward as is shown in position three (right figure) of Figure 1-11.

The Stirling cycle consists of isothermal expansion and compression and a constant volume addition and rejection of heat (15). The theoretical cycle shown in the pressure-volume and temperature-entropy diagram is:

1. 1-2 isothermal addition of heat.
2. 2-3 constant volume rejection of heat. This is accomplished by pushing the heated gas through a regenerator with high heat storing capacity.
3. 3-4 isothermal rejection of heat.
4. 4-1 constant volume addition of heat. This is done by passing the cooled gas through the hot regenerator which adds energy back into the system.

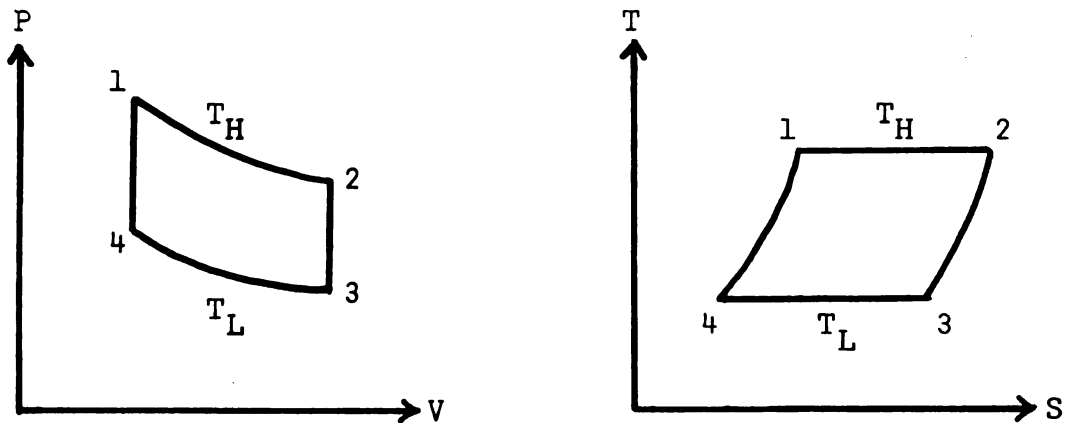


FIGURE 1-12. Stirling Cycle for a Gaseous Substance.

In actual working models, regenerators have been added. In Figure 1-13, the regenerators are shown. The displacement piston is on top of the work piston. The regenerator absorbs and stores the heat from the working medium. The displacement piston moves the gas through the connecting



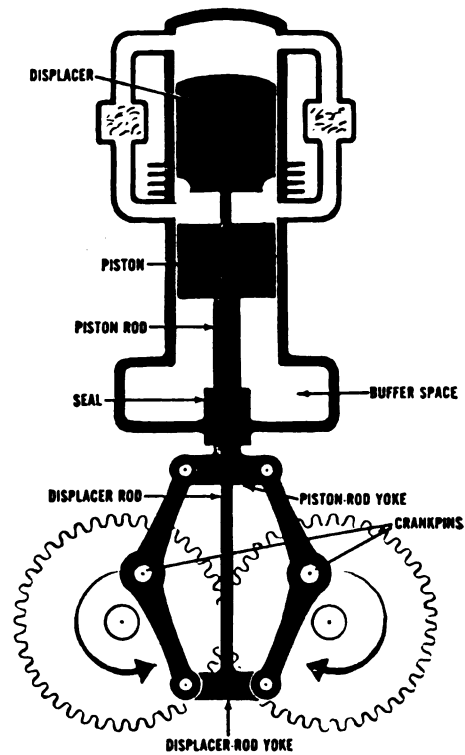


FIGURE 1-13. Stirling Engine with Regenerators.

tubes and into the regenerator.

Much less heat is rejected in this fashion and the efficiency is thereby increased.

In 1926, Stirling applied for a patent for an air engine representing what is known as the regenerative principle. Ericsson opposed this application. Ericsson evidently questioned the originality of the Rev. Dr. Robert Stirling. There is some overlapping of ideas between Stirling and Ericsson. Stirling had gotten his idea from "Jeffrey Respirators" used for T.B. patients. Ericsson's efforts were in vain. Stirling was granted a patent the following year. However, Ericsson was granted a patent on a regenerator later in 1833 (3).

#### 1.6 Patent Search of Solar Devices

Not everything that is patented is functional or practical. Some claims may defy the laws of nature. However, no review of solar engines would be complete without a current search of inventions. In Table 1-1 is a list of patents related to the subject.

The White radiation turbine, the first patent, shown in Figure 1-14 is an air turbine located at the focal point of a truncated cone collector.

TABLE 1-1. Patent Search on Solar Engines (31)

<u>Patent Number</u>	<u>Inventor(s)</u>	<u>Date</u>
3 031 852	W.W. White	May 1, 1962
3 157 024	R.J. McCrory, et al	Nov. 17, 1964
3 451 342	E.H. Schwartzman	June 24, 1969
3 491 554	E.G.U. Granryd	Jan. 27, 1970
3 495 402	J.W. Yates	Feb. 17, 1970
3 696 626	A. Daniels	Oct. 10, 1972
3 698 182	S. Knoos	Oct. 17, 1972
3 811 283	R. Hartmann, et al	May 21, 1974
3 916 626	G.O. Schur	Nov. 4, 1975
3 958 422	D.A. Kelly	May 25, 1976
3 965 683	S. Dix	June 29, 1976
4 002 031	R.L. Bell	_____
4 004 421	K.W. Cowans	Jan. 25, 1977
4 006 594	P.R. Horton	Feb. 8, 1977
4 010 614	D.M. Arthur	March 8, 1977
4 031 702	J.T. Burnett, et al	June 28, 1977
4 033 118	W.R. Powell	July 5, 1977
4 033 126	E.L. Newland	July 5, 1977
4 033 134	A.P. Bentley	July 5, 1977
4 041 705	A. Siegel	Aug. 16, 1977
4 041 707	D. Spector	Aug. 16, 1977
4 044 559	D.A. Kelley	Aug. 30, 1977
4 047 385	H.J. Brinjevec	Sept. 13, 1977

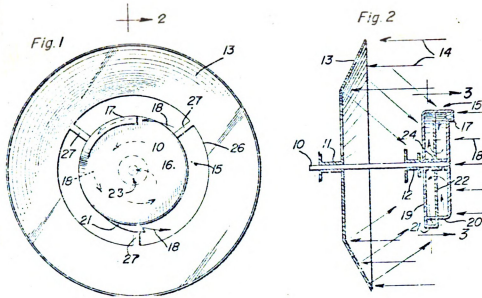


FIGURE 1-14. W.W. White Radiation Turbine.

The side 19 is transparent. Air enters at 17 and leaves at 18 (31). There are some unique features, but the performance is questionable.

Another turbine type invention is shown in Figure 1-15. Elwood Newland has a patent on an air turbine operating from a flat plate collector. The Newland device would probably have a low efficiency and would perhaps be used in connection with heating. The inventor was sensitive to cost effectiveness in the claims of the patent (31).

The inventions of Figures 1-14 and 1-15 are attempting to move air with the sun and then extract energy with an engine (31). In the earth's atmosphere, winds are formed by the same solar process. These inventions would have to compete effectively with windmills.

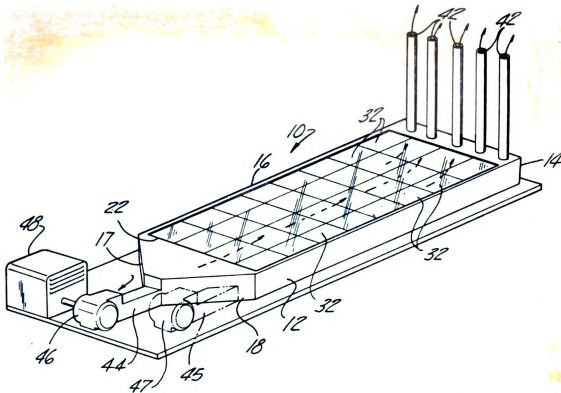


FIGURE 1-15. Newland Solar Energy Device.  
Patent No. 4 033 126.

Another class of inventions would be based on the thermal expansion of metal when heated. Such a device is shown in Figure 1-16 by Peoples and Kearns of the Marshall Space Flight Center in Alabama. Sun hitting the aluminum rod would cause thermal expansion. Work can be extracted from the motion.

Patent No. 4 006 594 by Paul Horton uses a complex system based on the heating and cooling of members to produce rotation. Two wheels at an angle to each other have connecting bars alternately heated and cooled, which supposedly produced motion. The device is pictured in Figure 1-17.

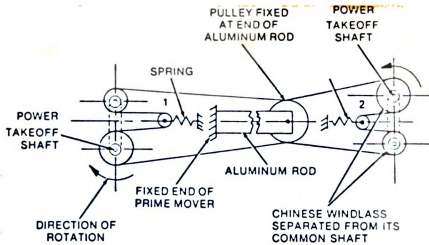


FIGURE 1-16. Solar Engine Based on Thermal Expansion.

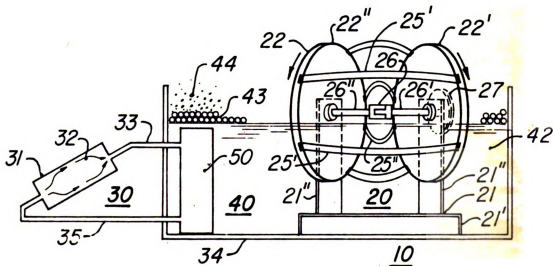


FIGURE 1-17. Horton Solar Power Plant.

A heat engine using air is presented in Figure 1-18. The engine by Arthur Bentley was designed to be heated by the sun (31).

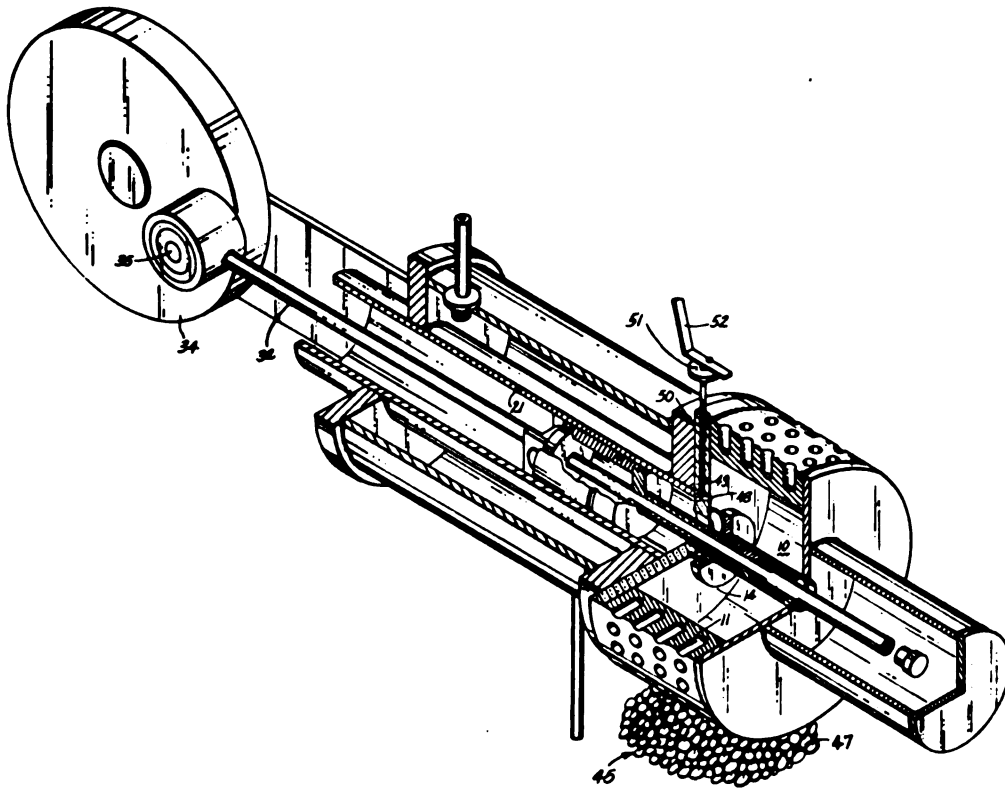


FIGURE 1-18. Bentley's Heat Engine.  
Patent No. 4 033 134.

Another novel idea connected with producing power using the traditional Rankine Cycle engine is given in Figure 1-19. In Bell's arrangement, photovoltaic cells using gallium arsenide convert light to direct current electricity. The waste heat from the cell area produces power from a Rankine Cycle engine (31).

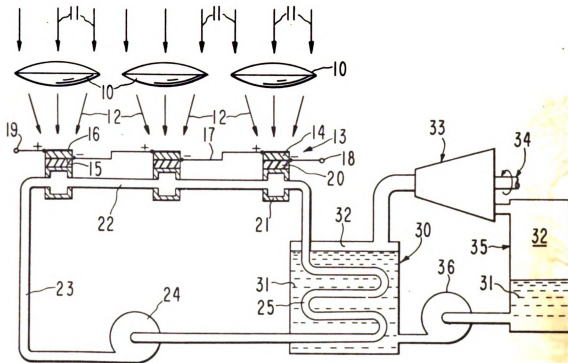


FIGURE 1-19. Bell's Solar Energy Converter with Waste Engine.  
Patent No. 4 002 031.



### 1.7 Summary

It is technically possible to produce mechanical power from the sun. There have been many workable engines. Table 1-2 gives a chronological order of developers.

TABLE 1-2. Solar Engine Developers

<u>Name</u>	<u>Date of First Solar Work</u>
Solomon de Caux (France)	1615
H.B. de Saussure (Sweden)	1766
Sir John Herschel (England)	1836
C.S.M. Pouillet (France)	1838
C.L. Althaus (Germany)	1853
Carl Giinter (Austria)	1854
August Mouchot (France)	1860
John Ericsson (U.S.A.)	1864
C.H. Pope (U.S.A.)	1875
William Adams (England)	1876
Abel Pifre (France)	1878
S.P. Langley (U.S.A.)	1881
J. Harding (England)	1883
Chas. Louis Abel Tellier (France)	1884
A.G. Eneas (U.S.A.)	1900
H.E. Willsie (U.S.A.)	1902
C.G. Abbott (U.S.A.)	1905
Frank Shuman	1906
Charles Fery (France)	1906
G. Millochau (France)	1906
Frederico Molero (Russia)	1941
M.L. Ghai (India)	1950
M.L. Khanna (India)	1950

There has been little systematic development of solar machines. Past developers have been accused of ignoring economic considerations so that the solar engine systems of the past were not cost-effective. Perhaps economics had always been a consideration of the early inventors. These inventors were pioneers and were enthusiastic about free solar power and probably realized that equipment depreciates. Fossil fuels were abundant and cheap. The demise of each

product, that was a technological success, was a result of the solar engines inability to compete with fossil fuel engines. With increasing difficulty in obtaining cheap fossil fuel, solar engines will continue to become more competitive. If the design of solar engines is approached with the proper economic perspective, then cost effective designs will result.

From the data of these historic engines, a level of expectation can be established. The areas (collector efficiency, engine efficiency, power output and collector area / one brake horsepower) are given in Table 1-3.

Table 1-3 gives an excellent guide to use in feasibility studies. Shuman and Boys, in the author's opinion, conducted reliable experiments. One of the problems of determining overall efficiency is the problem in determining the solar insolation. Many of the investigators had no way of being certain about the quantity of sunlight striking their collectors. However, the determination of horsepower is easily done, and the best information can be obtained in the value of collector area per one brake horsepower. It will be assumed that these solar enthusiasts published only the best results which would be recorded at solar noon on a clear day. It would also appear that:

1.  $100 \text{ ft}^2/\text{lbhp}$  is a goal that will be somewhat challenging to reach. (Willsie, Boyle and Ericsson claimed to have reached this.)
2.  $150 \text{ ft}^2/\text{lbhp}$  should be an easily obtainable figure with modern systems.

TABLE 1-3. Past Performances of Solar Engines and Collectors

INVESTIGATOR & DATE	COLLECTOR & SIZE	COLLECTOR EFFICIENCY	OUTPUT bhp	AREA bhp	ENGINE EFF.
Mouchot (1878)	5.22 m <sup>2</sup> Truncated Cone	49%			
Ericsson (1868- 1870)	Parabolic trough in series	72%			
Ericsson	Parabolic trough 16" x 11'		1 bhp	$\frac{100 \text{ ft}^2}{1 \text{ bhp}}$	12%
Adams (1876)	Hemisphere 40 ft. dia.	70%	2.5 bhp	$\frac{503}{1 \text{ bhp}}$	2.3%
Pifre (1880)	Parabolic		.065 bhp	$\frac{1538}{1 \text{ bhp}}$	0.54%
Eneas (1901)	Truncated Cone <sub>2</sub> 642 ft <sup>2</sup>	74.6%			
Eneas (1903)	Truncated Cone <sub>2</sub> 700 ft <sup>2</sup>	73.3%			
South Pasadena Ostrich Farm (1901)	Truncated Cone 33'6" major diameter. 15' minor diameter.		Claimed 10 hp Probable 4.25 hp	$\frac{166 \text{ ft}^2}{1 \text{ bhp}}$	7.32%
Willsie (1902)	Flat Plate Double glass	50%			
Willsie Boyle (1904)	Flat Plate 600 ft <sup>2</sup>	85%	6 hp	$\frac{100}{1 \text{ bhp}}$	12%
Shuman (1907)	Flat Plate 1200 ft <sup>2</sup>	50%	3.5 hp	$\frac{100}{1 \text{ bhp}}$	5%
Willsie Boyle (1908)	Double glass Flat Plate 1000 ft <sup>2</sup>	50%	15 hp	$\frac{343 \text{ ft}^2}{1 \text{ bhp}}$	25%

TABLE 1-3 (Cont'd)

INVESTIGATOR & DATE	COLLECTOR & SIZE	COLLECTOR EFFICIENCY	OUTPUT bhp	AREA bhp	ENGINE EFF.
Shuman (1911)	Trough with sides 10,296 ft <sup>2</sup>	30%		$\frac{245}{1 \text{ bhp}}$	
Shuman- Boys (1913)	Parabolic Tracked East-West 13,269	40.1%	55.5 bhp 63 max 52.4 min	$\frac{183}{1 \text{ bhp}}$	8.6%
C.G. Abbott (1936)	Parabolic Trough		1/2 hp		

The apparent engine efficiency from history range from 1/2% to 25%. The average engine efficiency would be 10%. For example, if a parabolic concentrator has 70% efficiency and the solar engine has 12% efficiency, the overall efficiency is:

$$\eta = .12 \times .70 = .084 = 8.4\%$$

Calculating the overall efficiency of an engine with a 100 ft<sup>2</sup>/lbhp ratio:

$$\frac{1 \text{ bhp} \times 100 \times 2545}{100 \times 300} = 8.5\%$$

The 300 BTU is the assumed average solar insolation per hr ft<sup>2</sup> at solar noon. From the example, it takes a 70% efficient collector coupled to a 12% efficient engine to equal a 100 ft<sup>2</sup>/lbhp efficiency ratio. For economic

feasibility studies, 10% efficiency overall seems possible if the assumption is made that past systems can be duplicated with minor improvements.

### 1.8 Objectives

There has been a need demonstrated for such research. The author received numerous letters from researchers in the third world countries asking for more information in response to a paper published at the Second World Hydrogen Conference in Zurich (5). The most important application of solar mechanical power is in water pumping applications in developing countries. After searching the literature, and the United States patent office, it became obvious that solar engine technology needs additional research efforts. Solar engine development appears to be a near virgin research area with immediate applications.

The objectives of the research were to:

1. Establish from the literature an expected level of performance.
2. Make economic judgments as to the feasibility of solar mechanical power.
3. Assemble the necessary theoretical tools to help produce a solar engine.
4. Build and analyze a demonstration model.

## CHAPTER 2

### SOLAR INSOLATION

#### 2.1 Solar Constant and Surface Insolation

Solar insolation is the energy per unit area per unit time that hits a specified location. This value is essentially a constant in outer space. The distance between the sun and earth varies with the seasons, and there is some minor variation of the solar constant (solar radiation in space). The present accepted value is  $1353 \text{ watts/m}^2$ , but variation ranges from  $1390$  to  $1310 \text{ watts/m}^2$  (6). However, the energy that reaches the earth's surface is significantly different. Shown in Figure 2-1 is the solar insolation versus time at the  $40^\circ$  North Latitude on February 21 (10).

The total area under this curve (Figure 2-1) would represent the daily normal solar insolation, and it equals  $29,981 \text{ kJ/m}^2 \text{ day}$  ( $2,640 \text{ BTU/ft}^2 \text{ day}$ ). For most practical applications, the solar insolation can be read from the ASHRAE tables included in the appendix. A sample has been included and is presented in Figure 2-2.

Radiation received at the earth's surface is attenuated by atmospheric scattering and absorption. The sun-earth distance varies, and the air mass is constantly changing. These factors must be considered if a mathematical model is to be developed for the surface insolation.

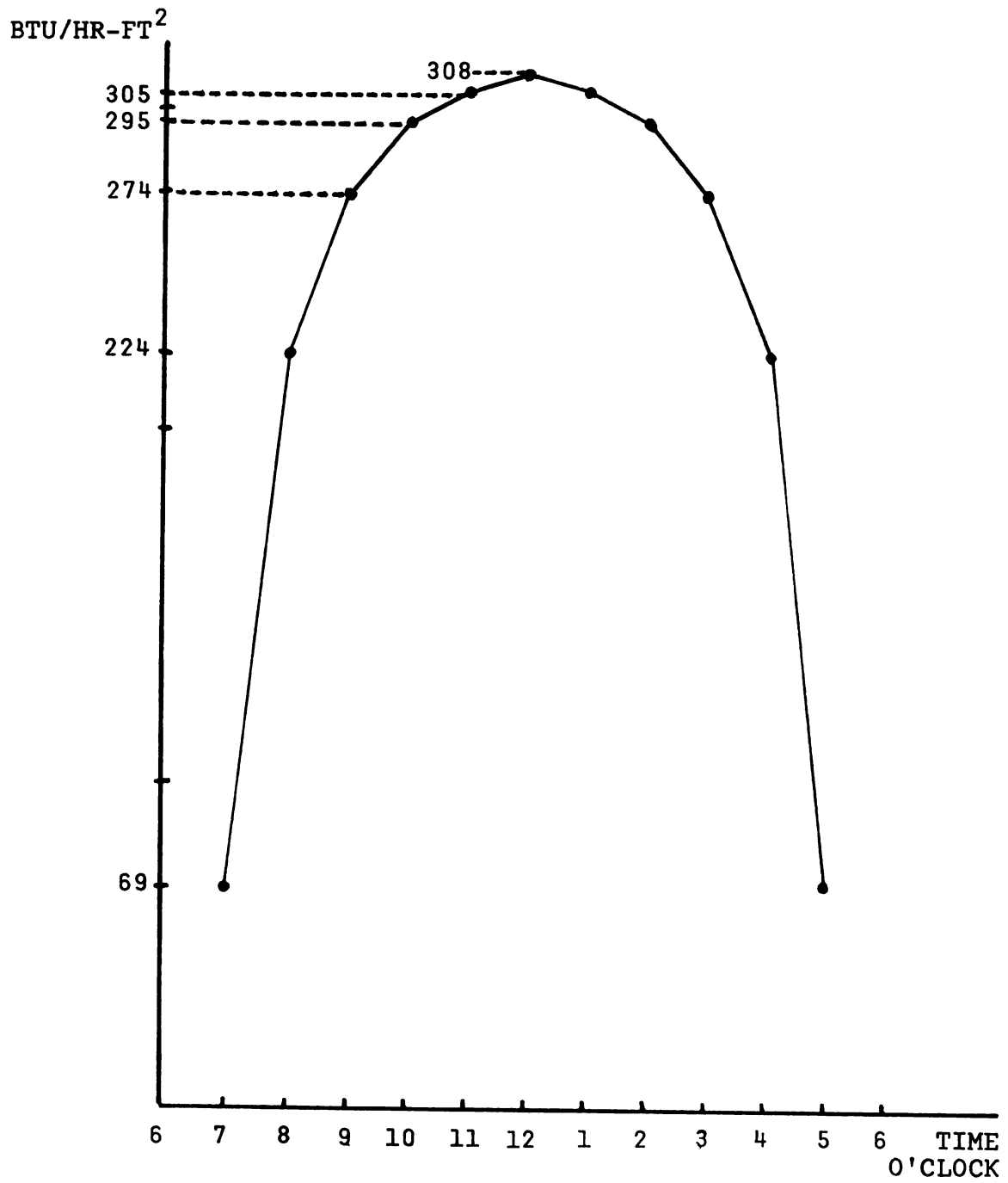


FIGURE 2-1.

Solar Insolation 40° North Latitude - February 21.

SOLAR POSITION AND INSOLATION, 40°N LATITUDE

DATE	SOLAR TIME		SOLAR POSITION		BTUH/SQ. FT.		TOTAL INSOLATION ON SURFACES					
	AM	PM	ALT	AZM	NORMAL	HORIZ.	SOUTH FACING SURFACE ANGLE WITH HORIZ.					
JAN 21	8	4	8.1	55.3	142	28	65	74	81	85	84	
	9	3	16.8	44.0	239	83	155	171	182	187	171	
	10	2	23.8	30.9	274	127	218	237	249	254	223	
	11	1	28.4	16.0	289	154	257	277	290	293	253	
	12		30.0	0.0	294	164	270	291	303	306	263	
SURFACE DAILY TOTALS					2182	948	1660	1810	1906	1944	1726	
FEB 21	7	5	4.8	72.7	69	10	19	21	23	24	22	
	8	4	15.4	62.2	224	73	114	122	126	127	107	
	9	3	25.0	50.2	274	132	195	205	209	208	167	
	10	2	32.8	35.9	295	178	256	267	271	267	210	
	11	1	38.1	18.9	305	206	293	306	310	304	236	
SURFACE DAILY TOTALS					308	216	306	319	323	317	245	
MAR 21	7	5	11.4	80.2	171	46	55	55	54	51	35	
	8	4	27.5	69.6	250	114	140	141	138	131	89	
	9	3	32.8	57.3	282	173	215	217	213	202	138	
	10	2	41.6	41.9	297	218	273	276	271	258	176	
	11	1	47.7	22.6	305	247	310	313	307	293	200	
SURFACE DAILY TOTALS					307	257	322	326	320	305	208	
SURFACE DAILY TOTALS					2916	1852	2308	2330	2284	2174	1484	

FIGURE 2-2. ASHRAE Tables.

## 2.2 Transmittance of Solar Radiation through the Air Mass

Radiation is equally absorbed or scattered in the earth's air envelope. Dust, air molecules, and water vapor attenuate the sun's energy. The amount of attenuation depends upon the mass of air the radiation must pass through. The quantity of air between the surface of the earth and the sun varies with time and terrestrial location. This amount of air is directly proportional to the air mass index. The air mass is defined as (6)

$$m = \frac{1}{\cos \theta_z} \quad (2.1)$$

where  $m$  is the air mass ratio and  $\theta_z$  is the angle between the zenith (perpendicular to the earth's surface) and the sun's rays.

If the sun is directly overhead, the  $\cos \theta_z$  is one and  $m$  equals one. If the sun is  $60^\circ$  from the zenith, then  $m$



equals two because the  $\cos \theta_z$  is one-half. In other words, the path that the solar radiation must traverse is twice as long at  $\theta_z = 60^\circ$  as it is at  $\theta_z = 0^\circ$ . The intensity of the radiation at the surface varies according to the zenith angle  $\theta_z$ . A sunset can be observed with the naked eye because the path length of radiation through the atmosphere is long as compared with path length when the sun is directly overhead.

There are two types of radiation received at the earth's surface. Beam radiation is the solar radiation that is received from the sun without direction change. This is the radiation that enters the earth's atmosphere. Diffuse radiation is the solar radiation after its direction is altered. The reflecting and scattering of the beam radiation by the atmosphere produces diffuse radiation. Flat plate collectors can use diffuse radiation, but solar collectors that concentrate the rays, generally, cannot utilize this small component.

As can be seen from the previous discussion on the air mass, the longer the path through the atmosphere, the greater is the attenuation of the terrestrial insolation. Using Bouger's law equation (9)

$$I_b = I_o e^{-km} \quad (2.2)$$

where  $I_b$  is the terrestrial insolation of beam radiation,  $I_o$  is the solar constant, "m" is the air mass, and "k" is a constant that represents the absorption constant. If m were

zero in (2.2),

$$I_b = I_o$$

and  $I_b$  would equal the extraterrestrial radiation, which is the solar constant.

The definition of the average atmosphere transmittance,  $\tau_{atm}$ , is the ratio of the radiation received on the collector to the solar constant

$$\tau_{atm} = I_b / I_o \quad (2.3)$$

In Figure 2-3, a schematic representation is given of the quantities involved.

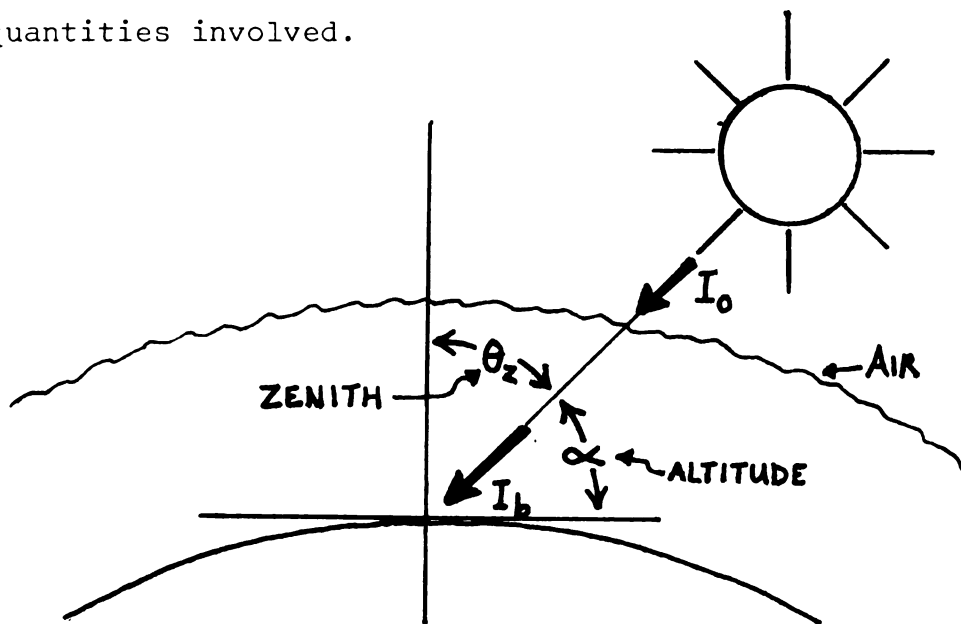


FIGURE 2-3. Air Mass.

$\tau_z$  is the zenith angle,  $\alpha$  is the altitude of the sun,  $\tau_{atm}$  can be found using (2.4) for clear and dry air.

$$\tau_{\text{atm}} = \frac{e^{-.095 m(z)} + e^{-.65 m(z)}}{2} \quad (2.4)$$

where

$$m(z) = \left[ [1229 + (614 \sin \alpha)^2]^{\frac{1}{2}} - 614 \sin \alpha \right] \frac{P(z)}{P(o)} \quad (2.5)$$

and  $P(z)$  equals the atmospheric pressure at elevation  $Z$  feet above sea level,  $P(o)$  is the atmospheric pressure at sea level,  $\alpha$  is the angle of the sun. To approximate  $P(z)$  in Equation 2-5, an aviator's rule of thumb, which states that pressure changes one inch of Hg per 1000 feet of elevation, can be used.

Equation 2.4 does not account for particulates and water vapor. Hottel (8) has developed an equation to correct for non-clear day transmittance.

$$\tau_{\text{atm}} = a_0 + a_1 e^{-k/\cos \theta_z} \quad (2.6)$$

where the constant  $a_0$ ,  $a_1$ , and  $k$  are compiled in table form. Some values are given in Table 2-1.  $a_0$ ,  $a_1$ , and  $k$  are a function of the altitude and visibility.

To illustrate the use of (2.6), for an air mass equal to 1 and 2 at 23 km haze model at sea level is calculated:

$$\begin{aligned} m = 1 \quad \tau &= .1283 + .7559e^{-.3878(1)} \\ \tau &= .64 \\ m = 2 \quad \tau &= .1283 + .7559e^{-.3878(2)} \\ \tau &= .48 \end{aligned}$$

TABLE 2-1. Coefficients of  $a_0$ ,  $a_1$ , and  $k$ 

	Altitude above sea level (km)					
	0	0.5	1	1.5	2	(2.5) <sup>b</sup>
23 km haze model Visibility						
$a_0$	0.1283	0.1742	0.2195	0.2582	0.2915	(0.320)
$a_1$	0.7559	0.7214	0.6848	0.6532	0.6265	(0.602)
$k$	0.3878	0.3436	0.3139	0.2910	0.2745	(0.268)
5 km haze model Visibility						
$a_0$	0.0270	(0.063)	0.0964	(0.126)	(0.153)	(0.177)
$a_1$	0.8101	(0.804)	0.7978	(0.793)	(0.788)	(0.784)
$k$	0.7552	(0.573)	0.4313	(0.330)	(0.269)	(0.249)

### 2.3 Solar Geometry

The  $I_b$  found in Section 2.2 is the direct normal beam radiation. For tracking solar collectors, the  $I_b$  found from Section 2.2 is sufficient. However, for fixed collectors, another important factor must be considered. The collector does not face the sun at all times, and therefore, the projected normal area will change. As an example, the projected area in Figure 2-4 is:

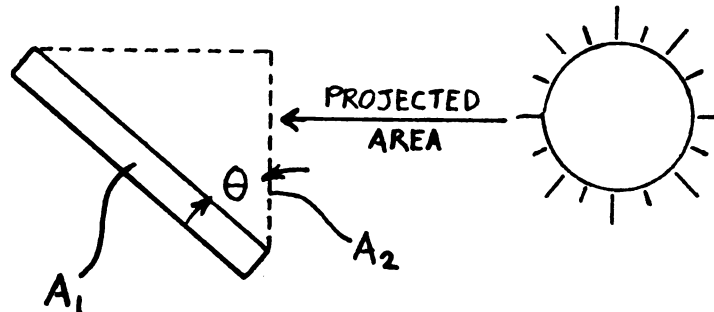


FIGURE 2-4. Projected Area.

$$A_2 = A_1 \cos \theta \quad (2.7)$$

As can be seen in this simple example,  $A_2$  approaches zero as  $\theta$  approaches  $90^\circ$ . ( $\theta$  is measured from the vertical.) It becomes obvious that for fixed collectors, this geometric projection in the path of the beam radiation must be determined.

To calculate the magnitude of the energy incident upon a horizontal surface, four quantities must be evaluated. These quantities are found from equations 2.8, 2.9, and 2.10. The angle of declination is given by

$$\delta = 23.45 \sin \left\{ 360 \left( \frac{284 + n}{365} \right) \right\} \quad (2.8)$$

where  $n$  is the day of the year. The angle of declination,  $\delta$ , is the angle the sun's rays make with the plane of the equator. The equinox is the time of the year when the sun is directly over the equator. At this time, the angle of declination,  $\delta$ , equals zero.

The sunrise hour angle,  $W_s$ , can be calculated from

$$\cos W_s = -\tan \phi \tan \delta \quad (2.9)$$

where  $W_s$  is the sunrise hour angle,  $\phi$  is the latitude with north positive, and  $\delta$  is the angle of declination obtained from (2.8). The hour angle  $W$  is the angle of the sun off the meridian. Solar noon would be zero. Each hour, the hour angle would move  $15^\circ$  with mornings as positive. In Figure 2-5, the hour angle, latitude, and angle of declination are shown.

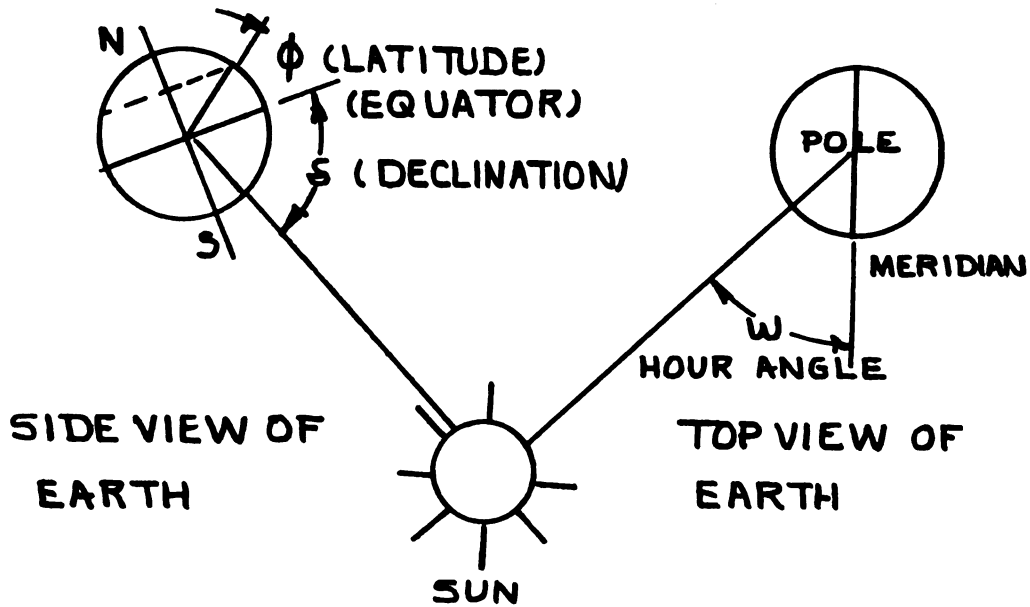


FIGURE 2-5. Angles Defined.

The length of the day,  $N$ , can be found from the equation:

$$N = \frac{2}{15} W_s \quad (2.10)$$

where the units on  $N$  are hours.

The final value needed is the daily extraterrestrial solar energy falling on a horizontal surface in  $\text{kJ/m}^2\text{-day}$

$$H_o = 7.64 I_o \left[ \left[ 1 + .033 \cos\left(\frac{360n}{365}\right) \right] [A + B] \right]$$

$$A = \cos \phi \cos \delta \sin W_s$$

$$B = \frac{2 W_s \pi \sin \phi \sin \delta}{360} \quad (2.11)$$

where  $I_o$  is the solar constant per hour,  $n$  is the day of year from 1 to 365.  $\phi$  is the latitude,  $\delta$  is the angle of declination, and  $W_s$  is the sunshine hour angle.

The average horizontal radiation can be calculated from

$$H_{av} = H_o (a + bx / 100) \quad (2.12)$$

where X is the percentage of sunshine and a and b are values related to meteorological conditions. Values of "a" and "b" for some locations are given in Table 2.2 (12).

To determine the hourly radiation from the daily,  $H_{av}$ , use Figure 2-6 from Liu and Jordan (1963) (7). The total hours from sunrise to sunset is found from (2.10). Reading upward from the total hours to the intersection of the proper "hour from solar noon" line, the ratio of hourly radiations on a horizontal surface to the daily radiation on a horizontal surface from Figure 2.6 will determine the amount of hourly radiation on a horizontal surface.

The values obtained thus far are for horizontal surfaces. To obtain the interterrestrial insolation on a tilted surface, (2.13) is used (6)

$$R_b = \frac{\cos \theta_t}{\cos \theta_z} = \frac{H}{H_{av}} \quad (2.13)$$

where H is the hourly or daily radiation depending on the units of  $H_{av}$  and

$$\cos \theta_t = \cos(\phi - s) \cos \delta \cos W + \sin(\phi - s) \sin \delta$$

and

$$\cos \theta_z = \cos \phi \cos \delta \cos W + \sin \phi \sin \delta$$

All the angles have been previously defined except "S"

TABLE 2-2. Constant for Equation 2-11\*

Location	Average X	a	b
Albuquerque, New Mexico	78	.41	.37
Atlanta, Georgia	59	.38	.26
Blue Hill, Massachusetts	52	.22	.50
Brownsville, Texas	62	.35	.31
Buenos Aires, Argentina	59	.26	.50
Charleston, South Carolina	67	.48	.19
Darien, Manchuria	67	.36	.23
El Paso, Texas	84	.54	.20
Ely, Nevada	77	.54	.18
Hamburg, Germany	36	.22	.57
Honolulu, Hawaii	65	.14	.73
Madison, Wisconsin	58	.30	.34
Malange, Angolia	58	.34	.34
Miami, Florida	65	.42	.22
Nice, France	61	.17	.63
Poona, India	37	.30	.51
(Monsoon Dry)	81	.41	.34
Stanleyville, Congo	48	.28	.39
Tamanrasset, Algeria	83	.30	.43

\* Where  $X = 0$ , the value of "a" would be representative of the diffuse radiation. When  $X = 100$  percent, the value of  $a + b$  would have to equal the atmospheric transmittance.



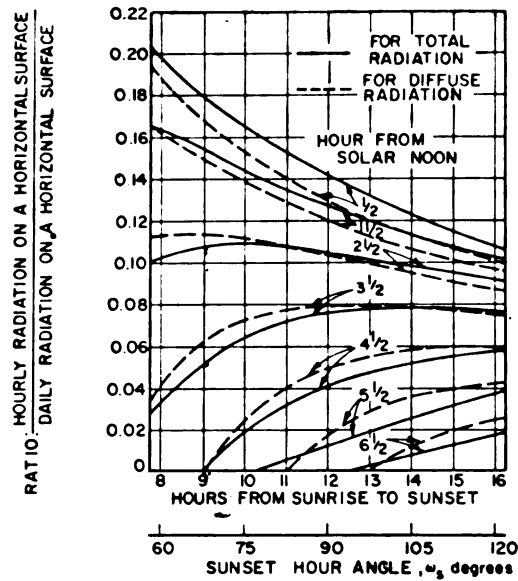


FIGURE 2-6. Hourly Radiation Chart ( 7).

which is the angle of the collector with respect to the ground.  $R_b$  is applicable only to beam radiation. Diffuse radiation is not directional to any extent and will not be as important in concentrating collectors. So the hourly or daily value is obtained from (2.13) where  $H_{av}$  is either the daily or hourly horizontal insolation,  $R_b$  is the factor to correct for orientation.

#### 2.4 Solar Time

Equation 2.14 gives a relationship between solar time and the local time:

$$\text{Solar time} = \text{Standard time} + E + 4(L_s - L_1) \quad (2.14)$$

"E" can be estimated from Table 2-3,  $L_s$  can be found in Table 2-4, and  $L_1$  is the local longitude. It should be noted that the published "E" values vary with time and must be read from current published charts.

TABLE 2-3. Equation of Time "E"

<u>MONTH</u>	<u>MINUTES</u>
January 1	- 5
February 1	- 13
March 1	- 13
April 1	- 5
May 1	+ 3
June 1	+ 3
July 1	- 3
August 1	- 6
September 1	0
October 1	+ 10
November 1	+ 16
December 1	+ 10

TABLE 2-4. Standard Meridian for  
Local Time Zone (6)

<u>ZONE</u>	<u>L<sub>s</sub></u>
Eastern	75° West
Central	90° West
Mountain	105° West
Pacific	120° West

## CHAPTER 3

### SOLAR COLLECTORS

#### 3.1 Introduction

There are two broad categories of solar collectors, concentrators and flat plate collectors. Most of the engines of past times used tracking concentrators. Shuman and Willis-Boyle engines both operated from fixed flat plate collectors. Ether and sulphur dioxide were heated from hot water flowing through a flat plate collector (1). In Table 1.3, the efficiencies for engines using flat plate collectors were, in general, higher than the concentrating type. Some of these quantities should be questioned, but the author has verified what Shuman reported. Shuman, in 1907, had 50% efficiency with a flat plate collector and 40.1% with a parabolic concentrator. The author has had similar results. Earlier investigators may have not known the correct amount of interterrestrial insolation. Published discussions on concentrating collectors expect higher efficiency because of a smaller absorber area. However, radiation losses are very high from non-selective absorber surfaces as can be determined.

It is difficult to look at an operating absorber with the unprotected eye which indicates large radiation losses. The author believes that flat plate collectors and concentrating collectors, under test, will have comparable efficiencies. The re-radiation losses are to the fourth

power of the absolute temperature. Unless special consideration is made in the absorber design, it may be difficult to exceed flat plate collector efficiency.

A design to lower re-radiation is shown in Figure 3-1. This invention by William R. Powell is included in the appendix (31).

Flat plate collectors will be the least expensive of the two types. If actual working models have comparable efficiencies, then the selection of the collector type will be made based on economics and engine efficiency. The concentrators have much higher temperatures. The efficiency of the engine is directly proportional to the peak operating temperature, and, therefore, engines operating from concentrating collectors will have higher efficiencies. This is verified with the Carnot engine principle:

$$\eta_{\text{Carnot}} = 1 - \frac{T_L}{T_H} \quad (3.1)$$

As the temperature,  $T_H$ , approaches infinity, the efficiency would approach 100%. Of course, the concentrator temperatures are limited. The absorber temperature is limited theoretically by the sun's temperature. The second law of thermodynamics would be violated if the absorber temperature exceeded 5,762°K., the average sun temperature. The technological aspect would further limit the absorber temperatures.

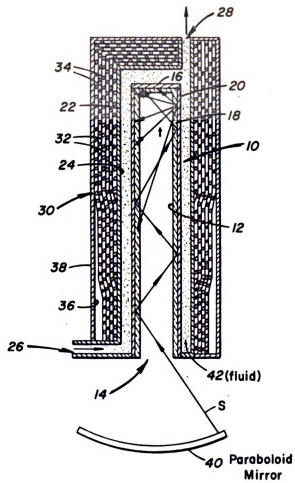


FIGURE 3-1. Patent No. 4 033 118 by Powell. Receiver for Collecting Solar Energy.

### 3.2 Flat Plate Collectors

Flat plate collectors have powered solar engines in the past and their analysis should be discussed. The application of solar engines may initially be centered in warm sunny regions or used in summers for agricultural purposes in colder climates. The treatise will be for single transparent covers which are more efficient than multiple covers in warm climates.

An analysis of flat plate collectors goes as follows. The first law of thermodynamics states that:

Energy in = Energy out + Change in stored energy.

$$E_i = E_o + \Delta E \quad (3.2)$$

In most flat plate collectors, the  $\Delta E$ , stored energy, is negligible. In the flat plate collector analysis, the objective is to analytically measure the energy leaving the system. The first law applied to a collector is (6)

$$E_i = A \left( [H(\tau\alpha)]_b + [H(\tau\alpha)]_d \right) \quad (3.3)$$

$$E_o = \dot{m}(h'_e - h'_i) + U_B A (T_{\text{plate}} - T_{\text{air}}) + U_T A (T_{\text{cover}} - T_{\text{sky}}) \quad (3.4)$$

where

$A$  = transparent cover area in  $m^2$ .

$H_b$  = normal (Equation 2.13) insolation.

$H_d$  = diffuse insolation.

$(\tau\alpha)$  = transmittance-absorptance product.

$\dot{m}$  = mass rate of flow through collector kg/hr.

$h'_e$  = enthalpy of fluid out of collector kJ/kg.

$h'_i$  = enthalpy of fluid into collector kJ/kg.

$U_B$  = the overall heat transfer coefficient out the back.  $kJ/hr\ m^2\ ^\circ C$ .

$U_T$  = the overall heat transfer coefficient out the top cover.  $kJ/hr\ m^2\ ^\circ C$ .

$T_{sky}$  = the temperature of the sky in  $^\circ K$ .

$T_{cover}$  = the temperature of the air in  $^\circ K$ .

The energy that is used to produce work in the solar engine is:

$$E_w = \dot{m}(h'_e - h'_i) \quad (3.5)$$

In a testing situation, (3.5) is obtained by direct measurements. If the collector is an air system, (3.5) becomes

$$E_w = 40.2\ CMM(T_e - T_i) \quad (3.6)$$

where CMM is the volume rate of flow of inlet air in cubic meters per minute.  $T_e$  and  $T_i$  are the respective exit and inlet temperatures. For water systems, (3.6) becomes

$$E_w = 139.4\ LPM(T_e - T_i) \quad (3.7)$$

where LPM is the liters per minute of water flow. The incoming radiation,  $A \left[ (H_b + H_d) \right]$ , can also be measured with a solarometer.

The efficiency could be easily found by direct measurements using (3.9):

$$\eta = \dot{m}(h_e' - h_i') / A(H_b + H_d) \quad (3.9)$$

If the collector system is a new design, then the quantities of (3.3) and (3.4) must be solved, and the numerator of (3.9) would represent the unknown quantity in (3.3) and (3.4). In Figure 3-2 is a small hand-held solarometer useful in measuring the denominator of (3.9).

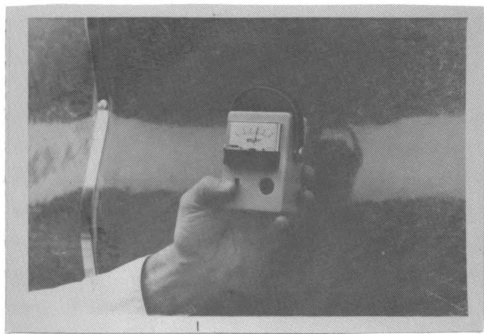


FIGURE 3-2. Solarometer Measuring  $A(H_b + H_d)$ .



The value of  $U_b$ , the overall heat transfer coefficient through the back of the collector can be determined from

$$U_b = \frac{1}{1/h_i + X_1/k_1 + X_2/k_2 + 1/h_o} \quad (3.10)$$

where

$h_i$  = convective heat transfer coefficient inside the collector BTU/hr-ft<sup>2</sup> ° F or kJ/hr-m<sup>2</sup> ° C.

$h_o$  = convective heat transfer coefficient outside the collector.

$x$  = thickness of material in feet or meter.

$k$  = thermal conductivity of material in BTU/hr-ft ° F.

The convective heat transfer coefficient can be found for a vertical surface using (16)

$$h = .99 + .21 \text{ Vel} \quad (3.11)$$

where "Vel" is the air velocity in ft/second.

Table 3-1 gives some simplified convective heat transfer coefficients.

As can be seen,  $U_b$  is easily obtained from (3.10).  $U_t$  is much more tedious to calculate, and is an iterating process. The problem is evident from Figure 3-3.  $U_t$ , the heat transfer coefficient through the cover plate, has radiation and convection in parallel. The temperature of the cover must be known to be able to determine the value of the radiation resistance.

TABLE 3-1. Convective Heat Transfer Coefficients (16)

DESCRIPTION	EQUATION BTU/hr-ft <sup>2</sup> °F.
<u>Air-Forced Convection</u>	
Vertical Plane with air velocity from 16 to 100 feet/sec and approximately 70° F.	$h = .5(V)^{0.8}$
Vertical plane with air velocity less than 16 feet/sec and air temperature approximately 70° F.	$h = .99 + .21 V$
-----	
<u>Air-Natural Convection with L a characteristic length in feet and ΔT the temperature difference between the surface and the fluid</u>	
Small Vertical Plates	$h = .29(\Delta T/L)^{0.25}$
Large Vertical Plates	$h = .19(\Delta T)^{.333}$
Small Horizontal Plates being heated facing upward	$h = .27(\Delta T/L)^{0.25}$
Large Horizontal Plates being heated facing upward	$h = .22(\Delta T)^{.333}$
Small Horizontal Plates being cooled facing upward	$h = .12(\Delta T/L)^{0.25}$

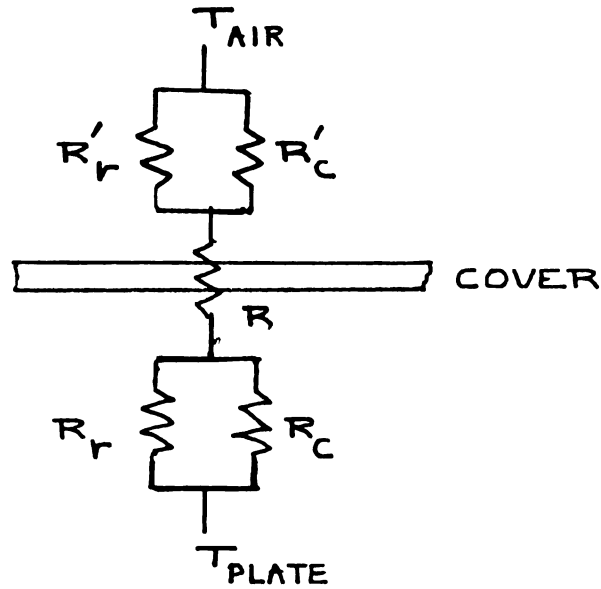


FIGURE 3-3. Heat Transfer Through Cover.

$R_r$ , the resistance to radiation flow, is

$$R_r = \frac{(1 - \epsilon_1)/\epsilon_1 + 1/F_{1-2} + (1 - \epsilon_2)A_1/\epsilon_2A_2}{\sigma(T_2^2 + T_1^2)(T_2 + T_1)} \quad (3.12)$$

where

$\epsilon_1$  = Emittance of surface 1.

$\epsilon_2$  = Emittance of surface 2.

$F_{1-2}$  = Shape factor from surface 1 to 2.

$A_1$  = Area of surface 1.

$A_2$  = Area of surface 2.

The resistance from the absorber plate to the transparent cover would have

$$A_1 = A_2$$

$$F_{1-2} = 1$$

and (3.12) is simplified to

$$R_r(\text{Plate} - \text{Cover}) = \frac{1/\epsilon_p - 1 + 1/\epsilon_c}{\sigma(T_c^2 + T_p^2)(T_c + T_p)} \quad (3.13)$$

where  $T_c$  and  $T_p$  are the respective temperatures of the cover and the absorber plate. The resistance to convective flow is

$$R_c(\text{Plate} - \text{Cover}) = \frac{1}{h_i} \quad (3.14)$$

where  $h_i$  is the convective heat transfer coefficient inside the collector.

The sum of the resistances across the system would give the overall heat transfer coefficient ( $U_t$ ) which is given by:

$$U_t = \frac{1}{\frac{1}{h_i} + \frac{1}{h_o} + \frac{1/\epsilon_p - 1 + 1/\epsilon_c}{\sigma(T_c^2 + T_p^2)(T_c + T_p)} + \frac{1/\epsilon_p}{\sigma(T_{sky}^2 + T_c^2)(T_{sky} + T_c)}} \quad (3.15)$$

$$U_t = \frac{1}{\Sigma R}$$

(The last term in the denominator comes from assuming  $\epsilon_{sky} = 1$ .) If the cover temperature,  $T_c$ , were known, (3.15) could be solved. To obtain  $T_c$  simply write the first law of thermodynamics around the cover plate. The system is shown in Figure 3-4.

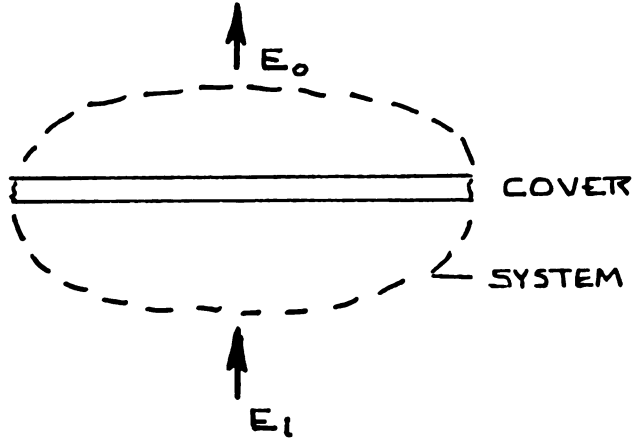


FIGURE 3-4. Energy Balance on Cover.

Equation (3.16) gives the  $E_i$  and (3.17) gives  $E_o$ .

$$E_i = h_i(T_p - T_c) + \frac{\sigma(T_p^4 - T_c^4)}{1/\epsilon_p + 1/\epsilon_c - 1} \quad (3.16)$$

$$E_o = h_o(T_c - T_{sky}) + \sigma\epsilon_c(T_c^4 - T_{sky}^4) \quad (3.17)$$

Equating (3.16) to (3.17) is the equivalent of stating that the heat into the cover equals the losses from the cover. Everything is known in the equation except  $T_c$  (temperature of the transparent cover).

The best method of solving  $T_c$  in (3.18) is by trial and error.

$$h_i(T_p + T_c) + \frac{\sigma(T_p^4 - T_c^4)}{1/\epsilon_p + 1/\epsilon_c - 1} = h_o(T_c - T_{sky}) + \sigma\epsilon_c(T_c^4 - T_{sky}^4) \quad (3.18)$$

When the left side equals the right side of (3.18), the correct value of  $T_c$  is known. This value of  $T_c$  is then substituted into (3.15) where  $U_t$  can be determined.

The temperature of the sky,  $T_{sky}$ , is found from

$$T_{sky} = T_{air} - 6 \quad (3.19)$$

where  $T_{sky}$  and  $T_{air}$  are in °C.

In determining  $U_b$  and  $U_t$ , some fixing of design parameters was necessary. The plate temperature,  $T_p$ , was established. The plate temperature is equal to

$$T_p = \frac{T_i + T_e}{2} \quad (3.20)$$

where  $T_i$  equals the inlet temperature of the collector and  $T_e$  equals the outlet temperature. From (3.20) and normal expected conditions placed upon  $T_i$  and  $T_e$ ,  $T_p$  can be determined. Re-examining (3.4) will show that the quantity  $\dot{m}$  is the only unknown in the equation. The energy coming onto the plate is found from (3.3) which is the next item to discuss. Then, (3.3) is equated to (3.4) which is shown in (3.21)

$$A \left( [H(\alpha \tau)]_b + [H(\tau \alpha)]_d \right) = \dot{m}(h'_e - h'_i) + U_B A (T_p - T_{air}) + U_T A (T_c - T_{sky}) \quad (3.21)$$

where the subscripts are

b = beam radiation

d = diffuse radiation.

The  $H_b$  is determined by methods of chapter two. The  $H_d$ , the diffuse radiation, is not precisely obtained. Three assumptions can be made:

1. The diffuse radiation comes from around the sun and the angular correction factor  $R_b$  would equal  $R_d$ . ( $R_b = R_d$  applicable on a clear day.)
2. The diffuse radiation is uniformly distributed across the sky. ( $R_d = 1$  in this case and would be applicable on cloudy days.)
3. The diffuse component is not used with concentrating collectors and is usually small and can be neglected for a conservative approach. (The system will work better than predicted.)

The  $(\tau\alpha)$  product is equal to

$$(\tau\alpha) = \tau\alpha \sum_{n=0}^{\infty} [(1-\alpha)\rho_d]^n = \tau\alpha / [1 - (1-\alpha)\rho_d] \quad (3.22)$$

where  $\tau$  is the transmittance through the glass and the  $\alpha$  is the absorption of the absorber plate,  $\rho_d$  is the diffuse reflectance,  $n$  is the number of covers and  $\rho_d$  can be determined from Table 3-2.

TABLE 3-2. Diffuse Reflectance  $\rho_d$  (6)

<u>Number of Covers</u>	<u><math>\rho_d</math></u>
1	.16
2	.24
3	.29

$\tau$  of equation 3.22 is determined from Figure 3-5 and  $\alpha$  from Table 3-3.

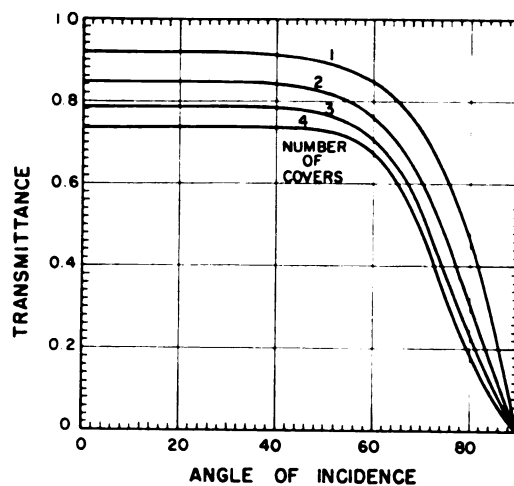


FIGURE 3-5. Transmittance,  $\tau$ , Neglecting Absorption (6).

TABLE 3-3. Absorption Emissivity of Various Surfaces (16)

Surface Material	$\alpha$	$\epsilon$
"Nickel Black" (Selective Surface)	.90	.10
Flat Black Paint	.96	.88
Green Paint	.50	.90
Concrete	.60	.88
Dry Sand	.82	.90
Black Tar Paper	.93	.93
Green Rolled Roofing	.88	.94
Water	.94	.96
White Paint	.20	.91
Aluminum Foil	.15	.05



It can be seen that all the quantities of Equation 3.22 can now be calculated except the mass flow rate  $\dot{m}$ . Being the only unknown,  $\dot{m}$  can be determined from (3.22). The collector efficiency can then be calculated from (3.9).

### 3.3 Simplified Analysis for Flat Plate Collectors

The method of this section has been verified by tests from solar installations. The solar module designed by the author is shown in Figure 3-6. Another vertical air system was designed by R.C. Schubert and the author (5). This vertical unit is pictured in Figure 3-7. Both of these systems use air as the medium of energy transfer. Both have air flowing between the inside of the cover and the absorber face. A comparison is made between this simplified analysis and actual test results.

Fluid enters the inlet of a flat collector at  $T_i$  and leaves at  $T_e$ . The simplification comes in assuming that the temperature in the fluid is equal to the discharge temperature throughout the collector. As an example, if the inlet temperature is  $90^\circ \text{ F}$  and the discharge temperature is  $140^\circ \text{ F}$ , the procedure assumes that the entire fluid temperature is  $140^\circ \text{ F}$ .

In the operating region for flat plate collectors, this simple modification has been quite accurate. The radiation component through the cover is neglected, and the increased fluid temperature increases the convective losses. This modification adjusts for the radiation losses which were not considered.

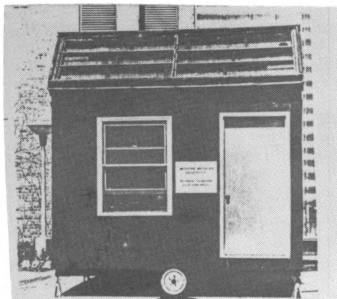


FIGURE 3-6. Solar Test Module.

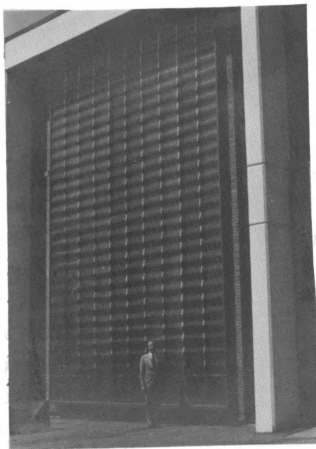


FIGURE 3-7. Vertical Solar Collector.

Figure 3-8 shows the electrical analogy of this concept.

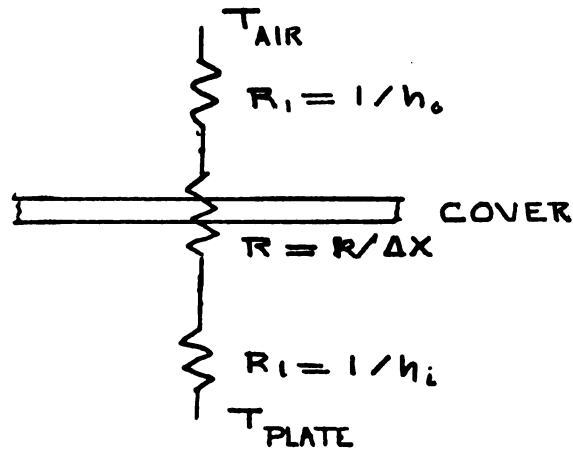


FIGURE 3-8. Heat Flow From Collector (Simplified).

The  $U_t$  of the cover becomes

$$U_t = \frac{1}{1/h_o + k/\Delta x + 1/h_i} \quad (3.23)$$

which is much simpler than (3.15).

Equation 3-10 is still used to calculate the back losses. In Figure 3-9 is shown a small 3 ft x 2 ft flat-plate solar collector. Test data taken from this panel include

$T_i = 3.3^\circ \text{ C}$  (Temperature in)

$T_e = 21^\circ \text{ C}$  (Temperature out)

$\dot{m} = 1.17 \text{ kg/min}$  (Mass flow rate)

$I = 3567.1 \text{ kJ/hr-m}^2$  (Solar insolation)

$A = 0.557 \text{ m}^2$  (Area)

$Vel_i = 12.95 \text{ m/sec.}$

The actual efficiency is:

$$\eta = \frac{\dot{m} C_p \Delta T}{I_a A} = \frac{1.17 \times 60 \times 1.012(21 - 3.3)}{3567.1 \times 0.557} = .63 = 63\%$$

Using the simplified method of analysis, proceed as follows:

Using Table 3-1 to find  $h_i$  and  $h_o$ , with 3 ft/sec inside air velocity.

$$h_i = .99 + .21(42.49) = 9.9 \text{ BTU/hr-ft}^2 \cdot ^\circ\text{F} = 202.4 \text{ kJ/hr-m}^2 \cdot ^\circ\text{C}$$

$$h_o = .99 + .21(22) = 5.61 \text{ BTU/hr-ft}^2 \cdot ^\circ\text{F} = 114.67 \text{ kJ/hr-m}^2 \cdot ^\circ\text{C}$$

$$U_t = \frac{1}{1/h_i + \Delta X_1/k_1 + 1/h_o}$$

$$U_t = \frac{1}{1/202.4 + .003/1.05 + 1/114.7}$$

$$U_t = \frac{1}{.0049 + .003 + .0087} = 60.24 \text{ kJ/hr-m}^2 \cdot ^\circ\text{C}$$

$$Q_{\text{cover}} = U_t A \Delta T$$

$$Q_{\text{cover}} = 60.24 \times .557 \times (21 - 3.33)$$

$$Q_{\text{cover}} = 592.9 \text{ kJ/hr}$$

Note, the temperature outside equaled  $3.33^\circ\text{C}$ . Assumed panel temperature was at  $21^\circ\text{C}$  throughout.

$$U_b = \frac{1}{.0049 + 0.213 + .0087} = 4.417 \text{ kJ/hr-m}^2 \cdot ^\circ\text{C}$$

$$Q_{\text{back}} = U_b A \Delta T = 4.417 \times .557(21 - 3.33) = 43.47 \text{ kJ/hr}$$

$$Q_{\text{insolation}} = 3567.1 \text{ kJ/hr}^2 \times 0.557 \text{ m}^2 = 1986.9 \text{ kJ/hr}$$

$$Q_{\text{useful}} = Q_{\text{insolation}} - Q_{\text{losses}}$$

$$Q_{\text{useful}} = 1986.9 - (592.9 + 43.47)$$

$$Q_{\text{useful}} = 1350.5 \text{ kJ/hr}$$

$$\eta = \frac{1350.5}{1986.9} = 67.9\%$$

This calculated efficiency is 67.7% as compared with actual efficiency. For the few test comparisons made, this simplification worked reasonably well. However, the tests were made on air systems operating with relatively low temperatures and should be used with caution. The tedious procedure of Section 3.2 shows a need for an apparent temperature.

The apparent temperature would be elevated high enough to account for radiation losses without actually having to include the traditional radiation equations.

The general form that the relationship might take is

$$T_{\text{apparent}} = T_{\text{exit}} + K$$

where K would be assumed constant over a certain range and would increase with elevated temperatures. By further development, this concept could be used for other types of collectors such as concentrators.

### 3.4 Solar Concentrators

Because of the potential for increased engine efficiency, as was discussed in Section 1.1 and 3.1, solar concentrators

will play an important role in the production of mechanical power. The concentrators are not necessarily more efficient than flat plate collectors. There is potential for lower efficiencies. The author has found that a concentrator can have a poor efficiency. The reasons for this poor efficiency were not always obvious. An analysis is developed here to show the ratios of concentration must be larger than one to have the flat plate and concentrating collectors equal in efficiency.

$A_R$  = Actual receiver area that is white from concentrated solar rays.

$A_C$  = Aperture of collector. Projected area normal to the collector.

$\eta_C$  = Instantaneous collector efficiency.

$\eta_0$  = Optical efficiency. The fraction of specularly reflected radiation that strikes the absorber. This quantity will, in general, be unknown because it is a function of the quality of the surface. A prudent engineer would use a value less than 100%.

$Q_u$  = Collected solar energy.

$I_b$  = Beam solar radiation at the collector aperture.

$U_L$  = Overall heat transfer coefficient.

An energy balance on a collector would give:

$$Q_u = \eta_0 I_b A_C - U_L (T_C - T_{air}) A_R \quad (3.24)$$

The instantaneous efficiency is:

$$\eta = \frac{Q_u}{I_b A_C} \quad (3.25)$$

By substituting (3.24) into (3.25), another form of the efficiency is

$$\eta = \eta_0 - \frac{U_L(T_C - T_{air})}{I_b} \frac{1}{C} \quad (3.26)$$

where the concentration ratio  $C$  equals one for a flat plate collector and  $C > 1$  for a concentrator. If the values of  $U_L$ ,  $T_C$ , and  $I_b$  are ignored, then the efficiency of a concentrator would be higher than a flat plate collector. However,  $I_b$ , the beam solar radiation, is less than the solar insolation for a flat plate collector which includes  $I_b$  and  $I_d$ , the diffuse radiation. Also  $T_C$  is much higher in a concentrator, and  $U_L$  is a function of the cube of the higher  $T_C$ .

As an example, compare the efficiency of a flat plate collector to a concentrator where the assumptions are:

1. Temperature of concentrating absorber is twice as hot as the temperature of the transparent cover on the flat plate collector.
2. Optical efficiency is 100% in both.
3. 
$$U_L = \frac{1}{1/h_{wind} + 1/\epsilon\sigma T^3}$$
4. Assume both are receiving the same insolation.
5.  $\epsilon = 1$  for both the cover and the concentrator absorber.

With these assumptions, equate the efficiency of both and calculate the necessary concentration ratio, C.

$$\eta_{\text{flat plate}} = \eta_{\text{concentrator}}$$

$$1 - \left( \frac{1}{1/h_{\text{wind}} + 1/\epsilon_C \sigma T^3} \right) \frac{T - T_{\text{air}}}{I_b} =$$

$$1 - \left( \frac{1}{1/h_{\text{wind}} + \epsilon_A \sigma 8T^3} \right) \frac{(2T - T_A)}{I_b} \frac{1}{C}$$

$$\left( \frac{1}{1/h_{\text{wind}} + 1/\sigma T^3} \right) (T - T_{\text{air}}) = \left( \frac{1}{1/h_{\text{wind}} + 1/8\sigma T^3} \right) \frac{(2T - T_A)}{C}$$

$$C = \frac{\left( \frac{1}{1/h_{\text{wind}} + 1/\sigma T^3} \right) (T - T_{\text{air}})}{\left( \frac{1}{1/h_{\text{wind}} + 1/8\sigma T^3} \right) \left( \frac{2T - T_A}{T - T_A} \right)} \quad (3.27)$$

In (3.27), the first quantity on the right is larger than one. The second quantity is also larger than one. Therefore, the concentration ratio must be larger than one to have the efficiency of a flat plate collector equal to a concentrating collector. It becomes obvious that solar concentrators do not have necessarily an inherent efficiency advantage.

The analysis of solar concentrators follow the same general approach as given in Section 3.2 for flat plate collectors. Writing an energy balance on the receiver gives

$$\text{Energy in} = \text{Energy out} + \text{Change in stored energy.}$$

The energy in would depend on the reflectance of the concentrator's surface, and the amount of reflected radiation that is intercepted by the absorber surface and would affect



the "energy in" quantity. The equation for the energy into the receiver is

$$E_i = A_a I_b \rho \eta_0 \alpha \quad (3.28)$$

where  $A_a$  is the aperture area,  $I_b$  is the beam radiation,  $\rho$  is the specular reflectance of the mirrored surface,  $\rho_0$  is the optical efficiency,  $\alpha$  is the absorption of the receiver. Equation (3.28) is for a tracking collector.

$I_b$  is found from (2.3) and (2.6) These equations are rewritten here for convenience.

$$I_b = I_0 \tau_{atm}$$

$$\tau_{atm} = a_0 + a_1 e^{-k/\cos \theta z}$$

If the concentrator is fixed or partially fixed, the "energy in" would be

$$E_i = A_a H \eta_0 \alpha \rho \quad (3.29)$$

where  $H$ , the hourly radiation, is found from (2.13).

The energy leaving the receiver would occur from heat losses through the walls of the absorber and from the useful energy transported to the engine. Equation 3.30 gives the analytical relationship as

$$E_0 = \dot{m}(h'_e - h'_i) + U_L A_r (T_r - T_a) \quad (3.30)$$

where  $\dot{m}$  is the mass flow rate,  $h'_e$  and  $h'_i$  are the respective enthalpies out and in,  $A_r$  is the area of the receiver,  $U_L$  is the overall heat transfer coefficient,  $T_r$  is the receiver

temperature,  $T_a$  is the environmental temperature.

The change in stored energy,  $\Delta E$ , within the receiver equals

$$\Delta E = \dot{m}_2 U_2 - \dot{m}_1 U_1 \quad (3.31)$$

where  $\dot{m}_2$  and  $\dot{m}_1$  are the masses inside the receiver at the end and beginning of the analysis.  $U_2$  and  $U_1$  are the internal energies of the fluid inside at the end and beginning of the consideration. Solar systems never obtain a steady state condition where  $\Delta E = 0$ , but for a short period of time, this value will be very small. Therefore, " $\Delta E$ " can be neglected in most cases.

Equating "energy in" to "energy out" gives:

$$A_a I_b \rho \eta_0 \alpha = \dot{m}(h'_e - h'_i) + U_L A_R (T_R - T_a) \quad (3.32)$$

The specular reflectance is reflectance where the angle of reflection equals the angle of incidence. Values for specular reflectance are given in Table 3-4.

TABLE 3-4. Specular Solar Reflectance

Surface	$\rho$
Aluminum Foil	.86
Back-aluminized 3M Acrylic	.86
Back-silvered White Glass	.88
Electroplated Silver	.96

The optical efficiency represents the percentage of energy that leaves the reflective surface and contacts the receiver. Because of poor alignment, small irregularities and manufacturing tolerances, some of the radiation will miss the receiver.

The optical efficiency is defined as:

$$\eta_0 = \frac{\text{Actual Radiation Flux on Receiver}}{\text{Total Radiation Flux Possible}} \quad (3.33)$$

These values have been obtained theoretically, but because of the large number of variables experimental measurements are preferred. The optical efficiency should be part of a construction specification and therefore established by the solar engine system designer. Values should be greater than 0.9 for most smaller systems.

The absorption,  $\alpha$ , can be easily found from the literature. Table 3-3 gives a few values that are applicable. Cavity absorbers should be used whenever possible where the value of  $\alpha$  would approach unity.

A large range of temperatures are possible with a solar concentrator. By adjusting the flow rates through the receiver, the temperature in and out can be controlled. The enthalpies are a function of the temperatures.

Referring to (3.32), the designers trial values would be:

$A_a$  = Aperture size of collector.

$\rho$  = Specular reflectance.

$\eta_0$  = Optical efficiency.

$\alpha$  = Receiver absorption.

$A_r$  = Area of the receiver.

$h_e'$  = Exist enthalpy.

$h_i'$  = Entering enthalpy.

The above values are chosen by the solar engineer and would be selected by various design requirements. The environmental terms in (3.32) that are determined by time and location would be:

$I_b$  = Beam component of solar insolation.

$T_a$  = Air temperature.

The values that require further calculations are:

$U_L$  = Overall heat transfer coefficient.

$T_r$  = Temperature of the receiver.

The unknown that must be computed from (3.32) is the mass flow rate,  $\dot{m}$ .

The electrical-thermal analogy of heat flow in the receiver is presented in Figure 3-9.

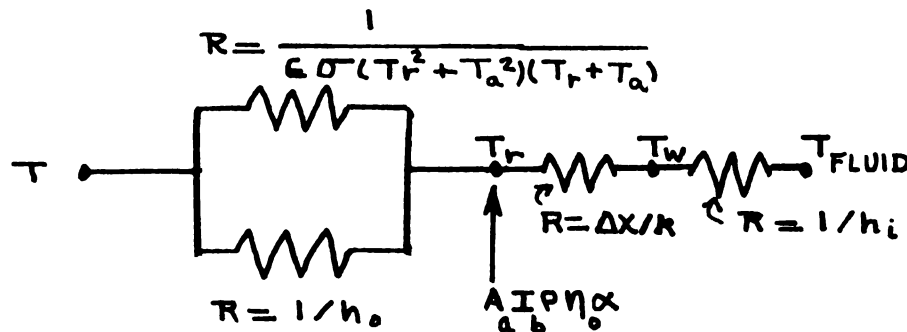


FIGURE 3-9. Heat Transfer into Receiver.

The value of heat flow through the receiver wall must equal  $\dot{m}(h'_e - h'_i)$ . The heat flow through the wall is:

$$\dot{m}(h'_e - h'_i) = A_r \frac{(T_r - T_{\text{fluid}})}{\Delta X/k + 1/h_i} \quad (3.34)$$

$U_L$  of (3.32) becomes:

$$U_L = \frac{1}{1/h_0 + 1/\epsilon_r \sigma (T_r^2 + T_a^2)(T_r + T_a)} \quad (3.35)$$

Equation 3-34 has been simplified by neglecting radiation. Also, the value of  $h_i$ , if the liquid is boiling, is usually large. Substituting (3.34) and (3.35) into (3.32) gives

$$A_a I_b \rho \eta_0^\alpha = \frac{A_r (T_r - T_{\text{fluid}})}{\Delta X/k + 1/h_i} + \frac{A_r (T_r - T_a)}{1/h_0 + 1/\epsilon_r \sigma (T_r^2 + T_a^2)(T_r + T_a)} \quad (3.36)$$

where  $T_{\text{fluid}}$  is the mean fluid temperature inside the receiver,  $\Delta X$  is the receiver wall thickness,  $k$  is the thermal conductivity of the receiver wall,  $h_i$  is the convective heat transfer coefficient on the inside of the receiver. The other terms have been previously defined.

If the temperature of the surface,  $T_r$ , can be found, the mass flow rate can be solved and the efficiency can be determined from (3.25) or (3.26). To calculate  $T_r$ , use (3.36). Every term in (3.36) is known except  $T_r$ . Because of the fact that  $T_r$  cannot be factored out easily, a trial and error solution becomes necessary. The correct value of  $T_r$  will equate the left side of (3.36) to the right.

## CHAPTER 4

### ACTUAL COLLECTOR TESTS COMPARED WITH ANALYSIS

#### 4.1 Parabolic Collector Test and Comparisons

In any science, it becomes important to compare the theoretical analysis to actual test data. Assumptions and simplifications can produce invalid theory. The material presented in Chapter 2 and Chapter 3 can be used to predict performance and then be compared with collected data.

Shown in Figure 4-1 is the spherical dished concentrating collector used to generate the data in Table 4-1. The four-wheeled cart in Figure 4-1 held the supply water that was kept at a fixed height manually. A tube coming out of the tank entered into a vertical cylinder. The face of the tube was white from the radiation flux. At the bottom of the tube is a discharge line that drained into a bucket.

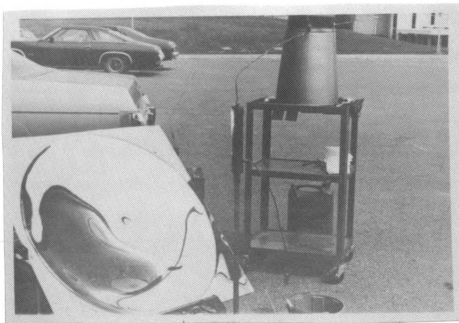


FIGURE 4-1. Testing System for Table 4-1.

TABLE 4-1. Data for Solar Concentrator

(Condensed from Data in the Appendix)

TIME EST	SOLAR METER BTU/HR-FT <sup>2</sup>	WIND VEL FT/MIN	TEMP AIR °F	TEMP AIR °F	TEMP OUT °F	FLOW RATE ML/SEC	DATE
1:55	270	400	78	78	86.5	6.25	May, 1978
2:00	270	600	75	76	86	6.6	May, 1978
2:05	275	600	76	76	86	6.6	May, 1978
2:10	270	600	76	77	87.5	6.6	May, 1978
-----							
2:32	150	150-300	58	70	79	3.31	May 17, 1978
2:34	125	150-300	58	70	75	3.21	May 17, 1978
2:37	100	300	58	70	75	--	May 17, 1978
2:40	150	300	58	70	76	--	May 17, 1978
2:45	160	350-300	58	70	75	3.25	May 17, 1978
-----							
1:30	265	100	86	77	98	2.38	June 1, 1978
1:35	265	200	87	77	104	2.39	June 1, 1978
1:38	265	350	87	78	104	2.37	June 1, 1978
1:55	265	400	87	79	118	2.3	June 1, 1978
1:58	268	350	87	79	120	2.07	June 1, 1978
2:00	265	50	86	80	124	2.03	June 1, 1978
2:03	265	300	86	80	122	2.11	June 1, 1978
2:05	205	350	86	80	122	2.03	June 1, 1978

The hand-held solarometer is shown in Figure 4-2. Measurement must be made at the site to accurately determine the solar insolation. The methods of Chapter 2 can be used to determine the solar radiation, and this method can be used to compare with the hand-meter readings.

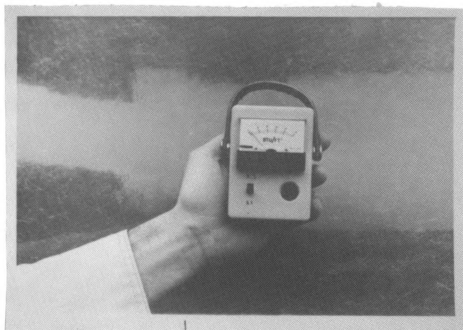


FIGURE 4-2. Hand-Held Solarometer.

#### Insolation Calculations

On June 1 from 1:30 - 2:00 p.m., the solarometer was reading 265 BTU/hr-ft<sup>2</sup>. From (2.3), (2.4), and (2.5), the solar insolation can be determined. However, the solar time must be known and the sun altitude must be found. The solution is as follows (located at 86° W longitude):



$$\text{Solar Time} = \text{Standard Time} + E - 4(L_S - L_L) \quad (2.14)$$

$$\text{Solar Time} = 12:45 + 3 \text{ minutes} + 4(75 - 86)$$

$$\text{Solar Time} = 12:45 + 3 \text{ minutes} + (-44)$$

$$\text{Solar Time} = 12:45 - 41 \text{ minutes}$$

$$\text{Solar Time} = 12:04.$$

The angle of declination from Equation 2.8 is:

$$\delta = 23.45 \sin [360 (284 + n)/385]$$

June the first is the 151st day of the year ( $n = 151$ ).

$$\delta = 21.9^\circ$$

The hour angle is easily calculated by multiplying the number of hours from solar noon by  $15^\circ$ .

$$W = 15 (1:45 - 12:00)$$

$$W = 15 (1.75 \text{ m})$$

$$W = 26.25$$

From (2.13b) (Latitude  $42.25^\circ \text{ N}$ )

$$\cos \theta_z = \cos \phi \cos \delta \cos W + \sin \phi \sin \delta$$

$$\cos \theta_z = \cos 42.25 \cos 21.9 \cos 26.25 + \sin 42.25 \sin 21.9$$

$$\cos \theta_z = .616 + .25 = .8668$$

$$\theta_z = 29.916^\circ$$

$$\alpha = 90 - 29.916 = 60^\circ.$$

$$m(z) = \left[ [1229 + (614 \sin 60^\circ)^2]^{1/2} - 614 \sin 60^\circ \right] \frac{P(z)}{P(O)} \quad (2.5)$$

$$m(z) = (1.15) \frac{P(z)}{P(O)} = (1.15) \frac{14.21}{14.70} = 1.11$$

$$\tau_{\text{atm}} = \frac{e^{-.095 \text{ m (z)}} + e^{-.65 \text{ m (z)}}}{2} = .693 \quad (2.4)$$

$$I_b = I_o \tau_{\text{atm}} \quad (2.3)$$

$$I_b = 4860.6 \times .693 = 3368.4 \text{ kJ/hr-m}^2$$

$$\text{CALCULATED: } I_b = 3368.4 \text{ kJ/hr-m}^2$$

$$\text{MEASURED: } I_b = 265 \text{ BTU/hr-ft}^2 = 3009.5 \text{ kJ/hr-m}^2.$$

By Equation 2.6

$$\tau_{\text{atm}} = a_o + a_1 e^{-k/\cos \theta_z} \quad (1.5 \text{ km alt})$$

$$\tau_{\text{atm}} = .2582 + .6523 e^{-.291/.866} = .725$$

$$\text{CALCULATED: } I_b = 3524 \text{ kJ/hr-m}^2.$$

As can be seen, the calculated values were higher than the measured values; but from an engineering viewpoint, there were correlation. What appears to be a clear day can be deceiving. Had the 5 km haze model been used for Equation 2.6, the results would have been:

$$\tau_a = .26 + .793 e^{-.330/.866} = .667$$

$$I_b = .667 \times 4860.6$$

$$I_b = 3242 \text{ kJ/hr-m}^2$$

### Efficiency Calculations

From the measured data, using the 2:05 time on Table 4-1

$$\dot{m} = 6.6 \text{ ml/sec} \times \text{g/ml} \frac{\text{kg}}{1000 \text{ g}} \frac{3600 \text{ sec}}{\text{hr}} = 23.76 \frac{\text{kg}}{\text{hr}}$$

$$Q_u = \dot{m} (h'_e - h'_i) = 23.76 \frac{\text{kg}}{\text{hr}} 4.19 \text{ kJ/kg } ^\circ\text{C} (30-24.4) ^\circ\text{C}$$

$$Q_u = 557.5 \frac{\text{kJ}}{\text{hr}}$$

$$A_a I_b = 1.1195 \times 3242$$

$$A_a I_b = 3629.4 \frac{\text{kJ}}{\text{hr}}$$

measured efficiency is

$$\eta = Q_u / A_a I_b = 557.6 / 3629.4 \approx .16$$

Testing  $\eta = 16 \%$ .

For calculating purposes:

$$A_a = 12.05 \text{ ft}^2 = 1.1195 \text{ m}^2$$

$$\rho = .9$$

$$\eta_o = .8$$

$$\alpha = .96$$

$$A_r = .02778 \text{ ft}^2 = .0026 \text{ m}^2$$

$$(h'_e - h'_i) = 10 \text{ BTU/lbms} = 23.23 \text{ kJ/kg}$$

$$I_b = 275 \text{ BTU/ft}^2\text{-hr} = 3123 \text{ kJ/m}^2\text{-hr}$$

$$T_a = 76^\circ \text{ F} = 24.44^\circ \text{ C}$$

$$k = 224 \text{ BTU/hr-ft } ^\circ \text{ F} = 1330.9 \text{ kJ/m } ^\circ \text{ C}$$

$$\Delta X = .125" = .00318 \text{ m}$$

$$h_i = 560 \text{ BTU/hr-ft}^2 \text{ } ^\circ \text{ F} = 11446.4 \text{ kJ/hr-m}^2 \text{ } ^\circ \text{ C}$$

$$h_o = 3.09 \text{ BTU/hr-ft}^2 \text{ } ^\circ \text{ F} = 63.16 \text{ kJ/hr-m}^2 \text{ } ^\circ \text{ C}$$

$$\dot{m} = 53.3 \text{ lb/hr} = 24.2 \text{ kg/hr.}$$

Substituting the above into Equation 3.36 and solving for  $T_r$  (Temperature on outside of receiver) gives:

$$A_a I_b \rho \eta_o \alpha = \frac{A_r (T_r - T_{\text{fluid}})}{\Delta x/k + 1/h_i} + \frac{A_r (T_r - T_a)}{1/h_o + 1/\epsilon_r \sigma (T_r^2 + T_a^2)(T_r + T_a)}$$

The first step in analyzing the efficiency is to solve  $T_r$  from the above equation. If the receiver has a

$$\frac{D_i}{D_o} > 0.6 \quad (\text{Threlkeld})$$

where  $D_i$  and  $D_o$  are the respective inside and outside diameters, the linear forms of the resistance to conduction can be used. If the walls are thicker than the stated limits, the conduction becomes:

$$Q = [2\pi k (T_1 - T_2)] / [\ln (D_o/D_i)]$$

Every element of (3.36) is known except the convective heat transfer coefficients  $h_i$  and  $h_o$ . With these values calculated,  $T_r$ , the surface temperature of the absorber, can be evaluated. To determine  $h_o$ , use

$$h_o = .99 + .21 \text{ vel} \quad (4.1)$$

where vel is in ft/sec and is less than 16 ft/sec.

This equation (Jinges), which is applicable for air flowing parallel to a vertical plate, is

$$h = a + b (V)^n \quad (4.2)$$

The values for (4.2) come from Table 4-2.

TABLE 4-2. Factors for Equation 4-2 (16)

Surface	Vel 16 ft/sec			16 ft/sec Vel 100 ft/sec		
	a	b	n	a	b	n
Smooth	.99	.21	1.0	0	.5	.78
Rough	1.09	.23	1.0	0	.53	.78

The focal point of the concentrating collector covered an area of approximately 2" x 2". For all practical purposes, this could be considered a vertical plain area.

The  $h_i$  is found from (4.3) (16). This equation is applicable for water flowing down the inside of a vertical

tube having inside diameters of 1.5 to 2.5 inches and height ranges from .407 to 6.08 feet.

$$h_i = 120 [\dot{m}/(\pi D_i)]^{1/3} \quad (4.3)$$

where  $\dot{m}$  is the lbs/hour of flow, and  $D_i$  is the inside diameter in feet. Calculating  $h_i$  and  $h_o$

$$h_i = 120 [53.3/(\pi \frac{2}{12})]^{1/3} = 560 \text{ BTU/hr-ft } ^\circ \text{ F} = 11464.4 \frac{\text{kJ}}{\text{hr-m}^2 ^\circ \text{ C}}$$

$$h_o = .99 + .21 \times 10 = 3.09 \text{ BTU/hr-ft } ^\circ \text{ F} = 63.16 \text{ kJ/hr-m}^2 ^\circ \text{ C}$$

Substituting the values into (3.36),  $T_r$ , the receiver temperature, can be found. The procedure is best solved by trial and error if all the terms of Equation 3.36 are involved. However, the  $1/h_r$  term in the denominator approaches zero as the receiver temperature increases.

Equation 3.36 is rewritten for convenience

$$A_c I_b \rho \eta_o \alpha = \frac{A_r (T_r - T_{\text{fluid}})}{\frac{X}{k} + \frac{1}{h_i}} + \frac{A_r (T_r - T_a)}{\frac{1}{h_o} + \frac{1}{\epsilon_r \alpha (T_r^2 + T_a^2)(T_r + T_a)}} \quad (3.36)$$

Equation 3.36 with higher receiver temperatures becomes

$$A_c I_b \rho \eta_o \alpha = \frac{A_r (T_r - T_{\text{fluid}})}{(\Delta X)/k + 1/(h_i)} + \frac{A_r (T_r - T_a)}{1/h_o + 0} \quad (4.4)$$

Substituting the values of this real problem gives

$$(1.1195) (3242) (.9) (.8) (.96) =$$

$$\frac{.0026 (T_r - 300.2)}{\frac{.00318}{1330.9} + \frac{1}{114464}} + \frac{.0026 (T_r - 279.4)}{\frac{1}{63.16}}$$

$$T_r = 860^\circ \text{ K}$$

The mass flow rate by (3.24) would be

$$\dot{m} (h'_e - h'_i) = \frac{A_r (T_r - T_{\text{fluid}})}{(\Delta X)/k + 1/h_i}$$

$$\dot{m} = 104.3 \text{ kg/hr.}$$

The efficiency by (3.25) will become

$$\eta = (Q_u)/(A_c I_b) = (104.3 \times 23.23)/(1.1195 \times 3242)$$

$$\eta = 66.6 \%$$

The actual measured efficiency was 16 % which indicates some fundamental problems with the test apparatus. The value of optical efficiency was essentially unknown, but the discrepancy between the actual and the theoretical seems too large for such a simple explanation.

Examining (4.4), it appears that the convective air film insulates the receiver regardless of the receiver temperatures. The  $1/h_r$  term approaches zero at high temperatures. By trying to solve (3.36) with an iterating process,

the author became aware of this limitation imposed upon radiation. The  $h_o$  term was assumed not a function of temperature. The calculated value of 66.6 % would be very reasonable and acceptable, but caution should be exercised. The assumptions used in connection with (3.36) were that parallel heat flow of convection and radiation occurred simultaneously, and that the convective term  $h_o$  was a function of air velocity only. The overall heat transfer coefficient of the receiver is (6)

$$U_L = (1/h_{wind} + 1/h_r)^{-1} \quad (4.5)$$

where

$$h_r = \epsilon \sigma (T_r^2 + T_{sky}^2) (T_r + T_{sky}).$$

The assumption will be made that radiation losses are much larger than the convection losses, and  $U_L$  will become

$$U_L = [1/\epsilon \sigma (T_r^2 + T_{sky}^2) (T_r + T_a)]^{-1} \quad (4.6)$$

where  $T_{sky}$  is found from (3.19).

$$T_{sky} = T_{air} - \theta$$

Equation 3.36 becomes

$$A_c I_{\rho n} \alpha = \frac{A_r (T_r - T_{fluid})}{(\Delta X)/k + 1/h_f} + A_r U_L (T_r - T_{sky}) \quad (3.36)$$

where  $U_L$  is found from (4.6).  $T_r$  is found by trial and error in (3.36).



The temperature of the receiver is around  $833^{\circ}\text{K}$  by these assumptions, and the efficiency is practically the same as before. The theoretical analysis is, therefore, valid if the receiver will actually absorb .96 % of the radiation flux. It appears that in actual installation, the receiver should be concaved to improve the absorptivity. The receiver used in the test had a convexed surface. The low efficiency of 16 % was produced, in part, by the improper angle of incidence of the radiation on the absorber surface.

#### 4.2 Flat Plate Collector Tests and Comparisons

Flat plate collector analysis as presented in Chapter 3 agrees well with actual data. Shown in Figure 4-3 is an auxilliary space heating system designed by the author.

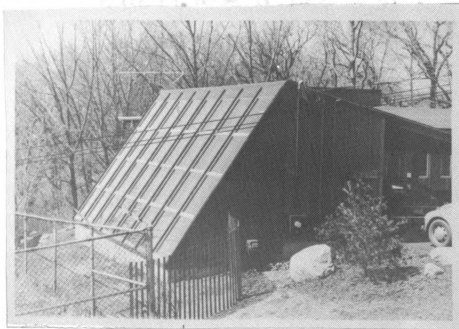


FIGURE 4-3. Auxilliary Space Heating System.

The collector is an air system with a single glass cover and a black cloth absorber glued onto fiber glass insulation.

In Figure 4-4 is shown another air collector. This vertical flat plate collector uses a Sun-Lite cover with a black painted aluminum foil absorber that is glued to insulation. The covering is undulated to provide for thermal expansion. This system was designed by R.C. Schubert and the author. Efficiencies have reached 63 % with snow reflection.



FIGURE 4-4. Vertical Solar Collector at Western Michigan University.

A small solar test panel is shown in Figure 4-5. The student is measuring the exit temperature and the solar insolation with a hand-held solarometer.



FIGURE 4-5. Solar Test Panel.

Tests were conducted on two identical panels with different absorbers. In Table 4-3 is a summary of the results. The entire test results are included in the Appendix. The panel is 2' x 3' and is described in the Appendix.

TABLE 4-3. Absorber Tests (March 25)

Mass Flow Rate lb/min		Temperature In		Temperature Out	
Collec- tor A	Collec- tor B	Collec- tor A	Collec- tor B	Collec- tor A	Collec- tor B
$\dot{m} = 2.750$	$\dot{m} = 2.546$	40 ° F	40 ° F	71.1 ° F	71.9 ° F

The efficiency of Collector A and B at 12:12 solar time on March the 25th from the test data of Table 4-3 is

$$Q/A = (\dot{m} C_p \Delta T)/A$$

$$(Q/A)_A = (2.750 \times 60 \times .24 \times 31.1)/6 = 205.25$$

$$\eta_A = 205.25/314.1 = 65.3 \%$$

$$(Q/A)_B = (\dot{m} C_p \Delta T)/A$$

$$(Q/A)_B = (2.546 \times 60 \times .24 \times 31.9)/6 = 194.92$$

$$\eta_B = 194.92/314.1 = 62.06 \%$$

Using the long form for flat plate collectors in Chapter 3 gives the following results from the test data of Table 4-3 (compared with Collector A) by

$$T_p = (40 + 71.1)/2 = 55.5^\circ \text{ F} = 13^\circ \text{ C}$$

by

$$h_o = .99 + .21 \text{ Vel} = .99 + .21 (14.6)$$

$$h_o \approx 4$$

$$h_i = .99 + .21 (13.5) = 3.8$$

by

$$T_{\text{sky}} = T_{\text{air}} - 6 = 4.44 - 6 = -1.55^\circ \text{ C} = 271.5^\circ \text{ K}.$$

Solving for  $T_c$ , temperature of cover, by Equation 3.18

$$h_i (T_p - T_c) + [\sigma (T_p^4 - T_c^4)] / (1/\epsilon_p + 1/\epsilon_c - 1) =$$

$$h_o (T_c - T_{air}) + \sigma \epsilon_c (T_c^4 - T_{sky}^4)$$

Assume  $\epsilon_p = .88$  and  $\epsilon_c = .9$ .  $U_T$  is solved from (3.15).

$$U_T = 10 \text{ kJ/hr-m}^2 \cdot \text{C}.$$

From (3.21)

$$\dot{m} = 86.26 \text{ kg/hr}$$

$$\eta = \frac{\dot{m} C_p \Delta T}{(5557)(3567)} = (86.26 \times 1.012 \times 17.3) / 1986.9 = .75$$

$$\eta = 75 \text{ \%}.$$

The calculated efficiency by the methods of Chapter 3 gives:

$$\eta = 75 \text{ \%}.$$

Actual efficiency is:

$$\eta = 65.3 \text{ \%}.$$

By careful examination of the process, it is seen that  $h_i$  and  $h_o$ , the convective heat transfer coefficients, effect the calculation greatly. Also, the sky temperature equation has much to do with the final results. The biggest factor

comes in using clear day insolation. The actual test was run under unknown solar insolation.

## CHAPTER 5

### SOLAR ENGINE ECONOMICS

#### 5.1 Introduction

Some very conclusive truths can be obtained from an economic analysis of solar engines. The fact that solar engines are not part of modern technology indicates past problems, since their development can be traced back to 1615. Ericsson in 1883 built a solar engine that will be a rival to modern developments, and he realized that his solar engine system could not compete with cheap fossil fuel. John Ericsson could see the demise of the fossil fuel era when heavy use of fossil fuel had barely started. As fossil fuels become more difficult to obtain, solar engine technology will become more competitive. Yet, fundamental changes in the engine design are necessary to eventually have working models that are cost effective. Cost effective design means that the cost to obtain power from the sun is equal to or less than the cost of power from fossil fuel engines. Chapter 6 deals with design problems to reduce cost and increase brake horsepower.

#### 5.2 Simple Payback Costing

The diesel engine has an overall efficiency of approximately 33%. There are 40,140 kJ/liter in diesel oil. Assume the engine's purchase price is  $C_1$  and the yearly cost for maintenance is  $C_2$ . The total annual cost per horsepower

for a diesel engine would be (5.1)

$$\left( \frac{\text{Cost}}{\text{bhp}} \right)_{\text{diesel engine}} = \frac{\frac{C_1}{N} + C_2 + \frac{(\text{bhp})_d}{.33} \times 2685 \frac{\text{kJ}}{\text{hr-hp}} \times \frac{C_3 \times t}{40,140 \frac{\text{kJ}}{\text{liter}}}}{(\text{bhp})_d}$$

where  $C_3$  is the cost per liter and  $t$  is the number of hours annually of operation. To compare the solar and the diesel engine, the bhp/hr of each engine must be equal. A diesel engine could run 24 hours while a solar engine might operate 6 hours. Therefore

$$\begin{aligned} (\text{bhp})_d \times 24 &= (\text{bhp})_s \times 6 \\ (\text{bhp})_d &= 1/4(\text{bhp})_s \end{aligned} \quad (5.2)$$

where the "d" and "s" are subscripts for diesel and solar respectively.

To compare systems, the solar engine will need to be four times larger at best because of its intermittent operation.

The annual cost of a solar engine is

$$\begin{aligned} (\text{Cost/bhp})_{\text{solar}} &= \frac{C'_1/N + C'_2}{4(\text{bhp})_s} \\ (\text{Cost/bhp})_{\text{solar}} &= \frac{4(C'_1/N + C'_2)}{(\text{bhp})_d} \end{aligned} \quad (5.3)$$

where  $C'_1$  is the cost of the system depreciated over "n" years.  $C'_2$  is the annual maintenance cost.



To determine a cost effective design, equate (5.1) to (5.3):

$$C_1/N + C_2 + (\text{bhp})_d \times 1760 \times C_3 = 4(C'_1/N + C'_2) \quad (5.4)$$

Assume maintenance cost such that  $C_2 = 4C'_2$ . Assume equal life of 20 years. For one brake horsepower, Table 5-1 gives the comparison of diesel engine cost to solar engine cost. Equation 5-4 with the assumptions becomes:

$$C'_1 = \frac{1}{4}(C_1 + 35,200 C_3) \quad (5.5)$$

As an example, consider a small 1 hp diesel costing \$600 with a fuel cost of \$0.40 per liter. What can the solar engine system cost?

Move to the left horizontally on the 0.40 line until the vertical \$600 column is intersected. Read the solar engine maximum cost at \$3,671.30.

The procedure of this section is called the simple payback method. The value of the energy is used to pay back the added investment in a solar engine system. The example given shows that \$3,671.30 could be invested in a solar device. The difference in the price between diesel and solar engines is about \$3,000. The simple payback method fails to take into account returns on the \$3,000 if it were invested. Considering the yearly inflation rate, the returns on the invested \$3,000 would have difficulty in matching the increased appreciation on the solar equipment. Therefore,

TABLE 5-1. Price/Horsepower for Solar Engine Versus Diesel Engine\*

Fuel Cost Per Liters in Dollars	Diesel Engine Cost/Horsepower					
	200	400	600	800	1000	2000
\$0.26	2397.5	2447.5	2497.5	2547.5	2597.5	2847.5
\$0.33	2984.4	3034.4	3084.4	3134.4	3184.4	3434.4
\$0.40	3571.3	3621.3	3671.3	3721.3	3771.3	4021.3
\$0.53	4745.0	4795.0	4845.0	4895.0	4945.0	5195.0
\$0.79	7093.5	7142.5	7192.5	7242.5	7292.5	7542.5

\* Based on 20 Years of Operation

the simple payback method seems sufficient for the times.

A brief study of Table 5-1 reveals that fuel costs are more important than initial equipment cost. Fuel in central Africa costs \$0.66 per liter and is rationed. For developing countries without fossil fuel, solar engines appear feasible now.

### 5.3 Flat Plate Collector Versus Concentrator as Engine Power Source

Since historical engines have operated from both flat plate and concentrating collectors, a simple study becomes relevant to the solar engine discussion. As has been discussed, concentrators produce higher discharge temperatures which, in turn, produce greater engine efficiencies. If the assumption is made that concentrators' overall efficiency would be higher than flat plate systems, there appears to be little reason to consider flat plate systems. With capital investment savings, it is possible for the cheaper flat plate systems to be considered. The symbols are:

$\eta_{FC}$  = Efficiency of flat plate collector.

$\eta_{FE}$  = Efficiency of engine driven by a flat plate collector.

$\eta_{CC}$  = Efficiency of a concentrating collector.

$\eta_{CE}$  = Efficiency of an engine driven by a concentrating collector.

$C_{FC}$  = Installed cost of flat plate collector per square foot.

$C_{CC}$  = Installed cost of concentrating collector per square foot.

Assuming 20 years of life, maintenance cost equal, and the Carnot efficiency, the efficiency of the solar engine, the following analysis was developed.

Assume an exit temperature in the concentrator of four times the flat plate collector.

$$T_C = 4 \times T_F$$

Assume the daily solar insolation is 22,713 kJ/m<sup>2</sup> day. The difference in the efficiency would have to pay for the added cost.

$$(\eta_{CC} \eta_{CE} - \eta_{FC} \eta_{FE}) 22,713 \times \text{Fuel cost/kJ} = C_{CC} - C_{FC} / 20 \times 365 \quad (5.5)$$

Assume

$$\eta_{CC} = 60\%$$

$$\eta_{FC} = 50\%$$

$$T_F = 366^\circ \text{ K}$$

$$T_C = 700^\circ \text{ K}$$

$$\eta_{CE} = 1 - 311/700 = .555$$

$$\eta_{FE} = 1 - 311/366 = .152$$

Then using (5.5), the  $\Delta$ cost becomes

$$(.60 \times .555 - .50 \times .152) 22,713 \times \text{Fuel Cost/kJ} = \Delta \text{Cost} / 7300$$

$$(.333 - .076)22,713 \times \text{Fuel Cost/kJ} = \Delta\text{Cost}/7300$$

$$\Delta\text{Cost} = \text{Fuel Cost/kJ} \times 42,611,859$$

Assume fuel cost at \$0.26 per liter.

$$\$0.26/\text{liter} \times \text{liter}/40,140 \text{ kJ} = 6.47 \times 10^{-6} \text{ \$/kJ}$$

$$\Delta\text{Cost} = 6.47 \times 10^{-6} \text{ \$/kJ} \times 42,611,859$$

$$\Delta\text{Cost} = \$275.70$$

In other words, the concentrator could cost \$275.70 more per square meter and be equivalent to the flat plate collector system. Table 5-2 illustrates the decision possibilities.

TABLE 5-2. Economic Comparison of Flat Plate To Concentrator

Fuel Cost/Liter	Additional Maximum Cost per Square Meter of Collector for a Concentrator to Make the Concentrator the Best Choice $\Delta\text{Cost}$
\$0.26	\$275.70
\$0.53	\$562.00
\$0.79	\$837.70
\$1.05	\$1113.40

It can be seen from Table 5-2 that solar concentrators would be the best choice if additional cost can be kept under \$275.70 per square meter with \$0.26 per liter oil. As oil prices increase, so does the increased justification cost.

## CHAPTER 6

### SOLAR ENGINE CYCLES

#### 6.1 Second Law Considerations - Carnot Cycle

The first law of thermodynamics states that "Energy cannot be created or destroyed, only transformed from one form to another." The energy of the universe is constant. Violations of the first law usually show up as perpetual motion devices, and of course, perpetual motion machines do not exist. The first law stated in equation form is:

$$\text{Energy in} = \text{Energy out} + \text{Change in stored energy.}$$

Newspapers are full of inventors claiming devices that create energy. One such device was an electric motor driving a generator that powered lights. The remaining energy from the generator powered the motor and the inventor had a system that created energy in the form of light. Another perpetual motion device used two mirrors to bounce light back and forth through a gas. The light was theorized to continue infinitely passing energy to the gas. The gadget exploded, which delighted the inventor. He was convinced of his energy creation until the author pointed to the electric cord connected to the light which carried energy into his system. The first law has not been disproved, and is understood and accepted by much of humanity. But without the second law of thermodynamics, further confusion would exist. The second law restricts the first law.

In fact, if there were no second law, there would be no energy crisis. Energy could be transformed without destruction and therefore, no shortage could ever exist. The second law stated in its best form says "Whenever transferring heat into work, energy must be rejected to return the cycle to the initial point." This means that heat cannot be completely transformed into work. No machine can be 100% efficient. A theoretical cycle has been developed to extract the maximum amount of work from a given amount of heat. This engine is the Carnot engine. Its efficiency is:

$$\eta_{\text{Carnot}} = 1 - \frac{T_L}{T_H} \quad (6.1)$$

The Carnot engine is a frictionless engine that is completely reversible. The process begins when the piston is at the top dead center position and the temperature is  $T_H$  as shown in Figure 6-1.

From State 1 heat is added from an infinite heat sink ( $T_H = \text{constant}$ ). The piston moves slowly downward at constant temperature. At just the proper moment in the process (State point 2) an insulated jacket replaces the heat source. The cycle expands reversibly and adiabatically until bottom dead center (State point 3). The temperature drops to  $T_L$ . To minimize the work required to return the piston, the infinite heat sink at  $T_L$  extracts heat (State point 3). Finally, an insulated cover is placed on the cylinder such that a reversible adiabatic process occurs

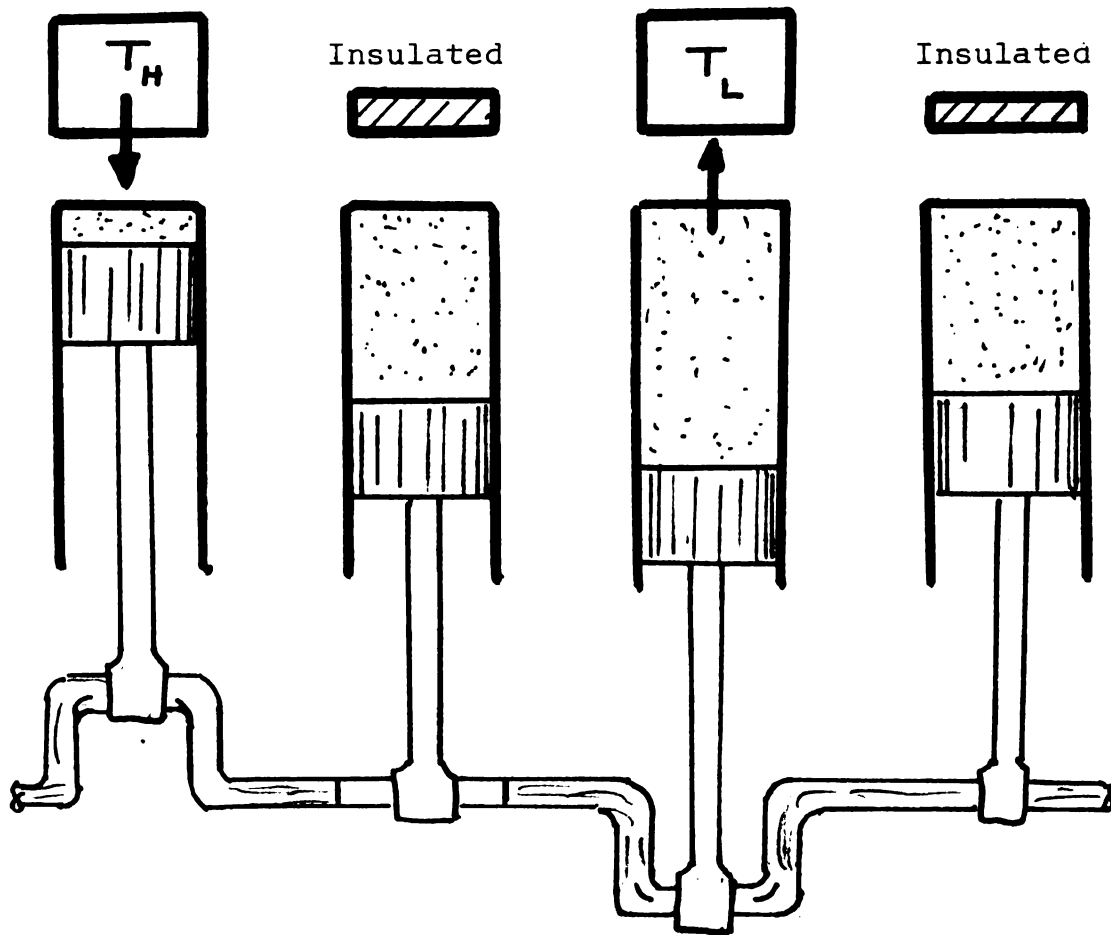


FIGURE 6-1. Carnot Engine.





from 3 to 4. The cycle returns to the initial state with a maximum net work. It would be difficult to conceive of an engine that could extract any more work from a given amount of heat. Therefore, the Carnot cycle is used to define available energy, since this cycle has the maximum possible efficiency. The available energy is defined as

$$\text{Available Energy} = \eta_c Q_s \quad (6.2)$$

where  $\eta_c$  is given in (6.1) and  $Q_s$  is the heat supplied. The total heat,  $Q_s$ , is composed of two parts:

$$Q_s = \text{Available Energy} + \text{Unavailable Energy} \quad (6.3)$$

The Carnot engine becomes important in defining and developing the property of entropy. Entropy,  $S$ , is defined as:

$$S = \frac{\text{Unavailable Energy}}{T_L} \quad (6.4)$$

From this discussion, entropy can be derived for a closed system and is:

$$dS = \frac{dQ}{T_H} \quad (6.5)$$

The Carnot cycle (Figure 6-2) becomes very important to solar engine technology.

The entire area under the  $T_H$  line in Figure 6-2 represents the total heat transfer. The available energy is the Carnot work which is the area above the  $T_L$  level. Anything below that line is unavailable to do work. The

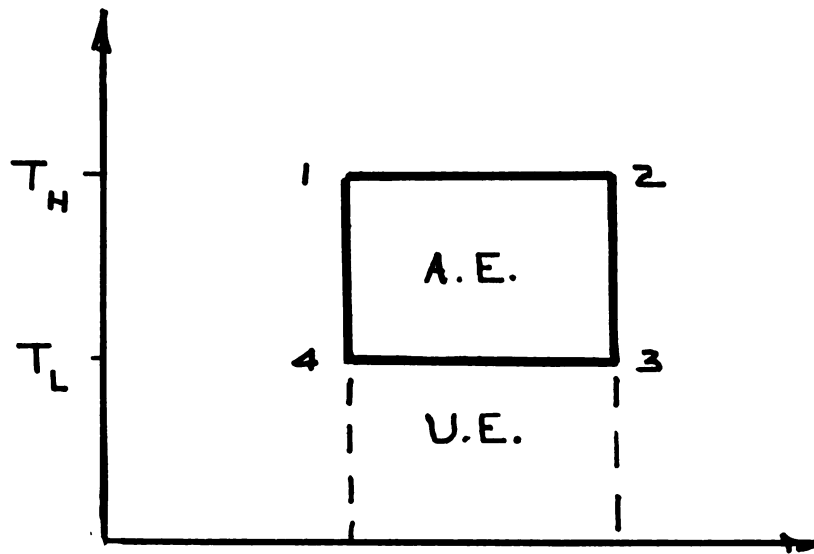


FIGURE 6-2. Carnot Cycle.

objective of any thermodynamic cycle is to use as much of the available energy as possible. See Figure 6-3.

The first law states the conservation of energy. The second law limits the first law in the conversion of heat to work. The Carnot engine is the most efficient cycle and is used to define available energy. The remaining energy is unavailable to do work. As energy processes continue, there is a natural increase in entropy. Energy tends to reach the most random state. Temperatures tend to reach some universal mean temperature where engines cease to operate and life becomes impossible. The second law stated another way would read "Energy is conserved, but becomes eventually unavailable to do work."

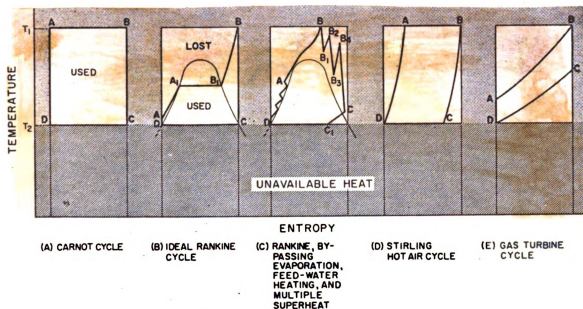


FIGURE 6-3. Heat Engine Cycle Comparison.

## 6.2 Rankine Cycle

The Rankine cycle was used in many of the past solar engines and will be used in the future ( 2). The cycle and schematic are pictured in Figures 6-4 and 6-5.

Steam is the working substance, and the system can be piped such that the rejected heat can be used for domestic water preheating or space heating. The output of the Rankine cycle, when the condenser rejected heat can be used, is improved. The efficiency in this case is

$$\eta = \frac{\text{work} + \dot{m}(h_2 - h_3)}{I_b A_c} \quad (6.6)$$

where  $\dot{m}$  is the flow rate and  $h_2$  and  $h_3$  are the respective enthalpies at Points 2 and 3. The engine efficiency would not improve, but the use of the heat rejected would improve the economic efficiency such that the Rankine cycle might be

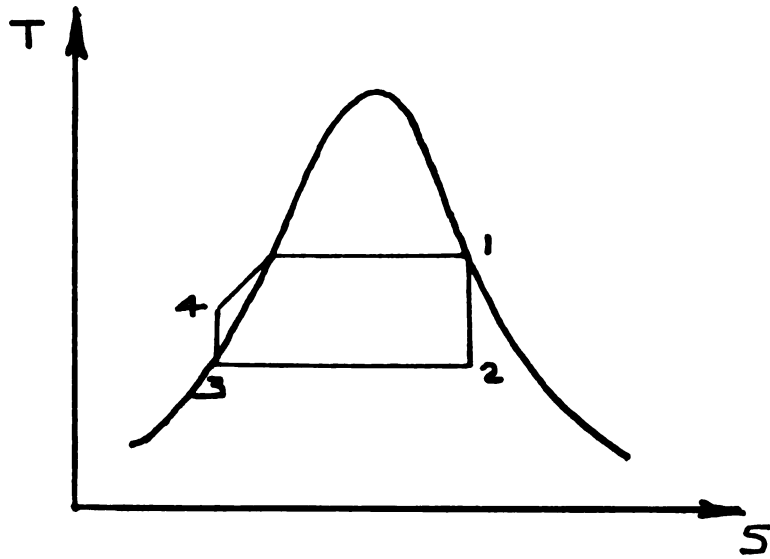


FIGURE 6-4. Rankine Cycle.

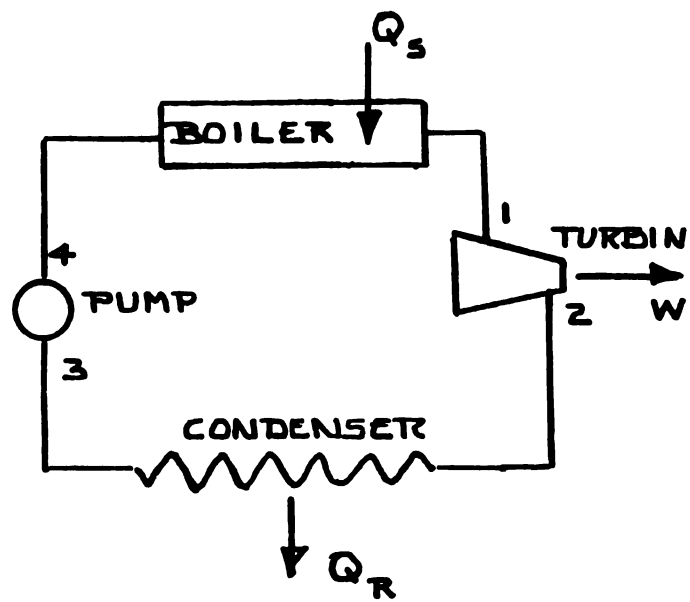


FIGURE 6-5. Rankine Cycle Schematic.

the best choice in certain cases. The hot air engine would have higher engine efficiencies but it would be difficult to capture the rejected heat. The Rankine efficiency is (15)

$$\eta = \frac{m(h_1 - h_2)}{m(h_1 - h_4)} \quad (6.7)$$

where the enthalpies,  $h$ , are references in Figures 6-4 and 6-5.

There are a number of ways to improve the Rankine cycle efficiency with such devices as reheaters or regenerators. These changes in the basic system must be justified economically. Since many of the engines are relatively small, it appears that the simple cycle without the frills should be used, and the condenser heat will be utilized for heating in cold climates.

### 6.3 Ericsson Cycle

The Ericsson cycle and the Stirling cycle are similar in design. The literature seems conflicting on how the engine worked, but actually Ericsson built one engine after another. It is possible to explain these discrepancies in the fact that details of operation on one engine may not fit another and good business practice protected trade secrets. In New York in 1870, Ericsson built his first "sun motor". The engine was steam driven and used a Rankine cycle. Another engine of different construction was designed and two or three experimental engines were built in 1874 (Churchill, 1935).

In a letter Ericsson wrote to a business associate, Harry Dilamater, he enthusiastically described how small caloric engines were unreliable because of valve adjustment. He then designed an air engine without valves. "Having found, by long experience, that small caloric engines cannot be made to work without fail, on account of the valves getting out of order, the above solar engine is operated without valves, and is therefore absolutely reliable" (Churchill).

In Figure 6-6 is one of Ericsson's hot air engines.

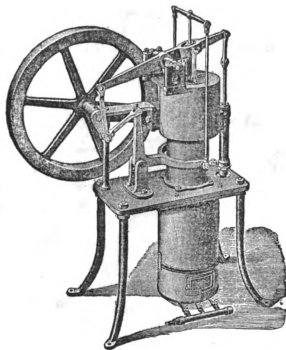


FIGURE 6-6. Solar Engine Adapted to Use Hot Air in 1880 ( 3)

In Figure 6-7 is a schematic of an Ericsson Engine using valves. The engine also resembles a Brayton cycle. The charging piston pumps air into the heating chamber where, with valves closed, the heat is added at constant volume. (The Brayton cycle adds heat at constant pressure.) The valves open and the pressure produces work on the piston.

The work piston would then vent the air through the regenerator (not shown) and out.

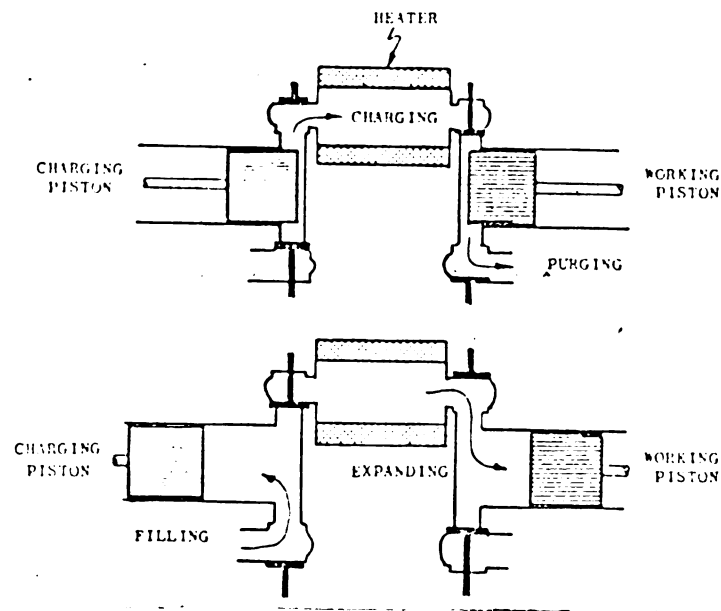


FIGURE 6-7. Schematic of One Type of John Ericsson's Hot Air Engine (Mernel).

The exact thermodynamic cycle that Ericsson's engine followed is uncertain. Most texts accept Figure 6-8. However, the engine of Figure 6-7 would not follow this cycle.



The engine has an isothermal compression from 1 to 2, an isobaric heating of the gas in the regenerator from 2 to 3, an isothermal expansion from 3 to 4, and an isobaric cooling in the regenerator from 4 to 1. The efficiency of this cycle is the same as a Carnot efficiency.

$$\eta = \frac{Q_s - Q_r}{Q_s} = \frac{T_H(S_4 - S_3) - T_L(S_1 - S_2)}{T_H(S_4 - S_3)}$$

$$S_4 - S_3 = S_1 - S_2$$

$$\eta = \frac{T_H + T_L}{T_H}$$

(6.8)

$$\eta = 1 - \frac{T_L}{T_H}$$

(Ericsson Cycle Efficiency)

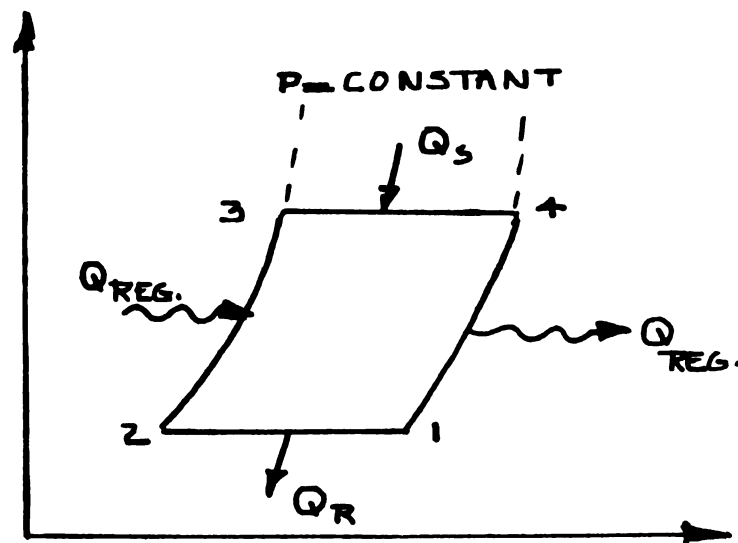


FIGURE 6-8. Ericsson Cycle.

#### 6.4 Stirling Cycle

The Stirling cycle, developed by Robert Stirling (1870-1878), is being studied for automotive applications using fossil fuel because of high theoretical efficiency (17). The engine has potential in reducing exhaust emissions that are associated with internal combustion engines.

The Stirling cycle consists of isothermal expansion and compression, and a constant volume addition and rejection of heat. The theoretical cycle shown in Figure 6-9 is an isothermal addition of heat from 1 to 2, and a constant volume rejection of heat from 2 to 3. This is accomplished by pushing the heated gas through a regenerator with high heat storing capacity.

There is an isothermal rejection of heat from 3 to 4. A constant volume addition of heat from 4 to 1 is accomplished by passing the cooled gas through the hot regenerator which adds energy back into the system.

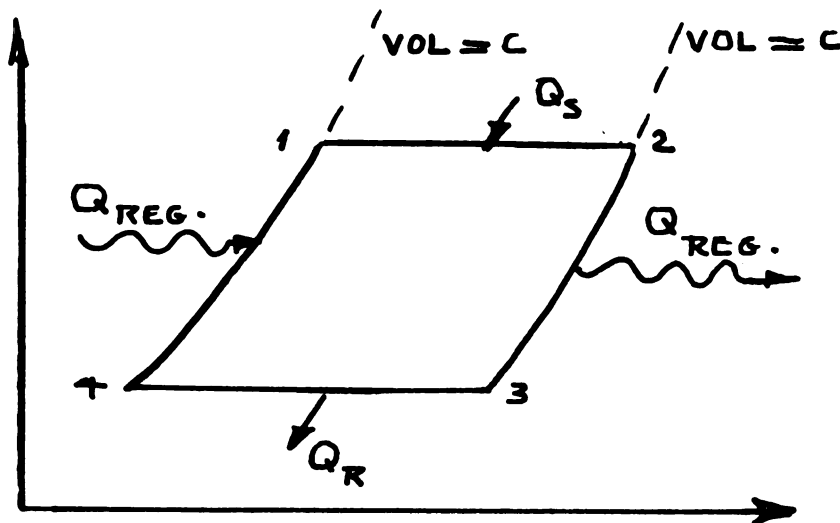


FIGURE 6-9. Stirling Cycle.

The Stirling efficiency is:

$$\eta = \frac{Q_S - Q_R}{Q_S}$$

$$Q_S = T_H(S_2 - S_1)$$

$$Q_R = T_L(S_3 - S_4) \quad (6.9)$$

$$\eta = \frac{T_H(S_2 - S_1) - T_L(S_3 - S_4)}{T_H(S_2 - S_1)}$$

$$\eta = \frac{T_H - T_L}{T_L} = 1 - \frac{T_L}{T_H}$$

Since July of 1972, N.V. Philips of Holland and Ford Motor Company have been trying to develop the Stirling engine for automotive applications (17). Ford's primary concern at that time was emission control which the Stirling could provide. Recently, Ford has abandoned the project temporarily because of other priorities, but not until tests were conducted on a 170 hp engine. One engine was tested on a dynamoter and one in a Torino test vehicle (17).

There was also a Ford/ERDA feasibility study made on an 80-100 hp Stirling engine. The car used was a 1976 Ford Pinto. The noise level was 10 dB below their current cars, but the fuel economy was 25 miles per gallon, lower than the desired 30 mpg. Engine friction and auxiliaries were blamed for the low efficiency. Emission objectives were not met either (17).

## CHAPTER 7

### A SOLAR ENGINE DESIGN

#### 7.1 Economic Comparison of Solar Designs

A new concept of design must precede the advent of solar mechanical power. Design technology used for fossil fuel engines cannot successfully be used on solar engines. Solar energy is essentially low density power. Fossil fuel is high density energy. The typical frictional horsepower of fossil fuel engines might exceed the brake horsepower of a solar engine. Solar engines are relatively slow and must be as frictionless as possible. One of the prime considerations is to introduce methodology to minimize friction. Another criteria in solar mechanical conversion is to use simple concepts. Simple concepts produce inexpensive engines which are necessary in order to have a cost-effective design. The investment in the capital must be recovered from the value of energy collected. The value of the energy collected would be based on a particular fossil fuel. If the logical competitor is diesel engines, then diesel oil would be used as an equivalent solar energy value.

Solar engines must be low cost, efficient, and, as previously stated, as frictionless as possible. The ideal engine would be cheap and efficient, but there are relationships between these platitudes that are important. If an engine were very efficient and very expensive, this engine might be rejected and an inexpensive low efficiency engine

chosen. The relationship between efficiency and cost is determined by cost-effectiveness. This concept was discussed in Chapter 5, but must be constantly stressed. The break-even cost of a solar engine as compared to a diesel engine was given by Equation 5-5. This equation related equivalent power from each engine. In this selection of one solar engine design versus another, (7.1) is applicable. Equation 7.1 gives the savings over N years.

$$\text{Savings} = (\eta I_b A_c C_3 N) . 009 - C_1 - C_2 \quad (7.1)$$

where  $\eta$  = overall efficiency.

$I_b$  = beam radiation ( $\text{kJ}/\text{m}^2\text{day}$ ).

$A_c$  = aperture area of concentrator ( $\text{m}^2$ ).

$C_3$  = cost of fuel oil/liter ( $\$/\text{liter}$ ).

$N$  = number of years of life.

$C_1$  = initial cost.

$C_2$  = total maintenance cost.

Equation 7-1 is based on simple payback, and no investment consideration was made. The engine design that would give the maximum savings from (7.1) should be the preferred design. From this equation, it is easily seen that at higher fossil fuel costs ( $C_3$ ), the more probability that a solar engine will be cost effective. The cost of the engine ( $C_1$ ) and the reliability which shows up as maintenance costs ( $C_2$ ) enter logically into this relationship.

## 7.2 Engine Design to Minimize Cost

One major factor in the success of getting mechanical power from the sun is to start with a simple concept. Ericsson and Stirling cycles have operated from the sun. Both engines will reveal one fault. The engines were not simple. A displacer moves back and forth pushing a gas into and out of the hot zone, and in general, both engines are somewhat complex. The Rankine cycle (steam engine) is simpler in design, but becomes more complex when a boiler, condenser, and pump must be added. The three cycles, Ericsson, Stirling, and Rankine cycles, should not be excluded from consideration, but these systems should be viewed as maximum in complexity. Successful solar engines will need to be simpler whenever possible.

Solar engines may find their initial application in pumping water in arid climates. A very simple device for pumping water is shown in Figure 7-1. Savery's ( 4 ) steam pump is operated by opening the steam valve which pressurizes the top of the tank forcing the water out and up through the discharge line. The steam valve would be shut and cooling water would flow over the tank. As the steam condensed, a vacuum would form allowing water to be pushed by the atmosphere into the tank.

By exploiting the idea of Savery's steam pump, a low cost solar pump concept can be developed. Since there are heating and cooling cycles in the steam pump, two complete systems are needed with a means of shifting the heating and

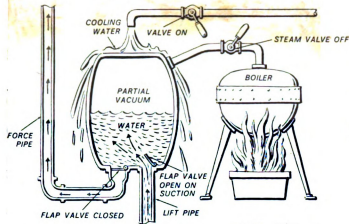


FIGURE 7-1. Savery's Steam Pump.

cooling modes at the proper time. Two identical tanks with check valves in the inlet and outlet area are required. Attached to the side of the main tanks are receivers. The receivers absorb solar energy and produce pressure by boiling water trapped in the chamber. Flexible hoses connect the receiver to the main tank. The two receivers are insulated from one another, but they are mechanically fastened together. A one-way hydraulic cylinder with a spring return is attached to the two receivers. When the pressure builds up high enough, the hydraulic cylinder will shift the heating-cooling mode. The system is sketched in Figure 7-2.

The simplicity of the system will result in a cheap pump. The four check valves and the spring loaded hydraulic cylinders are standard pieces of hardware. The rest of the apparatus is built by the fabricator of structural steel components. There would be a minimum of machining and very

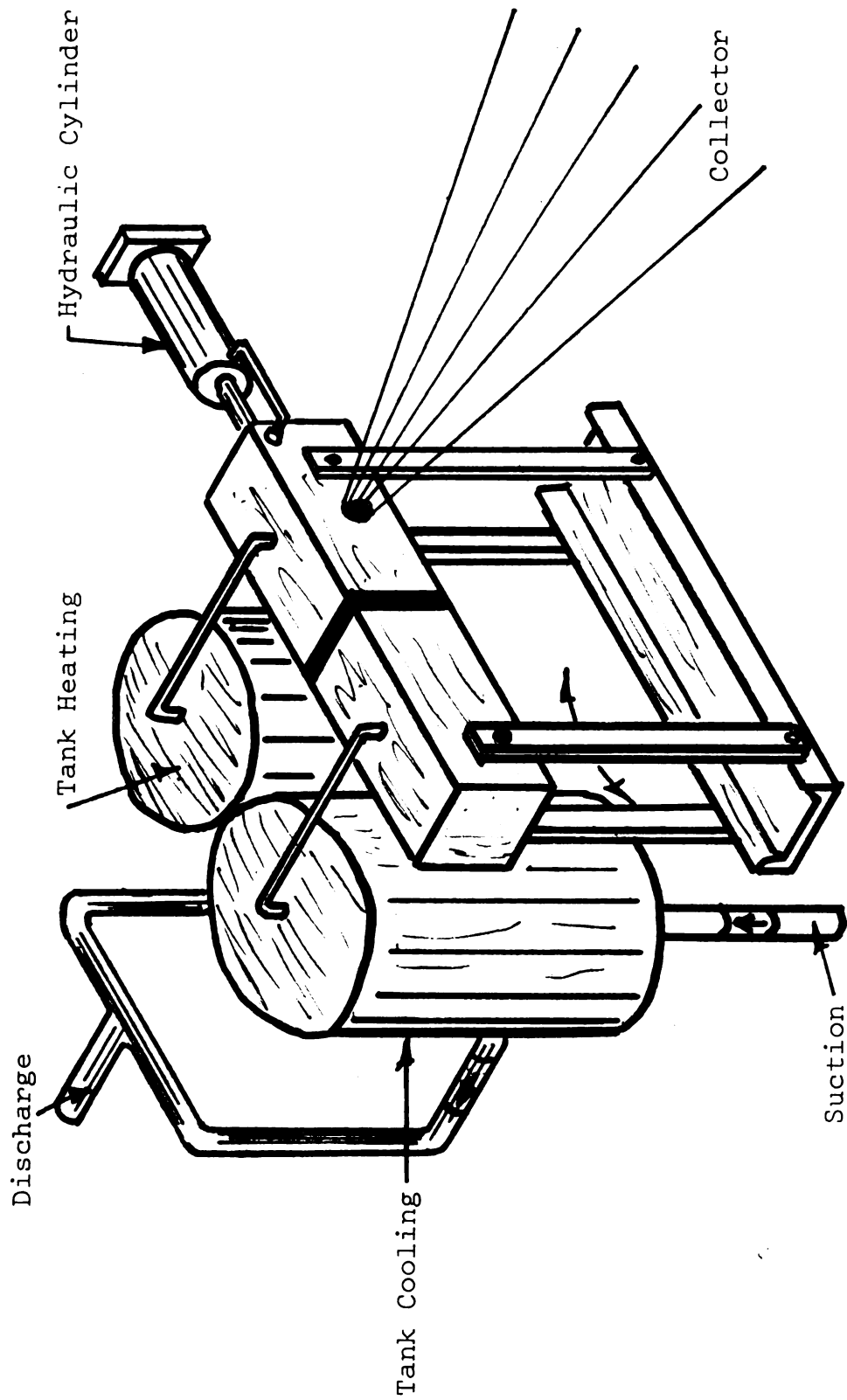


FIGURE 7-2. Solar Pump.





little precision fabrication. Most of the structure would be assembled by welding and punching operations. A lower cost pump would be difficult to perceive.

The recharging of the receivers with water could be done by the proper location of the flexible hoses on the side of the tank.

Another type of design developed by the author is the rotating air or gas engine. It became obvious that valves and displacement pistons were items that contributed greatly to the cost. The design goals were to eliminate both of these elements.

Shown in Figure 7-3a is a section through the new rotating engine. The construction consists of a fixed crank shaft with opposed pistons. The housing rotates and power is extracted from a gear or sprocket (not shown) attached to the housing. The solar concentrator hits an energy conducting ring that is something less than half a circle. One ring is being heated which pressurizes the gas inside the ring. The other ring is being air or water cooled since the ring is outside the focal point of the solar concentrator. A frontal view is shown in Figure 7-3b. Each heat conducting ring is divided into two parts. From A to B the ring surface is transparent or very readily conductive. With the energy being quickly added to the ring while the piston is near top dead center, the effect of adding energy at a constant volume is achieved. From B to C the rate of heat transfer is lessened by alterations in the energy

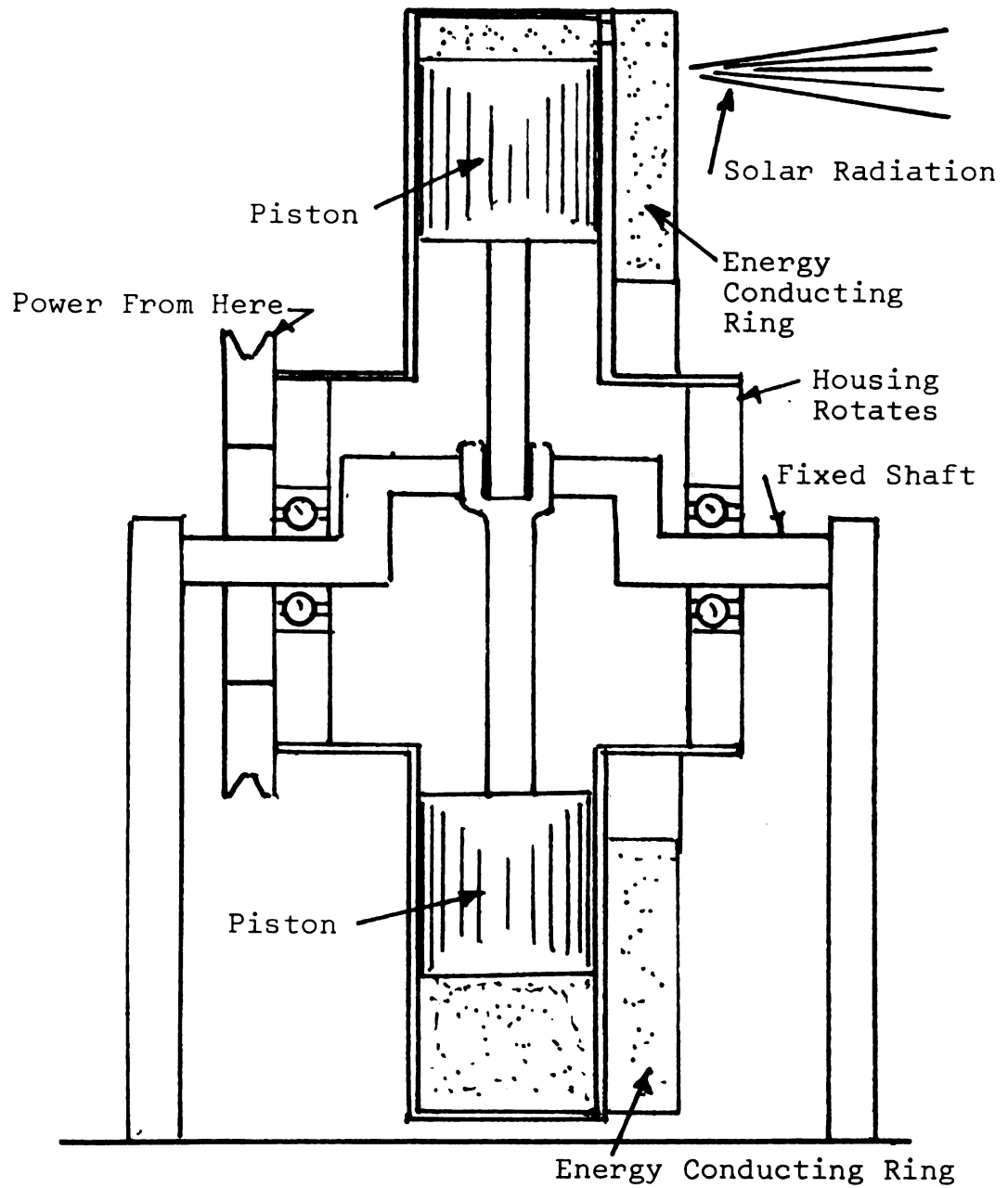


FIGURE 7-3a. Solar Engine Front View.

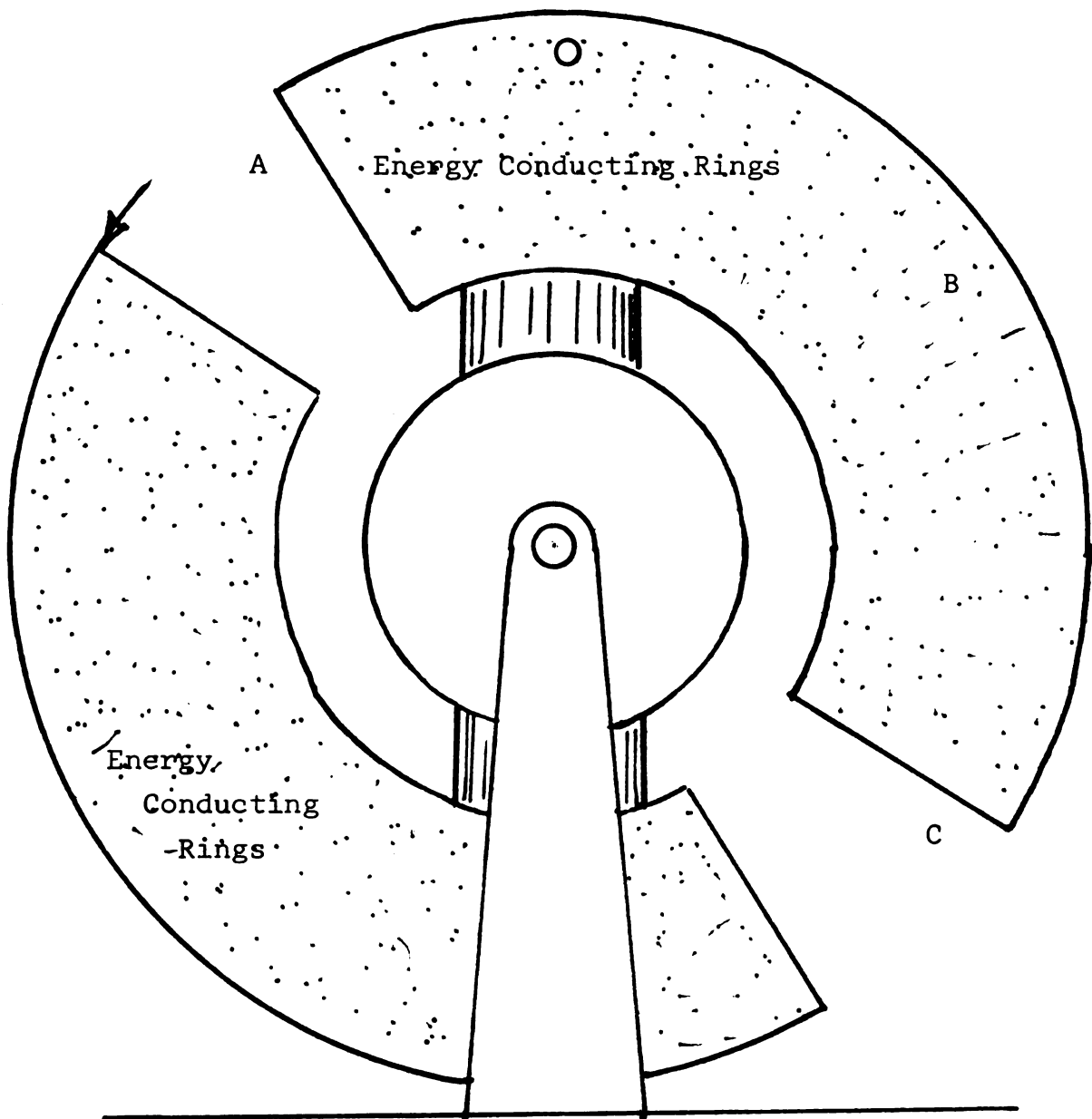


FIGURE 7-3b. Solar Engine Side View.

conducting ring. The surface could be thickened to reach the isothermal addition of heat which is necessary to have the theoretical efficiency equal to a Carnot cycle.

The cooling cycle would be more difficult to regulate for a tracing of a theoretical Stirling cycle. A coolant sprayed at one point  $180^\circ$  opposite the solar concentrator would produce the desired results.

Having the engine retrace a Stirling cycle would produce a theoretical cycle efficiency equivalent to the Carnot cycle. However, practical considerations must be made when using solar power. The sun cannot be regulated. If surfaces of the heat ring are operating at controlled temperatures just to proclaim high theoretical efficiency, it is obvious that available solar power would not be used. This would decrease the overall efficiency regardless of the theoretical analysis. The theoretical analysis considers only the temperature of the gas inside the engine. This analysis assumes the source is controllable. The future heat rings may just absorb the maximum energy over a somewhat shortened heat ring.

The rotating solar engine is conceptually simple. There are two power strokes per revolution. There are no mechanisms to displace air from the hot and cold zones. There are no valves. The simplicity of the engines meets the solar engine criteria of being non-complex.

In modifying the heat ring in the development process of the rotating engine, another useful element was

discovered. A new type of engine fulfilling the concept of being simple became possible. The details are discussed more thoroughly in Chapter 9. The engine is operated from a flat plate collector which is sealed and charged. The collector is connected to a piston of the design discussed in the following section. The cooling cycle can be accomplished in a number of ways. One possible system is shown in Figure 7-4. Another would be to use the pumped water to cool the collector. Solar energy enters the collector. The temperature and the pressure increase. The piston moves down which pumps water. A cable attached to the piston arm pulls a shade over the collector for the necessary cooling cycle. The pressure drops. The shade is removed. The system returns to the starting point where the process can be repeated.

### 7.3 Minimizing Friction in Solar Engines

Frictional losses must be reduced to a very low level in solar engines. The method of design used for fossil fuel engines will not in general be accepted in solar technology. Friction is developed in several areas. The largest and most difficult to overcome is the piston friction against the cylinder walls. Another source is the piston rod guide bushing that keeps the piston and cylinder concentric. Friction is also developed in the main bearings and the connecting rod bearings. All of this discussion assumes that reciprocating machinery is being used. Rotating machinery is a choice that is possible, but it is believed

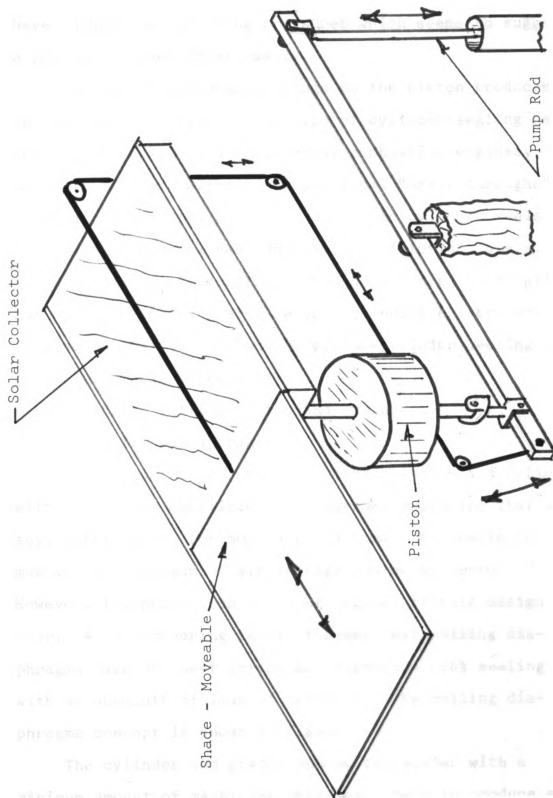


FIGURE 7-4. Flat Plate Solar Engine.





that cheaper equipment can be manufactured using reciprocating devices. Also, cost effective solar engines may have rather low operating pressures which seems to suggest a piston-cylinder arrangement.

The use of compression rings on the piston produces too much wall friction. This type of cylinder sealing has been successfully used in internal combustion engines, but will not work without technological "break-throughs" in solar engine applications. Hydraulic cylinder seals or "O" rings in general have unacceptable friction levels. There are materials available that do not need lubrication, but normally the synthetic seals will require lubrication. It appears that two methods of piston-cylinder sealing are possible. These types are:

1. Close fitting piston and cylinders.
2. Rolling Diaphragms.

It is possible to produce matched pistons and cylinders with compatible coefficients of thermal expansion that will seal sufficiently for most applications. By precision machining a minimum of air leakage can be achieved. However, the production costs of engines of this design will soar. At a pioneering level it seems that rolling diaphragms have the best potential to provide 100% sealing with an absolute minimum of friction. The rolling diaphragms concept is shown in Figure 7-5.

The cylinder and piston can be fabricated with a minimum amount of machining which will help to produce a

cost effective engine. The disadvantage from economic considerations is the guide that is essential in this design. The piston must be held concentric within the cylinder and the additional bearings add to the cost.

The fabric stresses of the diaphragms are given in the lbs. per inch and are easily calculated. Let "C" equal the radial clearance between the piston and the cylinder. The approximate area upon which the pressure reacts is given by equation

$$A = \pi DC \quad (7.2)$$

where D is the piston diameter and C is the clearance. As can be seen in Figure 7-6, the force,  $F_t$ , must support pressure.

The downward force equals

$$F = P\pi DC \quad (7.3)$$

where P is the gage pressure inside the cylinder. The fabric force,  $F_t$ , equals:

$$F_t = 1/2 P\pi DC \quad (7.4)$$

The fabric stress in lbs. per inch is given by (7.5)

$$S_t = 1/2 P\pi DC / \pi D \quad (7.5)$$

$$\text{or} \quad S_t = 1/2 PC$$

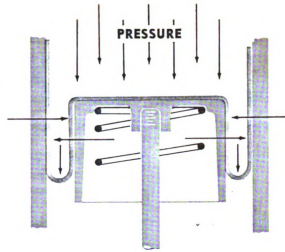


FIGURE 7-5. Rolling Diagrams Concept.

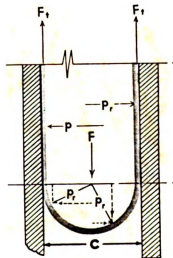


FIGURE 7-6. Free Body Diagram of Side Walls of Diaphragm.

Fabric stresses in many available materials can exceed 8 lbs. per inch. If a 4 inch diameter cylinder with a convolution width (C) of .125 were used a pressure of 128 lbs./in<sup>2</sup> could be safely contained.

Manufacturers state that pressure can range from 1 inch of water to 3,000 psi in special cases. However, pressure is directly proportional to the fabric stresses. At elevated temperatures, heat degradation occurs in most materials. Currently, ranges of -85° F to 550° F in operating temperatures have been encountered. By using special materials, temperatures above 700° have been affronted. At the elevated temperatures, stresses must be reduced. Therefore, there is a limit in pressure and temperature that most rolling diaphragms can sustain. Future technological advancement in rolling diaphragms will be made if manufacturers know there can be a demand for their product in solar engines.

Relatively large strokes are available with this system. In Figures 7-7 and 7-8 the piston is shown at top dead center and bottom dead center respectively.

$S_A$  is the upstroke,  $S_B$  is the downstroke. The companies making rolling diaphragms have specifications that limit these dimensions. In Table 7-1 are samples of sizes.

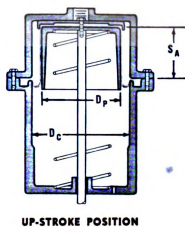


FIGURE 7-7. Diaphragm, Up-Stroke Position.

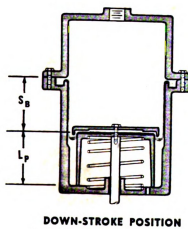


FIGURE 7-8. Diaphragm, Down-Stroke Position.

TABLE 7-1. Typical Sizes of Diaphragms (25)

Cylinder Bore ( $D_c$ )	Piston Dia ( $D_p$ )	Convolution (C)	Height of Diaphragm (H)
2.75	2.44	5/32	2.75
3.00	2.69	5/32	3.00
3.25	2.94	5/32	3.25
3.50	3.19	5/32	3.50
4.00	3.69	5/32	4.00

The maximum upstroke,  $S_A$ , or the maximum downstroke,  $S_B$ , is given by (7.6):

$$S_A = S_B = H - .90625 \quad (7.6)$$

From the table, and (7.6), it can be seen that a 4 inch cylinder could be fitted with a standard diaphragm that would have approximately a 3 inch up and down stroke. The total stroke for a 4 inch bore would be about 6 inches (25).

Cycle life of diaphragms is not objectively known. There is indication that they have a long flex life. In some cases 100 million cycles have been experienced. If a solar engine were turning at 300 rpm for 8 hours a day, 100 million cycles would give at one flex per revolution:

$$\frac{100 \times 10^6 \text{ cycles}}{300 \frac{\text{cycles}}{\text{min}} \times \frac{60 \text{ min}}{\text{hr}} \times \frac{8 \text{ hr}}{\text{day}}} = 694 \text{ days}$$

Nearly two years of operation could be expected at 100 million cycle life which would be adequate (25).

The author believes that rolling diaphragm is the best way to minimize cylinder friction in solar engines, but in conjunction with the rolling diaphragms, a guide bearing must be used. This topic is discussed in Section 7. The present level of diaphragm technology is adequate for pioneering efforts in solar engine design. Further research into the product should result in longer cycle life at elevated temperatures and pressures.

#### 7.4 Material Selection for Solar Engine Applications

As has been discussed in past sections, increasing the operating temperature will increase the efficiency. Therefore, future solar engines will probably have a trend of ever increasing head temperatures. At present, rolling diaphragms will somewhat limit the maximum working temperature. The other aspect of improved efficiency is to lower the temperature at the end of the expansion stroke. The efficiency is:

$$\eta = 1 - \frac{T_L}{T_H}$$

For Carnot, Ericsson and Stirling cycles, it is as important to reduce  $T_L$  as it is to raise  $T_H$ . Long stroke engines would tend to lower  $T_L$  as can be seen from the ideal gas law, but it would also raise the compression ratio which has limitations.

In hot air engines the temperature problems occur where the beam strikes the device. The equilibrium temperature that a machine element reaches depends upon several factors such as concentration ratio, environmental conditions, and the work output. energy in the form of heat is applied to an engine, heat is transferred away, and energy is taken out in the form of work. Material failure will occur most likely through high temperature failures. Creep or deformation failure will result. While operating, the engine elements, piston and cylinder, will be at their lowest temperature because of energy loss in the form of work.

The probable time for high temperature failures will happen during static conditions. Engine materials will require shielding or orientation away from the sun while inoperative. By using (3.35) and neglecting the energy that is carried away, the engine equilibrium temperature can be obtained

$$\text{Heat in} = \text{Heat out}$$

$$A_a I_b n_o \alpha = U_L A_r (T_r - T_a) \quad (7.7)$$

where  $U_L$  is defined by (7.8)

$$U_L = \frac{1}{1/h_o + 1/\epsilon_r (T_r^2 + T_a^2) (T_r + T_a)} \quad (7.8)$$

There are a number of basic properties that need to be considered when selecting materials to be used in solar engine design. Some of the major physical characteristics



that are important are:

1. Creep, yield strength, and fatigue strength at elevated temperatures.
2. Thermal conductivity.
3. Corrosion resistance at elevated temperatures.
4. Workability.
5. Cost.

The effect of increased temperature is to decrease the strength of materials. Such consideration must be made in conjunction with the other characteristics listed above. Given in Table 7-2 is the effect of temperature on the strength properties (29).

Creep is the time dependent deformation of materials that occur under constant temperature and stress.

The phenomenon of creep in metals (slow flow) increases with temperatures and stresses. In an engine and particularly a solar engine, creep will be an important consideration. A typical creep curve is shown in Figure 7-9 (24).

$\epsilon_0$  is the original strain that was placed on the test specimen. As a particular temperature  $T_1$  the strain consists of the initial strain  $\epsilon_0$  and the strain from creep  $\epsilon_c$ .

The initial part of the curve A-B represents the primary creep stage. The creep rate decreases during this primary stage. At Point B, the creep rate slows and remains practically constant. The second B-C is termed the secondary creep stage or the stage of quasi-viscous flow. The section B-C usually is very lengthy and terminates near C

TABLE 7-2. Effect of Temperature on Material Strength (26)

MATERIAL	Temperature ° F									
	70	300	450	500	600	750	950	1000		
Aluminum Bronze (5%) Yield psi	27740		15645		18420	6425		6230		
Red Brass Rolled Yield psi	45000	43200	39100		23735	15050				
Cold Rolled Shafting Yield psi	76800	77100	72850		54275		30400			
Iron Cast Tensile psi	22060	23260	20730		21240	21925		19820		
Iron Mall. Tensile psi	37625	33505	33280		34000	34055	27110			
Steel Cast Yield psi	39817	34020	34276		29422	27223	9650			

by either a brittle fracture or a ductile fracture with more deformation.

Creep is mainly a high-temperature process in most engineering material. Creep can occur at low temperatures but is not of any practical importance. It has been found that the temperature where creep becomes significant is related to the alloy's melting point. As the temperature is raised above  $0.3 T_m$  ( $T_m$  = melting temperature) creep is an important consideration (26). Equation 7.9 states this principle

$$T \leq 0.3 T_m \quad (7.9)$$

where  $T$  is the metal's operating temperature, and  $T_m$  is the melting temperature of the material.

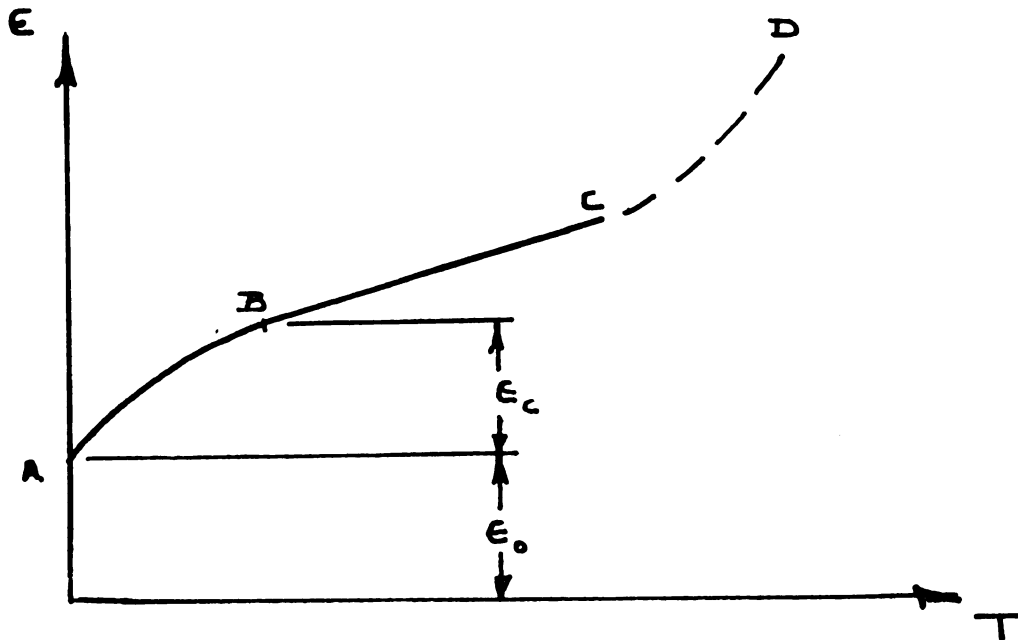


FIGURE 7-9. Typical Metallic Creep Curve.

As an example, lead melts at 327° C, thus:

$$T = .3 \times 327 = 98.1^{\circ} \text{ C}$$

This would mean that lead used on roofs could creep under its own weight in the summer. Steel that melts at 1500° C would become a concern if temperatures of 450° C were encountered.

$$T = .3 \times 1500 = 450^{\circ} \text{ C}$$

This relation between the creep resistance and the melting temperature is accepted as only a very crude guide and should be used with caution. However, the simplicity of the relationship gives the solar engine designer a point of reference for concern.

Many equations have been proposed to represent the time laws for creep. If the instantaneous strain is neglected, (7.10) would present the strain (26).

$$\epsilon = K_t^{-n} \quad (7.10)$$

where  $\epsilon$  is the strain rate, K and n are constant and t is the time. If the time is sufficiently large before failure occurs, users of solar mechanical devices will accept this as normal depreciation. In most cases, solar engine failures will not present a safety hazard and a certain amount of creep can be accepted.

Creep rates are very dependent upon stress. This

relationship of stress to creep is given in (7.11)

$$\dot{\epsilon} = K\sigma^n \quad (7.11)$$

where  $\sigma$  is stress and  $K$  and  $n$  are constants (23). For pure metals and some alloys  $n$  has been found to range from 3 to 5. If the stresses are doubled, the creep rate will increase 8 times with  $n$  equal to 3, and 32 times with  $n$  equal to 5.

Much of literature is devoted to creep resistance with steady temperatures and steady stresses. It has been thought that by using the results of steady state tests, conservative design procedures would result. There is some evidence that there is a weakening effect with non-steady state systems and thus possible decrease of creep resistance should be kept in mind (23).

Fatigue failure also increases with increasing temperatures. There are a number of other factors that affect fatigue strength besides temperature. The nature of the surface has much to do with fatigue value. In general, the rougher the finish of the machine element, the lower the fatigue strength. Steels show improvement in fatigue strength by mechanically working the surface. A process such as shot peening will improve the fatigue strength (28).

The relationship between the surface finish and the ultimate strength is given in Figure 7-10. Note the ultimate strength decreases as temperature increases.

The fatigue life of three steels as temperature is increased as shown in Figure 7-11.

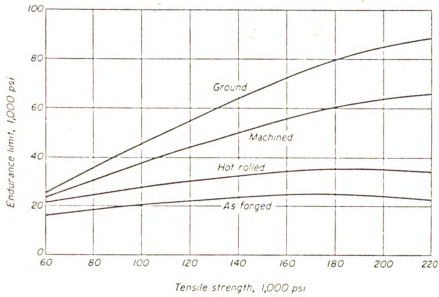


FIGURE 7-10. Fatigue Strength As a Function of  $\sigma_{ult}$  and Surface Finish (28).

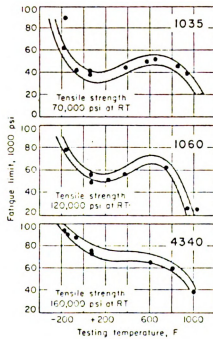


FIGURE 7-11. Effect of Temperature on the Fatigue Limits of Steels (26).

The last material characteristic to consider is thermal conductivity. Thermal conductivity is of prime importance in and out of the engine. Without successful transfer of energy, the engine will not operate. Therefore, top priority must be given to thermal conductivity. In Table 7-3 are given thermal conductivities of various metals.

TABLE 7-3. Thermal Conductivities of Various Metals (26)

METALS	68° F	k in BTU/hr-ft F				
		212	392	572	752	1112
Pure Aluminum	118	119	124	132	114	
Al-Cu (95%, 5%)	95	105	112			
Al-Si (86.5%, 12.5%)	79	83	88	93		
Carbon Steel						
0.5%	31	30	28	26	24	20
1.0%	25	25	24	23	21	19
1.5%	21	21	21	20	19	18
Nickel Steel						
20% Ni	11					
40% Ni	6					
Chrome Steel						
1%	35	32	30	27	24	21
5%	23	22	21	21	19	17
Pure Copper	223	212	216	213	210	204

The solar receiver, the heat ring, has to withstand much higher temperatures. There is always the possibility of an engine held in the static operational mode. Without work being extracted, temperature much higher than normal will be encountered. With production engines, all the questions of this section must be answered. The prototype that is discussed in the next chapter is a prototype that was

built to prove the principle of operation. Some of the design was based on expediency of fabrication.

The selection of material used in future solar engines will be a challenge to the science of metallurgy. At the present level of technology of the rolling diaphragms, the operating temperature is somewhat limited. If pure aluminum were to be used, the temperature should be under 182° C (360° F) to keep from having creep problems. This temperature would be acceptable as an operating temperature for the diaphragms. The 1100 alloy, commercially pure aluminum, has a yield stress of approximately 9000 psi at 360° F with an H14 temper. This material has good corrosion resistance, but the most important physical property is the high thermal conductivity. The information for each material is easily found in the "Metals Handbook" (26).

### 7.5 Working Media in Solar Engines

The engine design is an integrated process. One component affects the next which affects the next, and so goes the procedure. The weakest link in the chain becomes the principle criterion for the design, and satisfying this limiting factor will help fix the design. In the rotating hot air engine, the temperature was fixed at 182° C (360° F) in the cylinder because of creep, and the temperature limits placed on the rolling diaphragms. It can be assumed that the operating media could operate at approximately 182° C (360° F) and 882,530 N/m<sup>2</sup> (128 psi) (lbs. per square inch



gage) from the working stresses allowed in the rolling diaphragm. (See Section 7.3.) With the temperature and pressure fixed, the working media can be intelligently chosen.

Rankine cycles would utilize condensing vapors. The rotating engine will require highly superheated gases. Condensation could cause trouble with the operation. To insure that condensation will not occur, a sketch of the temperature-entropy diagram is helpful. A T-S diagram of water is shown in Figure 7-12 (15).

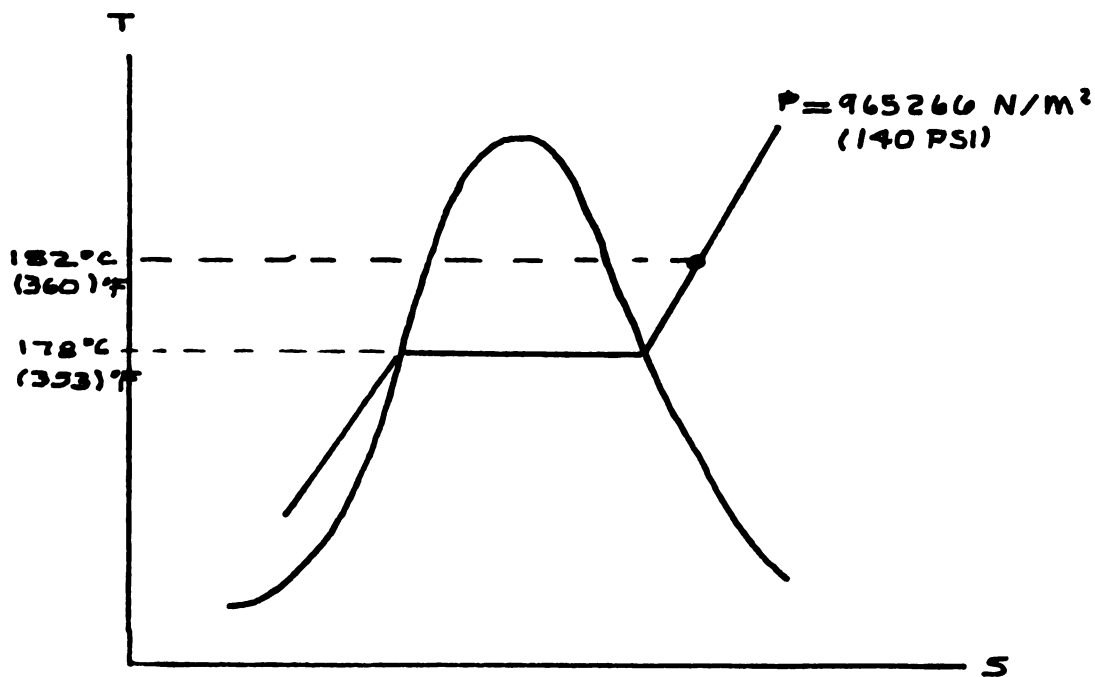


FIGURE 7-12. T-S Diagram of H<sub>2</sub>O.

The pressure and temperature maximums would be about  $965,266 \text{ N/m}^2$  (140 psia) and  $182^\circ \text{ C}$  ( $360^\circ \text{ F}$ ) which, as can be seen in Figure 7-12, is just barely in the superheated region.

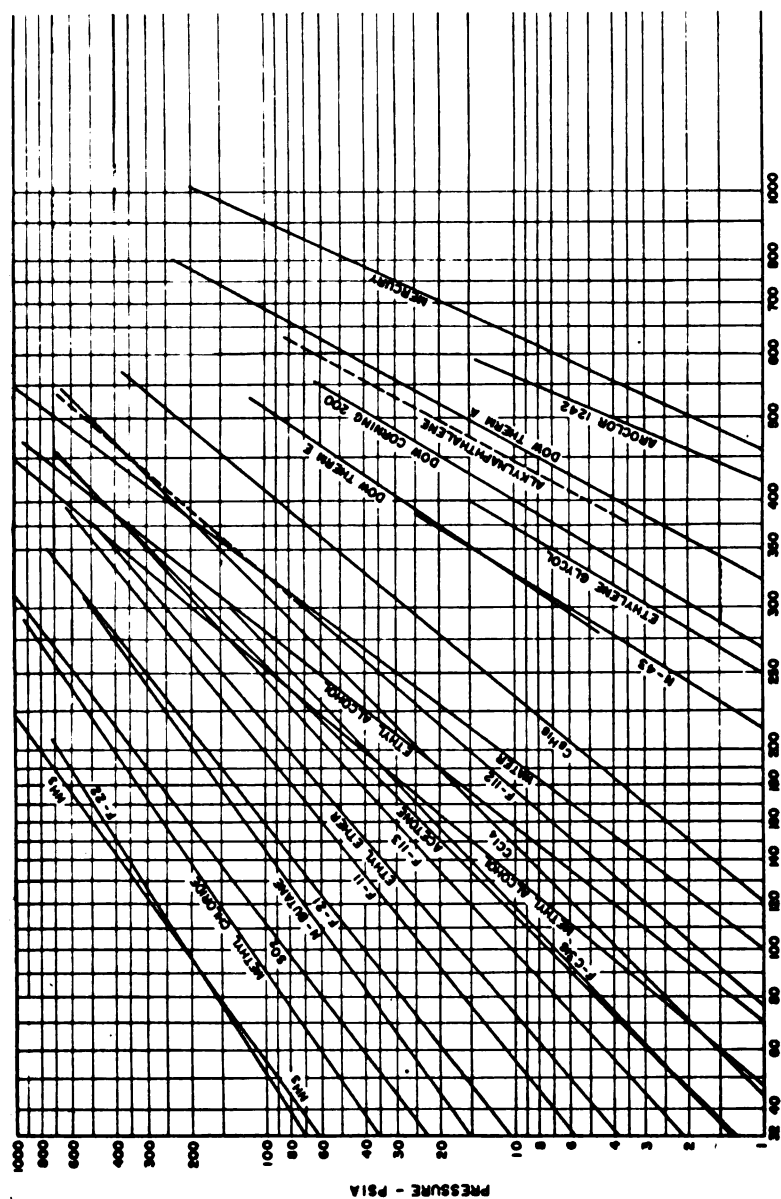
In Figure 7-13, vapor pressures for various working media are given ( 2). To the left the substance would be a liquid. As an example, by locating the point  $360^\circ \text{ F}$  and 140 pressure, the materials listed to the left would be in the superheated region given the two properties.

It can be seen from this figure that  $\text{NH}_3$ , F22, Methyl Chloride,  $\text{SO}_2$ , N-Butane, etc., would not stay in the superheated phase during the engine heating and cooling cycles. However, these materials are more applicable to the Rankine cycle since condensation is expected in the condenser. The proper substance would be selected from Figure 7-13.

In the rotating hot gas solar engine an ideal gas should be used. Air would make an acceptable gas if it were not for the corrosiveness of the oxygen, particularly at higher temperatures. Hydrogen is commonly used in Stirling engines. The ideal gas equation

$$\frac{PV}{T} = MR = \text{Constant} \quad (7.12)$$

shows that there is theoretically no advantage of one gas over another, since (7.12) equals a constant. The main consideration would be the chemical reaction of the gas with the machine components. Inert gases such as Helium and



Argon should be considered. It was found that Freon had definite advantages. This is discussed in Chapter 9.

### 7.6 Design of Machine Elements

It is not the intention of the author to cover topics in machine design that are readily found in texts on the subject. There are some unique areas in solar hot air engines that will require special treatment. Two of these areas are:

1. Thin wall cylinder design.
2. Guide Bushing and Transmission Angle.

The cylinder must both heat and cool. With the heat ring, less will be required of the cylinder for heat transmission, but in general the cylinder should be as thin as possible. The guide bushings were installed so that rolling diaphragms could be used to eliminate friction. Certain restrictions are involved to prevent the guide bushings from becoming a major source of friction.

The two basic problems are illustrated in Figure 7-14.

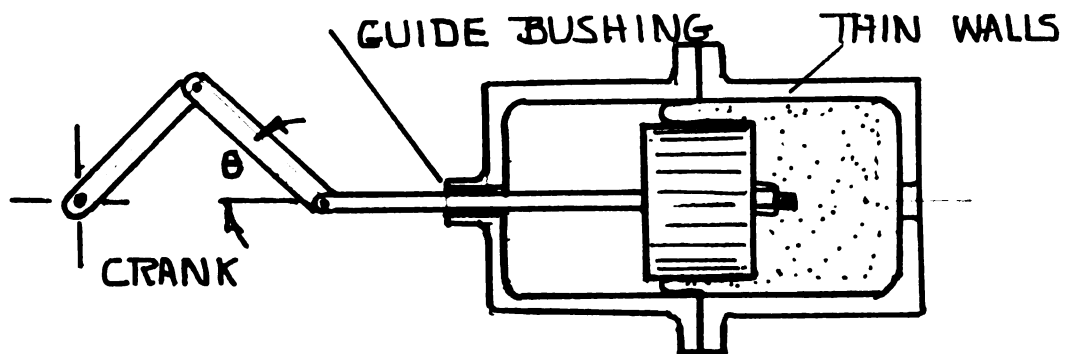


FIGURE 7-14. Hot Air Engine.

When the transmission angle,  $\theta$ , becomes large, heavy side loads are put on the bushing.

### Cylinder Design

The objective is to design the cylinder walls as thin as possible for good heat transfer. The first step to achieve this goal is to determine the working temperature using (7.9)

$$T \leq .3T_m \quad (7.9)$$

where  $T_m$  ° C is the melting temperature of the metal and  $T$  ° C would be the maximum working temperature.

Equation 7-9 defines the working temperature that is acceptable from a creep perspective. From this equation the yield stress is found at that particular temperature and with a suitable factor of safety, a working stress can be established. (See Table 7-4.)

As an example, assume 1100 alloy aluminum is used because of its superior thermal conductivity. From the "Metals Handbook" (26), the melting temperature is:

$$T_m = 1215^\circ \text{ F} = 657^\circ \text{ C}$$

The operating temperature would be:

$$T = (.3)1215 = 365^\circ \text{ F} = 185^\circ \text{ C}$$

The yield strengths for untempered 1100 aluminum is given in Table 7-4.

TABLE 7-4. Properties of 1100 Aluminum Alloy At Various Temperatures When Heated for 10,000 hr. (26)

TEMPERATURE		YIELD STRENGTH	
75 F	23.9 C	5,000 psi	34,474 kPa
300 F	148.9 C	4,500 psi	31,026 kPa
400 F	204.4 C	3,500 psi	24,132 kPa
500 F	260.0 C	2,000 psi	13,789 kPa
600 F	315.5 C	1,500 psi	10,342 kPa
700 F	371.1 C	1,000 psi	6,895 kPa

Interpolation of the 182.2° C (360° F) would give from Table 7-4 a yield stress of 3900 psi. With a factor of safety of an arbitrary 1.5, the working stress would equal:

$$\text{Working Stress} = 17,926 \text{ kPa (2600 psi)}$$

From the rolling diaphragm discussion in Section 7-3, the maximum pressure is 883 kPa (128 psi) inside the cylinder to avoid using a special diaphragm. The side wall thickness is calculated from the simple thin walled cylinder theory which is given in (7.13).

$$S_x = \frac{PD}{2t} \quad (7.13)$$

For a 4 inch cylinder the example described would give:

$$17,926.4 = 883 \times .106/2 \times t$$

$$t = .00261\text{m} = 0.1 \text{ inch}$$

The cylinder top thickness would be determined by using

the circular plate equation with clamped edges. The equation for stress at the center is (27)

$$S = \frac{3Pr^2}{4t^2} \quad (7.14)$$

where  $t$  is the plate thickness,  $P$  is the pressure in kPa,  $r$  is the radius of the cylinder. The maximum stress determined by Equation 7-14 is at the edge.

In our example the cylinder top is:

$$17,926.4 = 3 \times 883(.10612)^2/4t^2$$

$$t = 0.01019\text{m} = .4 \text{ in}$$

#### Guide Bushing

The initial step in designing the guide bushing is to determine the reactions at the extremities of the bushing. If the forces are excessive, two bushings are needed with the proper spacing. The piston pressure in general is known, as is the piston area. The reaction force would be the pressure multiplied by the area. The vector relationship is shown in Figure 7-15.

The downward reaction on the end of the piston rod is

$$F_y = PA \tan \theta_2 \quad (7.15)$$

where  $P$  is the piston pressure,  $A$  is the piston area and  $\theta_2$  is the angle between the piston center line and the connecting link. The reaction  $R$  on the outside of the

bushing would be given by summing the moments

$$R = F_y \frac{X_1}{X_2} \quad (7.16)$$

where  $X_1$  and  $X_2$  are the length of rod extension and the bushing length respectively.  $F_y$  is found from Equation 7.15. The value of  $R$  is the force that the guide bushing sustains without binding.

Bearing loads are determined mainly by experience. In Table 7-5 is a table of current practice for rotating shafts. The application is somewhat different in that there is linear motion through the bushing.

However, the same wedging mechanism that keeps the rotating shaft supported on an oil film is present to a certain degree in a linear bushing. The pressure in a linear bushing would range from minimum on the outer edge to zero somewhere internally.

Using the rotating hot air engine as an example, the connecting link is 4.5 inches and the pitman arm is 2 inches. At a rotational angle of 45 from the machine center line, the angle  $\phi_2$  defined in Figure 7-15 is 18.31. The  $F_y$ , from (7.15) using a 4 inch piston with 883 kPa (128 psi) pressure, is 2366N (532 lbs). Assuming a force distribution as shown in Figure 7-16, the average force would be  $R/2$ .



TABLE 7-5. Bearing Design Pressure (29)

<u>TYPE OF BEARING</u>	<u>DESIGN PRESSURE IN PSI</u>
Diesel Engine Mains	800-1500
Connecting Rods	1000-2000
Wrist Pins	1800-2000
Electric Motor	100-200
Marine Lineshaft	25-35
Steam Turbine and Reduction Gears	100-250
Automotive Gas Engine Mains	500-700
Connecting Rods	1500-2500
Air Craft Connecting Rods	700-2000
Centrifugal Pumps	80-100
Railway Axle	300-350
Light Lineshaft	15-25
Heavy Lineshaft	100-150

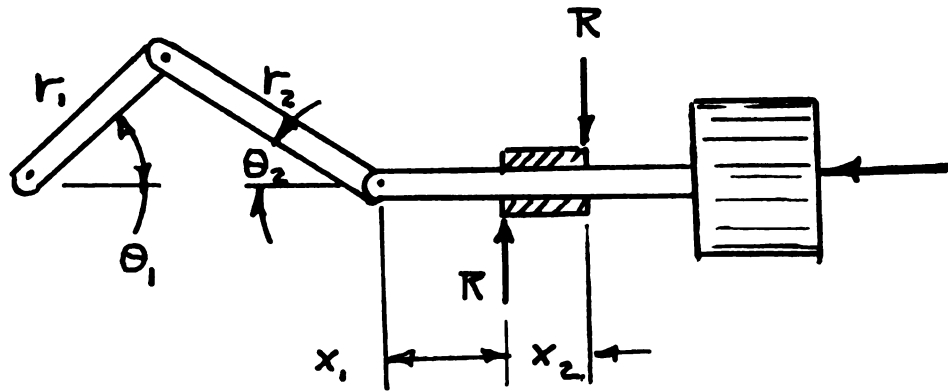


FIGURE 7-15. Forces on the Guide Bushing.

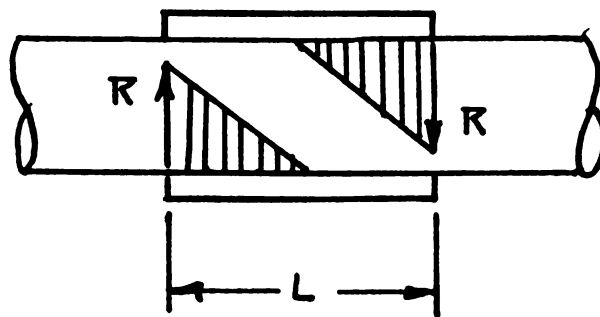


FIGURE 7-16. Force Distribution in Bushing.

The average pressure in the example would be

$$P = \frac{R}{2D \times L/2} = \frac{R}{LD} \quad (7.17)$$

where L is the bearing length, D is the diameter, and R is the reaction from (7.16). The pressure from the example is calculated to be:

$$P = \frac{532}{1 \times 1/2} = 7336 \text{ kPa (1064 psi)}$$

This amount of pressure caused metal to metal contact in the bushing, and excessive friction made the first engine inoperative. The bronze bushing was replaced with a Thomson ball bushing. It appears that pressures in a standard bronze bushing must be much less than 689 kPa (100 psi). Further research is needed in this area if this design is to be used. Considering Table 7-5, it would be expected that pressures under 689 kPa would be required. This lower pressure can be achieved in several ways. The bushing length "L" can be increased. If the length is excessive, two bushings can be used with a space between them. The stroke length could be shortened, which would decrease the angle  $\theta_z$ , or  $r_2$  could be lengthened.

It appears that the best solution would be to use linear ball bearings. A picture of the ball bushing is presented in Figure 7-17.

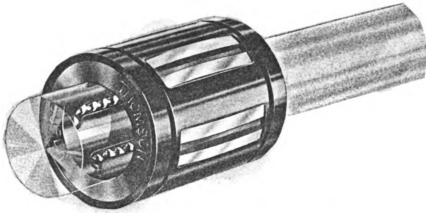


FIGURE 7-17. Typical Ball Bushing.

The engineering procedure to size a ball bushing is as follows:

1. Find the minimum allowable bushing size using (7.18). Use Figure 7-16 to find  $K_L$  in (7.18). Locate the bushing from the sample Table 7-6.
2. Compute the allowable load capacity from (7.19).
3. Predict the travel life expectancy from (7.20).
4. Find the minimum allowable shaft hardness from (7.21).

The minimum allowable bushing size is (25)

$$R_R = \frac{R_{av}}{K_L \times K_H} \quad (7.18)$$

where  $R_R$  is the rolling load rating,  $R_{av}$  is the average load capacity and  $K_L$  and  $K_H$  are found from Figures 7-19 and 7-20 respectively.

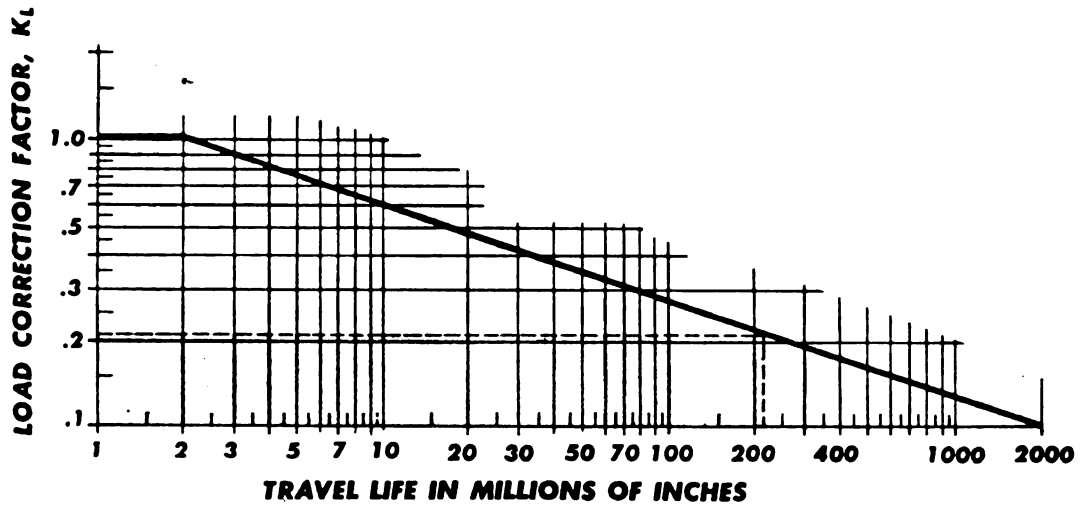


FIGURE 7-19. Ball Bushing Design Chart (25).

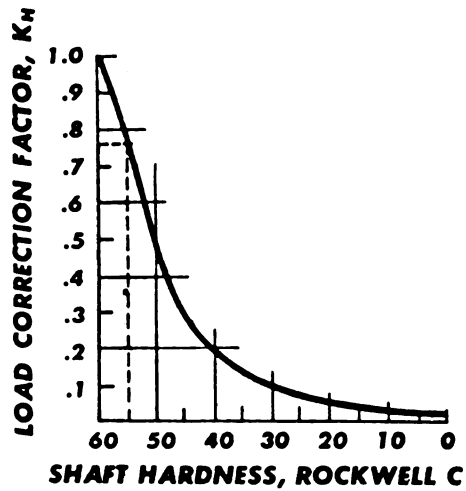


FIGURE 7-20. Ball Bushing Design Chart (25).

The allowable load capacity is calculated from (7.19)

$$R_A = K_L \times K_H R_R \quad (7.19)$$

where  $R_A$  is the allowable load capacity and  $R_R$  is the rolling load rating from (7.18).  $K_L$  and  $K_H$  are found from Figure 7-19 and 7-20. The difference between the allowable load capacity,  $R_A$ , and the rolling load rating,  $R_R$ , is based on a travel life of  $2 \times 10^6$  inches with a Rockwell 60C shaft hardness. The allowable load capacity is an adjustment for any variations from these initial specifications.

By reading the proper  $K_L$  which is found from (7.20), the travel life can be estimated.

$$K_L = \frac{R_{av}}{R_R \times K_H} \quad (7.20)$$

where  $R_{av}$  is the average load capacity actually on the bushing,  $R_R$  is the rolling load rating and  $K_H$  is selected from Figure 7-20.

The shaft hardness can be computed from:

$$K_L = \frac{R_{av}}{R_R \times K_L} \quad (7.21)$$

$K_H$  is used in Figure 7-20 to select the proper shaft hardness. The terms of (7.21) were previously defined. A sample bearing table is shown in Table 7-6.

TABLE 7-6. Ball Bushing (25)

Bushing Number	Bore $\pm .005$	Length	Rolling Load Rating	
			Normal ( $R_R$ )	Maximum
Super 8	.5000	1.250	180 lbs	255 lbs
Super 12	.7500	1.625	470	600
Super 16	1.000	2.250	780	1050
Super 24	1.500	3.000	1560	2000

Frictional force on the ball bushing is found from

$$F = \mu N \quad (7.22)$$

where  $\mu$  is the coefficient of friction from Table 7-7 and  $N$  is the applied load.  $N$  can be either equal to  $R_R$  or  $R_A$ .

The frictional horsepower can be calculated from

$$\text{hp friction} = FV/33.000 \quad (7.23)$$

where  $F$  is found from (7.22). The velocity, " $V$ ", in feet per minute, must be determined from the length of pitman arm " $r$ " (see Figure 7-15), and the revolutions per minute of the engine. The velocity of the rod through the bushing would be

$$\text{Vel} = 2\pi r_1 n \sin \theta_2 \quad (7.24)$$

where  $n$  is the rpm of the engine,  $r_1$  is the pitman length in feet, and  $\theta_2$  is the angle in degrees between the pitman arm,  $r_1$ , and the piston centerline. The form would be a constant found from (7.22), but the velocity will vary according to (7.24).

TABLE 7-7. Coefficient of Friction (25)

### Coefficients of Rolling Friction ( $f_r$ ) of Ball Bushings

$$f_r = \frac{P}{L} \text{ where } P \text{ equals frictional resistance} \\ \text{and } L \text{ equals applied load}$$

BUSHING I.D.	NUMBER of BALL CIRCUITS	CONDITION of LUBRICATION	LOAD IN % OF ROLLING LOAD RATING (for 2,000,000 inches of travel life)				
			125%	100%	75%	50%	25%
1/4", 3/8", 1/2", 5/8"	3 & 4	No Lube	.0011	.0011	.0012	.0016	.0025
		Grease Lube	.0019	.0021	.0024	.0029	.0044
		Oil Lube	.0022	.0023	.0027	.0032	.0045
3/4", 1"	5	No Lube	.0011	.0011	.0012	.0015	.0022
		Grease Lube	.0018	.0019	.0021	.0024	.0033
		Oil Lube	.0020	.0021	.0023	.0027	.0036
1 1/4" thru 4"	6	No Lube	.0011	.0011	.0012	.0014	.0019
		Grease Lube	.0016	.0016	.0017	.0018	.0022
		Oil Lube	.0018	.0018	.0019	.0021	.0027

### Coefficients of Static Friction ( $f_o$ ) of Ball Bushings

LOAD IN % OF ROLLING LOAD RATING				
125%	100%	75%	50%	25%
.0028	.0030	.0033	.0036	.0040

Values are based on use of shafts of recommended diameters,  
hardened to Rockwell 58-63C.

The unique features of solar engine technology are:

1. High temperature exposure of the engine.
2. Frictionless piston sealing by rolling diaphragms and ball bushings.

The design of the other engine components such as bearings, gears and structures can be found in traditional texts on design of machine elements. The engine designer will build prototypes with the theory presented here and in other machine design texts. Actual working commercial engines will result from the experience gained on experimental engines. No amount of analysis can replace the



art of applied engineering which simply makes the theoretical model work by trial and error techniques.

## CHAPTER 8

### ENGINEERING ANALYSIS OF A ROTATING SOLAR ENGINE

#### 8.1 Introduction and Engine Description

In Section 7.2, three engines were described. They were invented by stimulation from past experiences. By understanding how Savery's water pump works, hundreds of variations of this design could be imagined. Finally, the mind conceives of what the inventor perceives as the simplest design. The result is a "new invention". Later, added gadgets to overcome something overlooked often completely disguise the idea source. This new machine will help foster an idea in someone else, and so goes the process. The rotating hot air solar engine came from the same series of events. Heat must be applied externally to a piston after top dead center, and so as not to violate the second law, heat must be rejected after bottom dead center. This engine idea was born in understanding the Carnot engines. (See Section 6.1.)

The Stirling engine was also partially responsible. The mental creativity began to think of ways to add and subtract heat to the cycle. The rotating engine with a fixed crank came forth. The heat ring was added as a gadget to solve the adding and rejecting heat problem. An engine was born. From this engine better and simpler formulation may result. Therefore, with this solar engine design selected, the theory was applied. The design was

analyzed and the performance of the engine was predicted. Many practical "lessons" were learned in building three models. The design material of Chapter 7 resulted in part from Sun Engine I and Sun Engine II which never were totally completed. Problems encountered often found subjective solutions and finally Sun Engine III resulted.

The rotating engine, Sun Engine III, frame is pictured in Figure 8-1. The lower cylinders and the fixed crank are shown fastened to the frame.

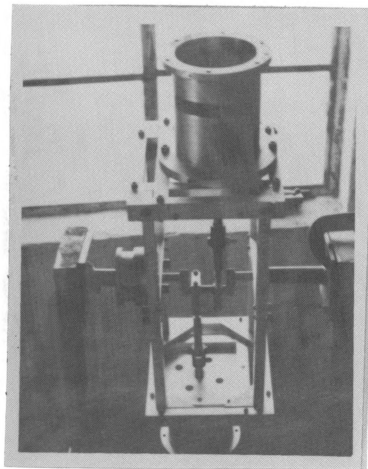


FIGURE 8-1. Solar Engine Frame.

In Figure 8-2, an exploded assembly photograph of the lower cylinder, the piston, the rolling diaphragm, washer, and the upper cylinder can be seen. The piston, the diaphragm and the washer are slipped over the piston rod where a nut secures the components. The lip on the diaphragm is clamped between the upper and lower cylinders.

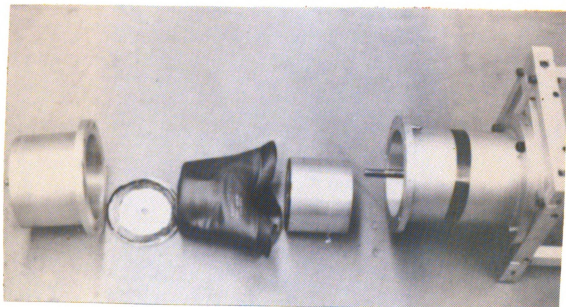


FIGURE 8-2. Solar Engine Piston Assembly.

The assembled engine is displayed in Figure 8-3. The stand holds the crankshaft in a fixed position. The entire engine rotates acting as a flywheel. Power is extracted from a sprocket fastened to the frame. The circular heat rings rotate in and out of solar concentration focal point.

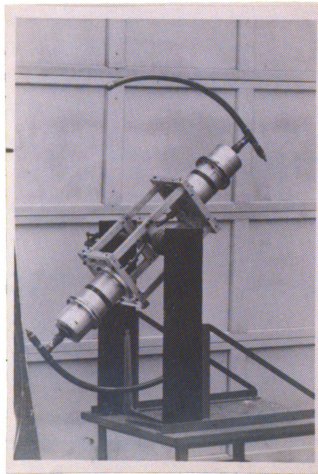


FIGURE 8-3. Solar Engine Assembly.

## 8.2 Cycle Analysis of the New Engine

Since the Ericsson and Stirling cycles have efficiencies theoretically equal to the Carnot cycle, it becomes important to achieve this efficiency in any new engine. To have the efficiency equal to the Carnot engine, simply make the engine expand and compress the gas at a constant temperature with the entropy difference equal for each isothermal process. This process is shown in Figure 8-4 (15).

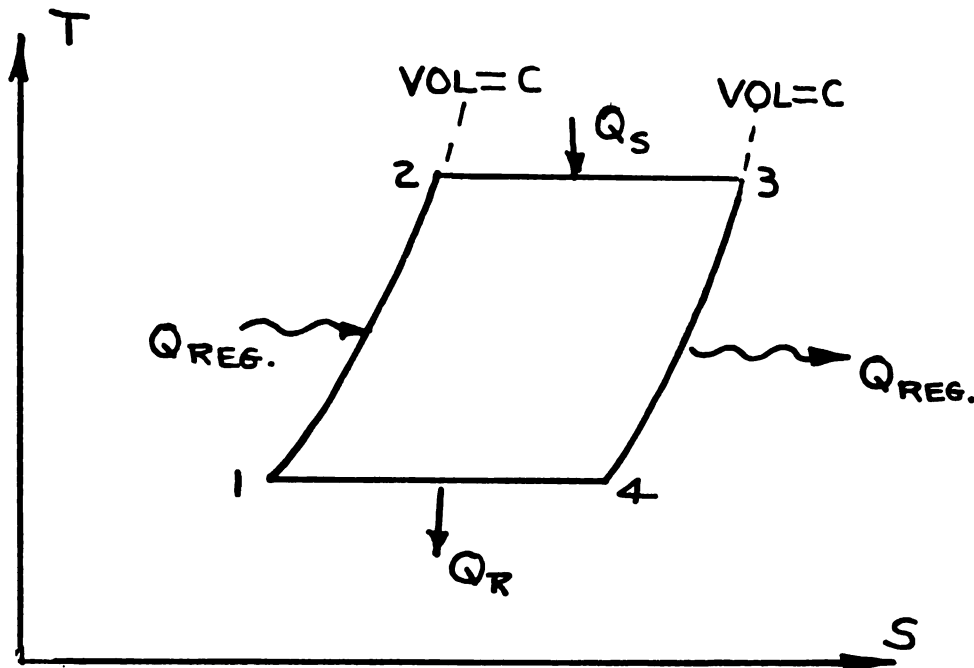


FIGURE 8-4. Cycle Diagram.

Heat is added in the Stirling cycle from the regenerator between 1 and 2. Heat is added isothermally between 2 and 3 and rejected to the regenerator from 3 to 4. Finally, heat is rejected to the environment from State 4 to 1. The process where heat is added and rejected, excluding the isothermal processes, could be constant entropy, volume, pressure, or any process. The important relationship is

$$S_3 - S_2 = S_4 - S_1 \quad (8.1)$$

and that heat is added or rejected to regenerators during the non-constant temperature processes. With this condition, heat is added or rejected outside the engine only in the isothermal processes.

As an example, prove that a constant volume process from State 1 to 2 and 3 to 4 does satisfy Equation 8.1. From State 1 to 2,

$$ds = dQ/T = mc_v dT/T$$

$$S_2 - S_1 = m c_v (\ln T_2 - \ln T_1)$$

$$S_2 - S_1 = m c_v \ln T_H/T_L$$

From State 3 to 4,

$$ds = dQ/T - mc_v dT/T$$

$$S_4 - S_3 = m c_v (\ln T_L - \ln T_H)$$

$$S_4 - S_3 = m c_v \ln T_L/T_H$$

$$S_3 - S_4 = m c_v \ln T_H/T_L$$

which gives:

$$S_2 - S_1 = S_3 - S_4 \quad (8.2)$$

Rearranging (8.2):

$$S_3 - S_2 = S_4 - S_1$$

With Equation 8-1 satisfied, the efficiency of this cycle is easily shown to be

$$\eta = \text{Work}/Q_S = Q_S - Q_R/Q_S$$

$$\eta = 1 - T_L \Delta S / T_H \Delta S$$

$$\eta = 1 - T_L/T_H$$

which is identical to the Carnot efficiency. Note the heat rejected to and from the regenerators is internal shifting of energy and does not enter into the efficiency calculation directly.

This cycle analysis is relevant to this section because the design concept was centered around making any new engine follow approximately a Stirling cycle.

The solar engine can be made to follow a Stirling cycle. The heat ring can have varying thermal conductivities such that the objectives are achieved. The schematic of Figure 8-5 will help to illustrate this cycle.



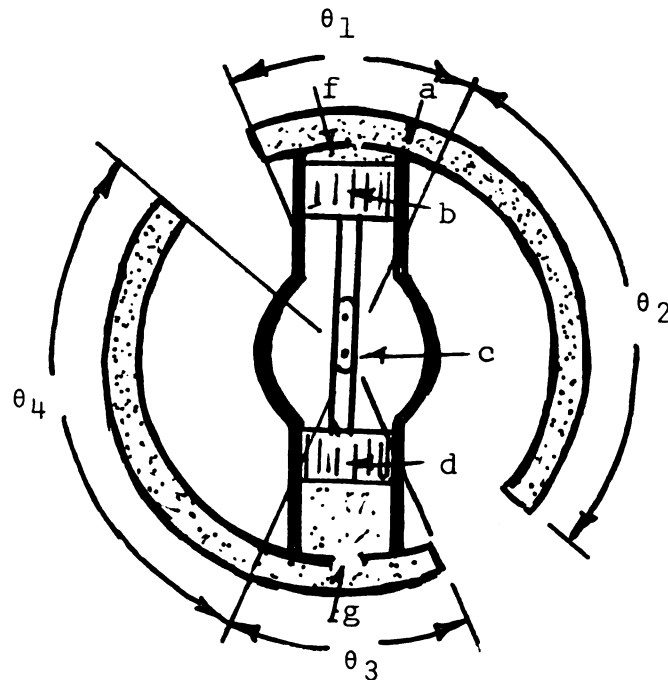


FIGURE 8-5. Solar Engine Schematic.

A curved tube called an energy conducting tube (a) is attached to the cylinder. This tube (a) is connected to the space above the cylinder (f). Concentrated solar radiation strikes this hollow energy conducting tube and transfers its energy to the gas that is above the piston (b). This tube spans an arc of 180 degrees, but it is divided into two parts,  $\theta_1$  and  $\theta_2$ . During the  $\theta_1$  portion of the tube, solar energy can readily transfer into the enclosed gas, but as the engine rotates, the focal point strikes the  $\theta_2$  section where thicker walls restrict the energy transfer. Since the piston is near top dead center at  $\theta_1$ , there is little volume change. If radiation from

the sun can be added quickly, then this portion of the cycle would approximate a constant volume process. Likewise, in  $\theta_2$  by proper selection of the materials and thickness of the wall of the tube, expansion of the gas could take place isothermally. The opposite end has identical hardware, and there are two power strokes per revolution. The crank-shaft (c) is locked between supporting brackets. The entire engine rotates, and power is taken from the rotating engine by such means as attaching a sheave to the engine housing. The pistons (b), (d) are 180 degrees apart. Since the engine rotates, the heat rings and cylinder heads alternately rotate into and out of the focal point of the solar concentrator. While one end is being heated, the other end is being cooled by convection and radiation.

The energy conducting heat rings (a), (g) can receive energy by conduction through a thin opaque surface or the side facing the solar concentrator can have a reinforced transparent cover. The process would start with piston (b) nearing top dead center and piston (d) approaching bottom dead center. The cylinder head and heat ring with piston (b) moves into the focal point of the solar concentrator. If this section of the energy tube were transparent, the pressure would rapidly increase with little change in the volume. Pressure above piston (b) produces a reactionary force on the engine housing that causes rotation. After a rotation of  $\theta_1$ , the construction of the energy conducting tube could be altered to an opaque surface with varying

materials or thickness so that during  $\theta_2$  the expansion could take place isothermally. During  $\theta_3$  the volume changes very little through a relatively large engine rotation. As before, this portion of the process could be considered to transfer heat at a constant volume. The remaining isothermal compression would occur during  $\theta_4$ .

The basic cycle is complete in one revolution with two power strokes per revolution. The cycle is divided into four segments:

1.  $\theta_1$  is the rotational section when the piston is near top dead center. The energy tube admits energy quickly during a time when little volume change occurs. The process is assumed constant volume.
2.  $\theta_2$  is the rotational period when a lesser amount of energy is added to the energy conducting ring. This is accomplished by changing the material of the energy ring. An isothermal process is obtained by adding a controlled amount of energy such that the internal energy remains constant. In other words, work is extracted in an isothermal process.
3.  $\theta_3$  is the rotational period where the energy conducting ring moves out from under the solar concentrator. Cooling begins. It is assumed that the process is constant volume because the piston is at bottom dead center where a small volume change occurs within a relatively long period of time.

4.  $\theta_4$  is the rotational period where the process is cooled isothermally. This is done by transferring heat at the same rate that work is performed in compressing the gas as the piston returns to top dead center.

$$\theta_1 + \theta_2 + \theta_3 + \theta_4 = 360 \quad (8.3)$$

The described processes follow the relationship

$$q/dt = mc_v dT/dt + W/dt \quad (8.4)$$

where internal energy term is zero during the isothermal processes and the work term is zero during the assumed constant volume processes near the bottom dead centers and the top dead centers.

The thermal efficiency would be:

$$\text{Efficiency} = \frac{\text{Work}}{\text{Heat Supplied}} = \frac{Q_A - Q_R}{Q_A}$$

The heat added is

$$Q_A = Q_{1-2} + Q_{2-3}$$

where  $Q_{1-2}$  is heat added during the constant volume process near top dead center and  $Q_{2-3}$  is the heat added during the isothermal expansion.

The heat rejected is

$$Q_R = Q_{3-4} + Q_{4-1}$$

where  $Q_{3-4}$  is the heat rejected during the constant volume process near bottom dead center and  $Q_{4-1}$  is the isothermal compression.

$$\text{Eff.} = \frac{Q_A - Q_R}{Q_A} = \frac{(Q_{1-2} + Q_{2-3}) - (Q_{3-4} + Q_{4-1})}{(Q_{1-2} + Q_{2-3})} \quad (8.5)$$

Writing (8.4) over the constant volume process 1-2 gives:

$$q = mc_v dT$$

$$Q_{1-2} = mc_v(T_H - T_L) \quad (8.6)$$

Writing (8.4) over the isothermal process, the internal energy term is zero and:

$$q = W$$

$$Q_{2-3} = \int P dv = MRT_H \ln V_3/V_4 \quad (8.7)$$

Writing (8.4) over the constant volume process 3-4 with work equal to zero and:

$$q = mc_v dT$$

$$Q_{3-4} = mc_v(T_H - T_L) \quad (8.8)$$

It should be noted that (8.6) equals (8.8).

Writing (8.4) over the final isothermal compression with the internal energy term zero,  $Q_{4-1}$  becomes:

$$q = W$$

$$Q_{4-1} = \int P dv = MRT_L \ln V_4/V_1 \quad (8.9)$$

Substituting (8.6), (8.7), (8.8), (8.9) into Equation 8-5 gives:

$$\text{Eff.} = \frac{(Q_{1-2} + Q_{2-3}) - (Q_{3-4} + Q_{4-1})}{(Q_{1-2} + Q_{2-3})} =$$

$$\frac{mc_v(T_H - T_L) + MRT_H \ln V_3/V_4 - mc_v(T_H - T_L) - MRT_L \ln V_4/V_1}{mc_v(T_H - T_L) + MRT_H \ln V_3/V_2} =$$

$$\frac{T_H \ln V_3/V_2 - T_L \ln V_4/V_1}{T_H \ln V_3/V_2}$$

Referring to Figure 8-4:

$$V_1 = V_2$$

$$V_3 = V_4$$

$$\text{so} \quad \frac{V_3}{V_2} = \frac{V_4}{V_1}$$

$$\text{Therefore,} \quad \ln \frac{V_3}{V_2} = \ln \frac{V_4}{V_1}$$

$$\text{and} \quad \text{Eff.} = \frac{T_H - T_L}{T_H} \quad (8.10)$$

Equation 8.10 is the efficiency of a Stirling engine and the approximate thermal efficiency of the new modification as described. This same equation is the equation of

the Carnot efficiency. The Stirling engine also has indicated mean effective pressure comparable to the Diesel and Otto cycle. Because of the isentropic processes in the Carnot cycle that are replaced with constant volume processes in the Stirling cycle, the Stirling engine becomes a practical possibility as compared with the Carnot engine.

### 8.3 Solar Insolation

To determine the solar insolation falling on the aperture of a solar concentrator, solve for the beam radiation in (2.3):

$$I_b = I_o \tau_{atm} \quad (8.11)$$

$I_o$  would equal 428 BTU/hr-ft<sup>2</sup>.  $\tau_{atm}$  is the transmittance through the atmosphere and is best given by (2.6):

$$\tau_{atm} = a_o + a_1 e^{-k/(\cos \theta z)} \quad (8.12)$$

The constants in (8.12) are found from Table 2-2. The value of  $\cos \theta z$  is found by solving first the angle of declination " $\delta$ " from (2.8) which is rewritten here as

$$\delta = 23.45 \sin [360 (284 + n)/365] \quad (8.13)$$

where  $n$  is the number of days. The hour angle,  $W$ , is next required.

After calculating the solar time from (2.14),

$$\text{Solar time} = \text{Standard time} + E + 4(L_s - L_L) \quad (8.14)$$

the number of hours,  $N'$ , away from solar noon is needed.

W is found from:

$$W = N' \times 15^\circ \quad (8.15)$$

Solve for the  $\cos \theta_z$  from:

$$\cos \theta_z = \cos \phi \cos S \cos W + \sin \phi \sin S \quad (8.16)$$

where  $\phi$  is the local latitude. Equation 8.16 is then substituted into Equation 8.12. With the  $\tau_{\text{atm}}$  solved, the beam radiation can be found. A June 1 calculation was made in Chapter 4. The results for the 5 km haze with 1.5 m altitude are:

$$I_b = 286 \text{ BTU/hr-ft}^2$$

#### 8.4 Energy Transferred to the Gas

In Section 8-3, the procedure for determining the energy striking the outside surface of the energy tube was reviewed. From Chapter 4, a sample calculation using June 1, km haze, and a 1.5 m altitude was made. The results for  $42^\circ$  N latitude at solar noon were  $286 \text{ BTU/hr-ft}^2$ . This theoretical value will be used to analyze the engine.

For stationary receivers, the procedure of Section 3-4 is applicable. The solution of (3.36) gives the temperature of the receiver surface. Equation 3.36 is rewritten for convenience.

$$A_a I_b \rho \eta_0^\alpha = \frac{A_r (T_r - T_{\text{fluid}})}{\Delta X/k + 1/h_i} + \frac{A_r (T_r - T_a)}{1/h_0 + 1/\epsilon_r \sigma (T_r^2 + T_a^2) (T_r + T_a)} \quad (3.36)$$



Once the surface temperature  $T_r$  is known, the mass flow rate is calculated using:

$$\dot{m}(h'_e - h'_i) = \frac{A_r(T_r - T_{\text{fluid}})}{\Delta X/k + 1/h_i} = Q_u \quad (8.18)$$

The efficiency is calculated from (3.25) which is:

$$\eta = \frac{Q_u}{A_c \bar{I}_b} \quad (8.19)$$

Sections 3-1 and 4-1 should be reviewed if there are questions on this method. The fundamental problem of this section is to modify the procedure described above to fit the energy tube that is essential to this design. The solar concentrator has the energy tube moving through its focal point which makes the heat transfer problem unique. The surface receives a transient application of solar radiation. The non-steady state conduction is affected by both the varying solar radiation on the outside and the changing temperatures inside the tube resulting from the work of the piston.

Several assumptions can be made without affecting the analysis appreciably. These assumptions are:

1. Conduction is one dimensional. The heat flow is normal to the tube surface.
2. The tube temperature follows the theoretical diagram as shown in Figure 8-4.
3. Reradiation will be a minimum. Most of the losses

from the surface of the tube will result from convection.

The problem is best illustrated discretely in Figure 8-6. The heat ring is divided into elements.

The energy in the top of the element is:

$$Q_z = kA \partial T / \partial z$$

The energy out the bottom of the element is:

$$Q_z + d_z = A[k \partial T / \partial z + \partial / \partial x (k \partial T / \partial z) dx]$$

The change in internal energy is:

$$\Delta U = \rho c A \partial T / \partial \tau dx$$

The differential equation becomes:

$$\partial / \partial z (k \partial T / \partial z) = \rho c \partial T / \partial \tau$$

For constant thermal conductivity:

$$\partial^2 T / \partial z^2 = (\rho c / k) \partial T / \partial \tau \quad (8.20)$$

which applies internally in the energy tube's wall. The boundaries have radiation and convection losses which require energy balances at the boundaries. For the areas where convection is involved, which is the entire inside and the outside except for the brief period where the focal point is on the element, the energy balance gives:

$$kA \partial T / \partial z = -hA(T_{\text{wall}} - T_{\infty}) \quad (8.21)$$

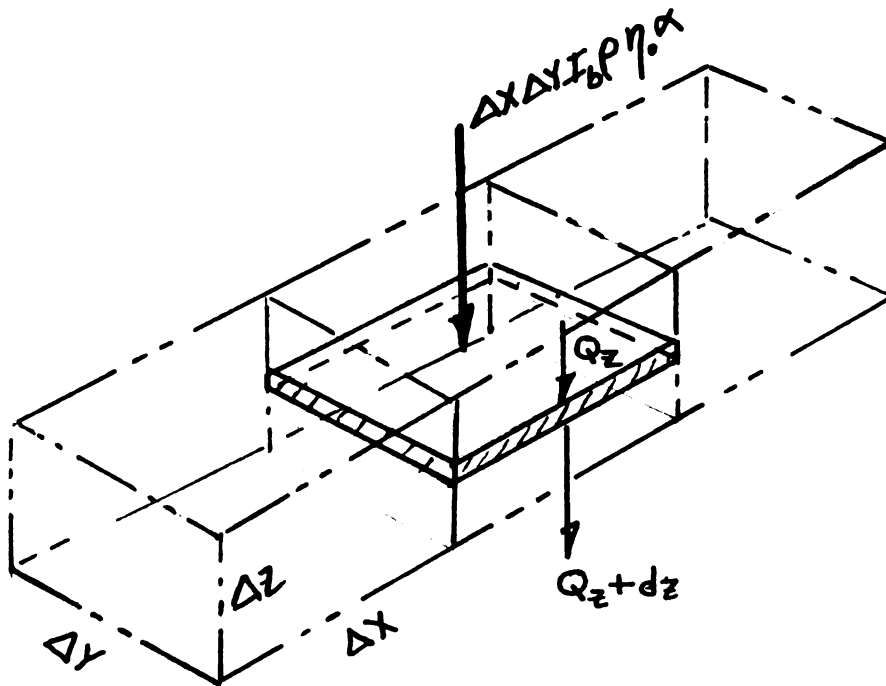


FIGURE 8-6. Energy Balance on Heat Ring.

•  
•  
•  
•  
•

•  
•  
•

The energy balance while the focal point is on the element is:

$$-kA \partial T / \partial Z = hA(T_w - T_\infty) + AI_b \rho \eta_0^\alpha \quad (8.22)$$

The remainder of the time, the energy balance is:

$$-kA \partial T / \partial Z = hA(T_w - T_\infty) \quad (8.23)$$

The last term in (8.22) would be considered a constant over the time interval  $\Delta\tau$  which is equal to

$$\Delta\tau = \Delta x / rw \quad (8.24)$$

where  $\Delta x$  is the length of the element,  $r$  is the mean radius of the heat ring and  $w$  is the angular rotation in radians per second.

The problem can be approached using finite difference techniques. The  $\partial^2 T / \partial Z^2$  is approximated by

$$\partial^2 T / \partial Z^2 = (1 / \Delta Z^2) (T_{n+1} - 2T_n + T_{n-1}) \quad (8.25)$$

where  $\Delta Z$  is the thickness of the element and  $T_n$  is the nodal temperature with  $T_{n+1}$  and  $T_{n-1}$  representing the temperature on each side respectively of the elements temperature. The  $\partial T / \partial \tau$  is also approximated by the equation

$$\partial T / \partial \tau = (T'_n - T_n) / \Delta\tau \quad (8.26)$$

where  $T'_n$  is the next transient temperature after the time  $\Delta\tau$ . To ensure convergence of the numerical solution:

$$(\Delta Z)^2/\alpha\Delta\tau \geq 2(h\Delta Z/k + 1) \quad (8.27)$$

Substituting (8.25) and (8.26) into (8.20), (8.21), and (8.22) gives the respective finite difference equations:

$$T_{n+1} - 2T_n + T_{n-1} = (\Delta Z^2 \rho c/k\Delta\tau)(T'_n - T_n) \quad (8.28)$$

For any particular problem:

$$\Delta Z^2 \rho c/k\Delta\tau = \text{constant}$$

$$T_{n+1} - T_n = (h\Delta Z/k)(T_{n+1} - T_\infty) \quad (8.29)$$

$$T_{n+1} - T_n = (h\Delta Z/k)(T_{n+1} - T_\infty) + \Delta Z I_b \rho \eta_o \alpha/k \quad (8.30)$$

where the last term is a constant applied over one interval.

Equation 8.28 is applicable inside the conducting wall. Equation 8.29 is used at the boundaries of every interval except when the focal point strikes the element. At this point, (8.30) is valid. The  $T_\infty$  is assumed equal to the cycle temperature and varies with the crank rotation. As can be seen, the described approach is very tedious. The convective heat transfer coefficients, "h", on the tube inside as well as the outside are difficult to compute. Therefore, a simplified analysis is essential to find the gas temperature.

The analysis can be simplified by writing the general energy equation:

$$I\alpha A \eta_o \rho - hA_T[(T_H + T_L)/2 - T_{air}] = \quad (8.31)$$

$$P_1 V_1 C_V (T_H - T_L)/(RT_L \tau) + (P_1 V_1/\tau J) \ln V_2/V_1$$

where  $\tau$  is the time for the ring to move through the focal point in hours. The tube surface temperature can be conservatively assumed to equal:

$$T_R = \frac{T_H + T_L}{2} \quad (8.32)$$

The terms in (8.32) which were not previously defined are:

$P_1$  = Initial pressure.

$V_1$  = Initial volume.

$V_2$  = Final volume.

$C_v$  = Specific heat for air at constant volume which equals (1714 BTU/lbm° R.) 0.717 kJ/kg° K

$\tau$  = Time for half a revolution.

$R$  = Gas constant for air.

Assuming the rotating hot air engine has approximately

$$P_1 = 101.35 \text{ kPa}$$

$$V_1 = 0.0003 \text{ m}^3$$

$$V_2 = 0.00113 \text{ m}^3$$

$$h = 511.1 \text{ kJ/hr-m}^2 \cdot \text{C}$$

$$A_t = .0278 \text{ m}^2$$

$$A = 1.119 \text{ m}^2$$

$$\rho = .9$$

$$\eta_o = .8$$

$$\alpha = .96$$

$$\tau = .6 \text{ sec}$$

$$\tau = 1.67 \times 10^{-4} \text{ hr}$$

The resulting high temperature is 325° K which is obtained by substitution into (8.31).  $T_L$  was assumed to be 38° C.

### 8.5 Engine Efficiency

The simplified method of Section 8.4 resulted in a high temperature of 325° K. The calculation was based on the prototype engine that reflected an attempt at having an operational engine and not a totally optimized design. It was assumed that the low temperature was at 38° C, and that the tube and the film offered no resistance to heat flow. The efficiency is:

$$\eta = 1 - T_L/T_H \quad (8.33)$$

which would equal:

$$\eta = 1 - T_L/T_H$$

$$\eta = 1 - 311/325$$

$$\eta = 4.4\%$$

The resulting efficiency could be improved by increasing the compression ratio  $V_2/V_1$  coupled with other design changes. From a prototype design viewpoint, 5% efficiency would be an acceptable beginning. Ericsson achieved a claimed 12% engine efficiency which will be a challenging goal for modern solar engines. The actual test results are given in Chapter 9.



### 8.6 Mechanism and Stress Analysis

Since the solar engine is a relatively slow moving engine, dynamic loading will, in general, be of minor interest. Efficiency improvements can be made by increasing the compression ratio, and the stroke length should be adjusted to maximize the  $V_2/V_1$  value. Lightweight pistons and connecting rods will keep forces small. The dynamic forces are related by:

$$F = ma/g_c \quad (8.34)$$

It is obvious that the mass "m" is equally as important as the acceleration, "a", in dynamic forces.

The design of the cylinder was discussed in Section 7.6. In Chapter 7, consideration was given to stresses. In general, the engine application will fix the factor of safety used in the design which will establish the stresses. If the market develops for agricultural irrigation engines, then lower factors of safety and higher stress levels will be encountered. However, if critical industrial applications are developed for the engine, where safety is involved, lower stress levels will be used. Basically, outside the heat ring and cylinder, there is little that is unique with this engine. General machine design procedures will be sufficient to solve the necessary details.

### 8.7 Servicing and Engine Life

The design presented in this text is extremely simple. Little difficulty was found in repairing the engine. The

failures will be obvious to the mechanic. Engine life will be determined primarily by the diaphragm and at present levels of technology, two years of operation seems possible with the diaphragms. The guide bushing and the main and connecting rod bearings also require preventive and progressive maintenance. It is perceived that servicing and engine life will be a developing art with this engine design, and with competitive manufacturers, improvements can be expected with time.

CHAPTER 9  
OPERATION OF THE SOLAR ENGINE

9.1 Discussion of the Rotating Engine

It became apparent from the development process that the rotating heat ring was theoretically sound, but technically difficult from a functional viewpoint. During part of the cycle, heat had to be added with minimum losses. The remaining 180 degrees of revolution had to allow the heated gas to expand and to minimize heat losses. The return stroke required heat to be transferred away. These requirements of adding heat and extracting heat during different portions of the cycle produced the design shown in Figure 9-1.

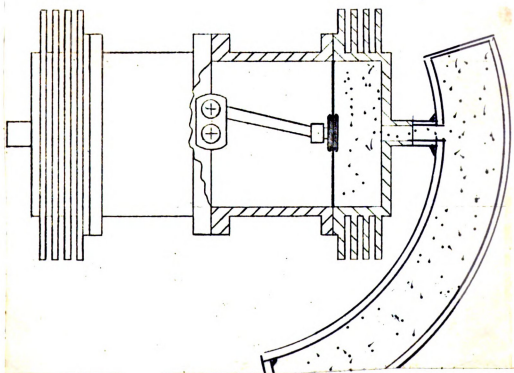


FIGURE 9-1. Solar Engine Schematic with Revised Heat Ring.

The design was changed by utilizing the greenhouse effect of a transparent or translucent cover. Kalwal, the trade name for a fiberglass reinforced plastic material, was used. The heat ring was moved toward the inside of the circle to minimize surface areas. Short wave radiation passed through the cover and was turned to longer wave radiation which was trapped. The gas was heated and the pressure increased. The pistons moved downward. This movement of the piston exposed the cylinder walls, which are finned for heat transfer purposes. With this design, the criteria of controlled losses can be achieved.

The heat ring has a transparent cover. Tests were conducted on a small test chamber with a transparent cover. The results are discussed in Sections 9.2 and 9.3. The test showed that insulation placed beneath commercially available selective surface was necessary. Reinforcement of the cover became important because of the pressure increase. The supply line from the heat ring was relatively large and insulated.

Pictures of the large four inch bore engine are shown in Figures 9-2 and 9-3. A smaller model is shown in Figure 9-4.

The entire engine rotates. Power is taken off a pulley on the crank center line which is fixed to the frame. The engine sits vertically on the ground. Manual cranking is required to start. The dished concentrator is focused on the heat ring, which is difficult with high sun altitude

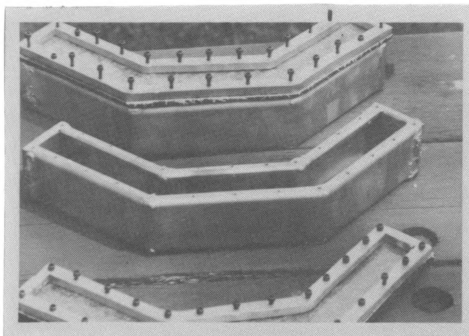


FIGURE 9-2. Four Inch Bore Engine.

angles. The general arrangement of engine to concentrator is rather awkward and tends to lower the collector efficiency. In other words, the engine is in the way of the collector. If the concentrating mirror is placed to one side, a distorted focal point results. Not all of the energy impinging upon the dished mirror can strike the heat ring because of the physical arrangement of mirror to engine. Another problem is found in the concentrating collector. The optical efficiency of the collector was low enough to be rejected by the manufacturer. The mirror was purchased by the author with limited funds and this reject was all that was affordable. The actual test data presented in Chapter 4 gave a sixteen percent efficiency for the collector, which verifies some optical efficiency problems.



FIGURE 9-3. Four Inch Bore Engine.





FIGURE 9-4. Small Model of Solar Engine.



The determining of the engine efficiency of both rotating engines with several built in "problems" became meaningless. The engines of Figures 9-2, 9-3, and 9-4 simply proved that the concept was feasible.

## 9.2 Results of Tests

When it became apparent that radiation through a cover into the heat ring was the only way to meet the design objectives, tests were conducted upon a small chamber. The chamber is shown in Figure 9-5. The body of the test chamber was machined from aluminum. A .040 inch premium Kalwal cover was attached.

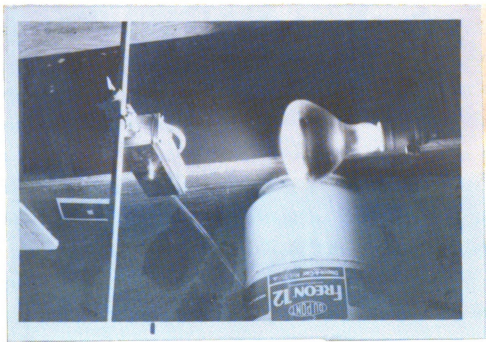


FIGURE 9-5. Test Chamber.

Two ports were located on each end which were used to purge and charge the test chamber. Two mediums, air and Freon-12, were used.

A 150 watt flood light was placed eight inches from the face. Pressure in inches of water was recorded as a function of time in seconds. The two gases were tested with different pressures. The result is shown in Figure 9-6.

At first the system failed to respond. The aluminum acted as a heat sink and also reflected out much of the radiant energy. The results of Figure 9-6 came after insulating the inside to the test chamber and covering the insulation with a selective surface (black chrome).

Probably the most significant finding of the entire thesis came in this simple test. The results of the tests indicated that an engine can be operated from the increased pressure developed inside a transparent covered enclosure that is exposed to solar radiation. By transferring energy through a transparent cover onto a selective surface, the enclosed gas pressurized according to the ideal gas laws. The increase in gas temperature with its resulting pressure increase can be made to occur rapidly. Other engine designs can use simple flat plate collectors similar to the test chamber. The flat plate collector can be connected to a piston using the techniques of Section 7.3 with various methods of producing a cooling cycle. A simple water seal piston (inverted can over water) could produce a cost

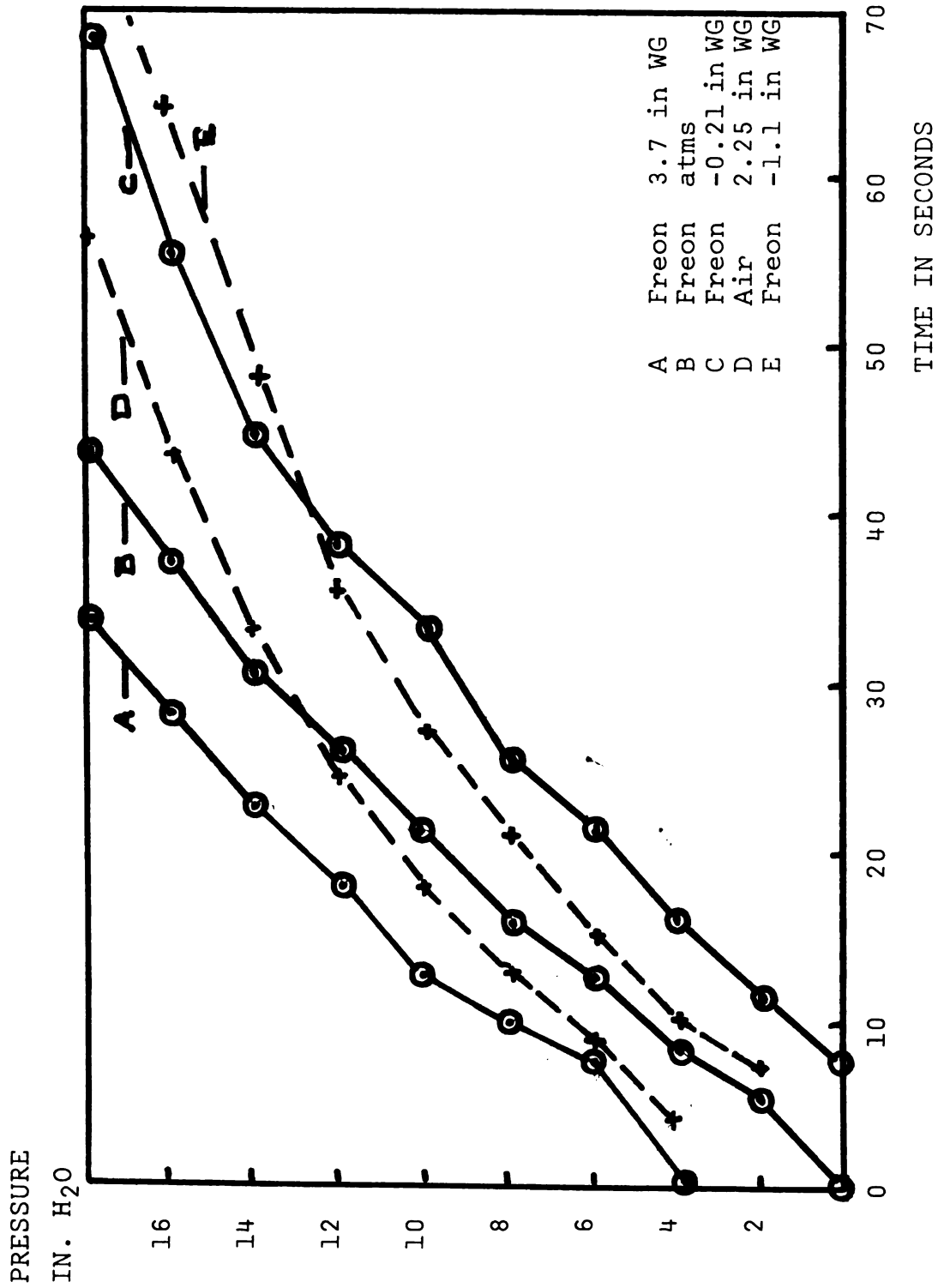


FIGURE 9-6. Test Results.



effective design.

Shown in Figure 9-7 is a small model engine operating from the test chamber.

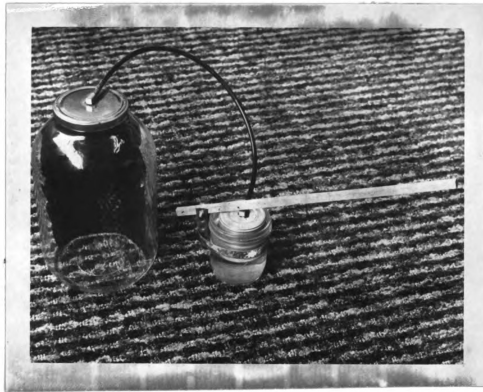


FIGURE 9-7. Flat Plate Collector Engine.

From Figure 9-6, several important facts can be ascertained. Increased mass of gas increased the pressure rise in a given time. This just verified the ideal gas law.

$$PV/T = mR$$

Freon-12 responded better than air. Not only was the initial rate of pressure increase higher in Freon than air,



but the rate of change of the slope was less in Freon. The air curves tended to decrease their slope. In other words, the air charge test chamber began to reach a steady state condition more rapidly than Freon. When steady state conditions are reached the pressure remains constant. The energy going in will equal the energy coming out. Such a condition cannot produce work. The Freon had faster pressure increases and would reach steady state conditions at a much higher pressure than air. The non-ideal gas, Freon 12, is a better solar engine medium than the ideal gas, air. Other gases should be tested and compared. This is certainly a future research project in developing solar engines.

### 9.3 Proposed Solar Engine Design

The initial design of the rotating solar engine was influenced by the Stirling and Ericsson engines. In these engines, heat applied externally was transferred through solid walls by conduction. This method did not work well in the rotating engine design. To overcome the problem, the heat ring was designed with a transparent side toward the tracking collector. The focal point was concentrated on the absorber inside the heat ring. The cover stopped most of the losses and solved the problem. The ease with which the gas pressure could be increased with radiation resulted in a simple source of power for engines of the type shown in Figures 9-7 and 7-4. The choice of this engine over the

rotating engine was verified by the ease of building models. Many attempts were made before the rotating engine produced power. Complex machining was also required on this engine. The flat plate engine was easily fabricated and was operational with little effort.

The necessary theoretical tools are very simple. The compression ratios must be low. ( $V_1/V_2$  = compression ratio.) The temperature near the top dead center cannot exceed the temperature of the gas being heated from the sun. The logic can be seen from (9.1)

$$T_2 = T_1(V_1/V_2)^{n-1} \quad (9.1)$$

where  $T_1$  is the initial temperature,  $T_2$  is the temperature at the top of the stroke,  $V_1/V_2$  is the compression ratio and  $n$  is a function of the process. If the process of returning the piston to the top of its stroke were assumed reversible and adiabatic, then  $n$  would equal 1.4 for air. If the temperatures were assumed to be  $T_2$  equal to 43.3° C and  $T_1$  equal to 37.7° C, the compression ratio would be:

$$V_1/V_2 = 1.045 \quad (9.2)$$

A system with a 9.29 m<sup>2</sup> (100 ft<sup>2</sup>) collector could have 127.42 liters (4.5 ft<sup>3</sup>) of displacement with a deep solar panel. The collector size and piston displacement from this example have values that make the system feasible to construct.

From the author's experience, a static temperature of 93.3° C (200° F) is quickly obtainable in a flat plate



collector. Using the ideal gas relationship

$$P_2 = P_1(V_1/V_2)(T_2/T_1) \quad (9.3)$$

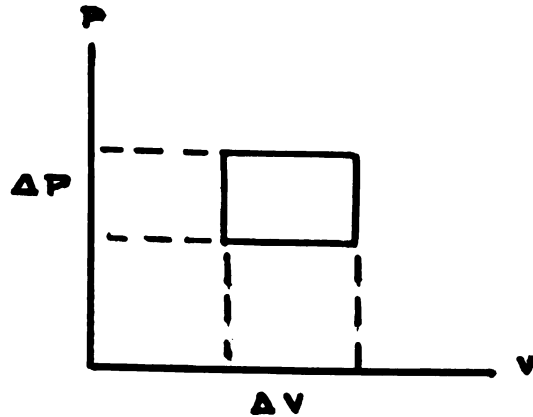
a pressure increase of 13.8 becomes obtainable.

The flat plate collector would be charged with an initial pressure of  $P_1$ . The gas would be Freon.  $T_2$  would reach a stagnation temperature of 93.3° C.  $T_1$  would be somewhat larger than the environmental temperature.  $V_1/V_2$  would be designed close to unity by having the surface area of the collector large as compared to the piston area. The stroke would be as short as practical. The end objective is to have  $P_2 = P_1 + 13.8$  kPa(2 psi). With the final pressure  $P_2$ , a force can be developed by applying the pressure to a relatively large piston area. The piston is a rolling diaphragm with a ball bushing or an inverted barrel in water. The piston is attached to one end of a lever. The other end could be a pump rod. When the piston pushes downward, the lever pulls the pump upward. Through a mechanism shading is provided for the cooling cycle or water from the reciprocating pump could produce the necessary intermittent cooling. In this resulting design, the cost of equipment will justify the decrease in engine efficiency.

The rotating engine served its purpose. Instead of being the reported design to pursue, the rotating engine caused the research which fostered a simpler engine.

The efficiency of this flat plate collector engine is easy to determine. The pressure-volume diagram can be a

rectangle when lifting water.



The work is

$$W = \Delta P \Delta V$$

where  $\Delta P$  is the pressure change and  $\Delta V$  is the volume change.

The efficiency is

$$\eta = W/Q_s = (\Delta P \Delta V / \tau) / (I_a A \eta) \quad (9.4)$$

where  $\tau$  is the time in hours per cycle,  $I_a$  is the actual solar insolation, and  $A$  is the collector area with an efficiency of  $\eta$ .

There are many ways of achieving a cooling cycle with the flat plate engine. If the engine is pumping water, the discharge water provides the necessary cooling. Or, the motion of the piston closes the shutter to allow cooling. Another possibility is to have the absorbing surface reflective on the back. Through a mechanism, the absorber flips over to the mirrored surface to reject the incoming energy

so that cooling takes place. A more direct approach is to use valves. By inclining the collector, natural flow is possible if valves in the top and bottom are opened. Cooling can also be accomplished through the cylinder walls. As the piston is pushed downward, the walls that are finned are exposed. To determine the efficiency from (9.4), the time,  $\tau$ , must be determined. If  $\tau$  is large, then the efficiency is small. This can be seen from (9.4). On the heating cycle it becomes important to have the collector well insulated. On the cooling cycle the opposite is required. Valving is one of the most certain ways to solve the problem of reducing the time of the cycle. However, engine cost must be weighed against efficiency. Shading with a simple device might be the proper solution in some instances. Another related problem is the presence of energy sinks. Mass that is thermally conductive should be avoided. The less mass used in the collector, the better is the efficiency. The absorbing surface is a future area of research. The surface requires extensive contact with the gas to be heated. A black cloth undulated for maximum contact gives good results.

#### 9.4 Failures

There is a learning experience in failure. Solar engine technology reached its peak of development one hundred years ago. With the advent of low cost energy came the demise of solar engines. The state of the art has, in

general, been buried with its inventors and entrepreneurs. It seems prudent to publish the errors the author made. Had Ericsson, Pifre, or Shuman been alive and consulted, many hours of development time could have been saved.

The very first rotating engine was designed using piston rings. The frictional energy consumed was larger than the available power. Consequently, this engine sat motionless when heated. The first challenge came in developing a frictionless piston. Close fitting brass pistons in aluminum cylinders were tried. The height of the piston versus the diameter was too small in one case. This caused the piston to bite into the cylinder walls. Close fitting pistons can be made to work satisfactorily if the skirt length is larger than the diameter, but the process holds little promise for mass production. The use of rolling diaphragms became the simplest solution (30) and was the topic of discussion in Section 7-3.

To use the diaphragms the piston is held away from the cylinder wall. This is accomplished by using linear bushings. If rotary motion is desired, a crank mechanism is used. Large piston displacements will place proportionally large side loads on the bushings.

The second engine had a 4 inch stroke. The piston through a link was connected to a crank. The large displacement caused the piston rod to lock in the bronze bushings and the second engine could not be rotated. (See Section 7.6.)

The second engine with the 4 inch stroke had too much compression. The temperatures in the engine were being elevated above the source temperature. The stroke was shortened to two inches, which lowered the compression temperature and allowed the engine inertia to smoothly rotate against the compression.

Finally, the initial heat ring, which was a one inch copper tube formed into a semi-circle, transferred heat away as fast as it was added. Conduction heat transfer was inadequate. The problem was solved by using the "greenhouse effect". The heat ring was given a transparent cover facing the sun. Radiation passed through the cover and was trapped. Heat was then rejected in the piston which needed fins.

## CHAPTER 10

### CONCLUSION

The scope of the thesis was to investigate the possibilities and methodology of converting solar radiation to work. Some technology had been developed a century ago. From this early development, it appears that one brake horsepower can be extracted from 100 square feet of collector area. (See Chapter 1.) Patent and literature searches indicate these past inventions were, in general, too complex to be cost effective.

Solar engine development requires competency in collector analysis and evaluation of solar insolation. Collected energy is a function of time, location, orientation and type of collector.

An important aspect of solar development is cost effective design. To be cost effective, a design must compete with fossil fuel engines economically. With fuel prices of \$0.53/liter (\$2.00 a gallon), solar engines could cost approximately \$5,000 per horsepower and be cost effective. Concentrators could cost \$562.00 more per square meter than flat plate collectors. With rising fuel costs it appears that solar engines can be used principally in applications such as water pumping. (See Chapter 5.)

Contrary to many publications, it was found that theoretically, flat plate and concentrating collectors have nearly the same efficiency. Under actual tests the flat

plate collectors had higher efficiencies. The absorber used in testing the dished mirror concentrator reradiated large amounts of solar energy, and special design efforts must be made to stop these losses. However, with assumed equal efficiency of concentrating and flat plate collectors, the engine efficiencies are higher with concentrators. The efficiency of the engine follows:

$$\text{Efficiency} = 1 - T_L/T_H$$

for the Carnot, Stirling and Ericsson cycles. With assumed equal collector efficiency and higher engine efficiency using concentrators, the overall product efficiency will be higher using concentrators. Economic considerations may cause the flat plate with its lower overall efficiency to be the best choice because of lower capital investment.

Thermodynamics was in its infancy when Ericsson and Stirling developed their engines. Most theoreticians criticized Ericsson's engines as being unsound. These critics were silenced when Ericsson's engines were seen producing power. Theoretical thermodynamic cycles follow the development of the engines. Initially, the author concentrated on having a new engine follow a particular cycle such as the Stirling cycle. It was soon realized that the cost per horsepower is more important than having the engine follow a particular cycle. Deviation from a cycle may soon become necessary to build a cost effective engine.

There are many possible cycles that a solar engine

could use. The Rankine cycle can be used if the rejected heat from the condenser has some use. In northern latitudes a solar steam engine could pump water and the condenser could heat domestic water. The added cost of this cycle could be justified by using the waste heat. The Ericsson and the Stirling cycles have promise, but tend to be expensive engines. The salient principle is to inexpensively add and reject heat during the cycle. Cycle tracing is of lesser importance when compared with capital investment in the engine. Chapters 7, 8, and 9 discuss the methods necessary to accomplish the conversion of radiant energy to work inexpensively.

Solar engine design centers around building frictionless pistons. Turbine type devices were not considered because it appeared to be difficult to compete with the oldest type of solar engine called a wind mill. The piston design uses a rolling diaphragm with a roll ball bushing. This type of construction requires a minimum of machining with liberal tolerances. Aluminum alloy pistons and cylinders will meet the other requirements of heat transfer, strength, and product life.

Initially, a rotating engine using a heat ring and a concentrator was investigated. By rotating the engine, a means of adding and rejecting heat became possible without valves or displacement pistons. An analysis of the engine was made theoretically and with the assumptions made in Chapter 8, an efficiency of 4.46% was determined.



The engine described in Chapter 8 was not operational initially. The problem of adding heat to the rotating heat rings was solved by constructing semi-circular flat plate collectors. A concentrating mirror focused its energy inside the flat plate collectors. Before building the new heat rings, tests were conducted on a small test chamber filled with varying pressures of Freon-12 and air. The most important findings of the project came from these tests. A flat plate collector could be designed to rapidly change the pressure of the trapped gas. By insulating the inside of the chamber and covering this surface with a black selective surface, significant pressure changes could be obtained. For most simple applications, 13.8 kPa (2 psi) pressure increase is possible inside a flat plate collector. These changes occur rapidly and follow the ideal gas relationships.

With the redesigned heat rings, the rotating engine became operational. Because of equipment limitations, no efficiency measurements could be made. The small model shown in Figure 9-4 was the model completed at the time of thesis publication. The mirror available is too large for this engine. The model was operated from a light bulb.

With a 13.8 kPa (2 psi) increase possible in an enclosed flat plate collector, many new possibilities exist. Relatively large diameter pistons connected to even larger flat plate collectors are able to produce significant forces. The motion of the piston can provide shading through a

mechanism or water pumped could cool the collector. The rotating engine is novel, but somewhat complicated to build. The engine that operates from a simple flat plate collector can be very simple. A thirty gallon barrel with the end cut out makes a piston. By inverting this smaller barrel into a fifty gallon drum, a simple piston is made. A flexible hose is attached to the flat plate collector. A simple lever arrangement fastened to a fixed post and the top of the thirty gallon barrel completes the system. The end of the lever is fastened to a pump rod. As the pressure builds up in the collector, the water is displaced out of the thirty gallon barrel. The lever pushes upward lifting water which flows through coils in the collector. The water provides the cooling cycle. Such an engine will find an application in third world countries. Other more sophisticated engines are possible using the techniques described in previous chapters.

The extraction of mechanical power from the sun has been proven possible. The results of this work should show the potential of producing cost effective solar engines using elementary thermodynamics and simple designs. The initial research and development must produce engines that have a place in the free market. If high efficiency engines require costly technology, then perhaps the prudent designer will find simple, cost effective engines with lower efficiency that shall be classified as appropriate technology for our times.

## CHAPTER 11

### RECOMMENDATIONS

Several research and development projects can develop from this work. Tests should continue on flat plate collectors designed to produce pressure. The design of the absorbing surface to produce pressure will be different from the surfaces used in typical heating applications. Only two gases were used in this study. Many other gases should be tried. Curves relating the type of gas, surface, initial pressure, and final pressure to time need to be developed. Methods of alternating the heating and cooling cycle should be studied in the flat plate collector engine. Both the rotating and the flat plate collector engines require further development.

## BIBLIOGRAPHY

## BIBLIOGRAPHY

1. Ackerman, A.S.E., The Utilization of Solar Energy. Government Printing Office, "Annual Report of the Smithsonian Institution, 1915".
2. Jordan, R.C., Mechanical Energy from Solar Energy. N.Y. Johnson Reprint Corporation. "World Symposium on Applied Solar Energy Proceedings".
3. Church, W.C., John Ericsson. Charles Scribner & Sons, New York.
4. Walton, H., The How and Why of Mechanical Movements. Popular Science Publishing Company, E.P. Dulton & Company, New York.
5. Ryan, L.D., "The Theoretical Design of a Solar Engine for the Production of Hydrogen", 2nd World Hydrogen Energy Conference Proceedings, August 1978.
6. Duffie, J.A., Solar Energy Thermal Process. John Wiley & Sons, 1974.
7. Liu, B.Y.H., Solar Energy, 4, No. 3, (1960), "The Interrelationships and Characteristic Distribution of Direct, Diffuse, and Total Solar Radiation".
8. Hottel, H.C. "A Simple Model for Estimating and Transmittance of Direct Solar Radiation Through Clear Atmospheres", Solar Energy, Vol. 18, pp. 129-134, 1976.
9. Krieth, F., Principles of Solar Engineering. McGraw-Hill Publishing Company, 1978.
10. ASHRAE Handbook of Fundamentals, American Society of Heating, Refrigeration, and Air Conditioning Engineers, New York, New York, 1972.

11. Hottel, H.C., Transactions of the Conference on The Use of Solar Energy, 2, Part I, 74, University of Arizona Press, 1958. "Evaluation of Flat-Plate Collector Performance".
12. Ryan, L.D., Fundamentals of Solar Energy. Prentice-Hall, 1981.
13. Cherenusinoff, P., Principles and Applications of Solar Energy. Ann Arbor Science Publisher, 1978.
14. Gupta, A., "Digital Simulation of a Solar Collector", Paper presented to the Honors College, Western Michigan University, Kalamazoo, Michigan, 1978.
15. Wark, K., Thermodynamics. 2nd Ed., McGraw-Hill, 1971.
16. McAdams, W.H., Heat Transmission. 3rd Ed., McGraw-Hill, New York, 1954.
17. "Automotive Stirling Engine Development Program", Contractors Co-ordination Meeting Report, Ford Motor Company, Engineering and Research Staff, Dearborn, Michigan, October 1978.
19. "Fatigue at High Temperature", ASTM Special Technical Publication 459, A symposium presented at 71 annual meeting, American Society of Testing and Materials, San Francisco, California, June 23-28, 1968.
20. Colangilo, V.J., Analysis of Metallurgical Failures. John Wiley & Sons, New York, New York.
21. Dorn, J.E., Editor, Mechanical Behavior of Materials at Elevated Temperatures. McGraw-Hill, New York, New York, 1961.
22. Greenfield, P., Creep of Metals at Higher Temperatures. Mills and Boon Limited, London, 1972.
23. Sully, A.H., Metallic Creep. Interscience Publisher Inc., New York, New York, 1949.
24. Kachanov, Translated by E. Bishop, Theory of Creep. National Lending Library for Science and Technology, Boston, 1967.

25. "Thomson Ball Bushings for Linear Motion", Thomson Industries, Ind., Manhasset, New York.
26. American Society for Metals, Metals Handbook. Vol. 1, 8th Ed., Metals Park, Ohio.
27. Roark, R.J., Formulas for Stress and Steam. 3rd Ed., McGraw-Hill, New York, 1954.
28. Spotts, M.F., Design of Machine Elements, 4th Ed., Prentice-Hall, Inc., Englewood Cliffs, New Jersey.
29. Kent, W., Kent's Mechanical Engineers Handbook. 10th Ed., John Wiley & Sons, New York, New York, 1923.
30. "Design Manual Bellofram", Burlington, Massachussetts, 1962.
31. U.S. Patents. United States Patent Office.
32. Klein, R.S. "John Ericsson: The Successful Failure", Industrial Education, Vol. 52, pp. 63-64, 1978.





MICHIGAN STATE UNIVERSITY LIBRARIES



3 1293 03169 1631